Determination of Maturity Relations for Steel-Fiber Reinforced Concrete

Saeid Kamkar

Submitted to the
Institute of Graduate Studies and Research
in partial fulfillment of the requirements for the degree of

Doctor of Philosophy
in
Civil Engineering

Eastern Mediterranean University
September 2017
Gazimağusa, North Cyprus

Approval of the Institute of Graduate Studies and Research

Assoc. Prof. Dr. Ali Hakan Ulusoy
Acting Director

I certify that this thesis satisfies the requirements as a thesis for the degree of Doctor of Philosophy in Civil Engineering.

Assoc. Prof. Dr. Serhan Şensoy
Chair, Department of Civil Engineering

We certify that we have read this thesis and that in our opinion, it is fully adequate in scope and quality as a thesis for the degree of Doctor of Philosophy in Civil Engineering.

Prof. Dr. Özgür Eren
Supervisor

Examining Committee

1. Prof. Dr. Özgür Eren _____

2. Prof. Dr. M.Hulusi Özkul _____

3. Prof. Dr. İsmail Özgür Yaman _____

4. Assoc. Prof. Dr. Khaled Marar _____

5. Asst. Prof. Dr. Tülin Akçaoğlu _____

ABSTRACT

The evaluation of steel-fiber reinforced concrete using the maturity method was investigated in this study. There were five different volume fractions of fibers (0, 0.5, 1, 1.5 and 2% by volume of concrete) and three different curing temperatures (8°C, 22°C and 32°C) considered. Maturity method has been widely used to predict compressive strength of concrete, although less research have been used to investigate other properties of concrete by maturity method. In this study, compressive strength, flexural strength, flexural toughness and splitting tensile of steel fiber reinforced concrete were also evaluated by maturity method. The compressive strength, flexural strength and splitting tensile strength were tested at 1, 3, 7, 10, 14, 28 and 56 days for all of the volume fractions of fibers and at different curing temperatures. However, flexural toughness were tested at ages of 3, 7, 14, 28 and 56 days for all volume fractions of fibers at different curing temperatures.

The apparent activation energy was determined for all volume fractions of fibers by three methods (linear hyperbolic, parabolic hyperbolic and exponential). The results show that activation energy decrease by increasing volume fractions of fibers in all methods. In order, to determine apparent activation energy, the compressive strength of mortar were tested at ages of 1, 2, 4, 8, 16, 32 and 64 days and at curing temperatures of 8°C, 22°C and 32°C for all the five-volume fractions of fibers.

In this study, two maturity methods were used to calculate equivalent age and maturity index, these were the Arrhenius and Nurse-Saul methods. However, according to different apparent

activation energies, three equivalent ages were calculated as namely LH_{eq}, PH_{eq} and EXP_{eq}. The predicted models obtain by LH_{eq} have a very good correlation with experimental results.

Four different strength-maturity equations (linear hyperbolic, parabolic hyperbolic, logarithmic and exponential) were used to predict the compressive strength, flexural strength, flexural toughness and splitting tensile strength for three equivalent ages and maturity index. All of these four equations have good correlations with the experimental results. However, the accuracy linear hyperbolic and exponential is slightly higher parabolic and logarithmic equations.

In this study totally 320 new maturity models were established and for each test, the predicted models were compared with each other. In addition, the validation of each model was evaluated.

Moreover, some necessary factors for using maturity method such as temperature histories and datum temperature were evaluated for all mixes. The temperature histories at first 24 hours are slightly increased by increasing volume fractions of fibers.

Keyword: Maturity method, Activation energy, Steel fiber, Compressive strength, Flexural strength, Splitting tensile strength, Flexural toughness.

ÖZ

Bu çalışmada çelik elyaflı betonun bazı özellikleri betonun olgunluğu kullanılarak elde edilmeye çalışılmıştır. Beş değişik hacimsel oranda (%0, 0.5, 1.0, 1.5 ve 2.0) çelik elyaf karışımı ile üretilen betonlar üç farklı sıcaktaki (8°C, 22°C ve 32°C) su küründe bekletilmiştir. Bilindiği üzere betonun olgunluk (sıcaklık-zaman ilişkisi) özelliği kullanılarak beton basınç dayanımı kolaylıkla tahribatsız bir deney seçeneği olarak yaygın bir biçimde kullanılmaktadır. Bu çalışmada ise betonun olgunluk özelliği kullanılmak sureti ile çelik elyaflı betonların basınç dayanımı, eğilme dayanımı, eğilmede tokluk ve basmada yarma dayanımı ölçülecektir. Basınç dayanımı, eğilme dayanımı ve basmada yarma dayanımı 1, 3, 7, 10, 14, 28 ve 56 günlerde, eğilmede tokluğu ise 3, 7, 14, 28 ve 56 günlerde ölçülmüştür.

Açık aktivasyon enerjiler ise tüm beton çeşitleri için üç model ile belirlenmiştir. Bunlar lineer hiperbolik, parabolik hiperbolik ve eksponansiyel olarak belirlenmiştir. Sonuçlara bakıldığı zaman tüm metodlarda çelik elyaf oranı arttıkça açık aktivasyon enerjisinin azaldığı görülmüştür. Açık aktivasyon enerjisini bulmak için ise beş değişik elyaf oranı olan harçların 1, 2, 4, 8, 16, 32 ve 64 günde (8 °C, 22 °C ve 32 °C'de su küründe) elde edilen basınç mukavemetleri kullanılmıştır.

Bu çalışmada eşdeğer yaş ve olgunluk endeksi iki çeşit beton olgunluk ilişkisi modeli kullanılarak (Arrhenius ve Nurse-Saul) hesaplanmıştır. Bunun yanında farklı açık aktivasyon enerjilerinden dolayı üç farklı eşdeğer yaş hesaplanmıştır (LH_{eq}, PH_{eq} ve EXP_{eq}). Sonuçlara bakıldığı zaman eq_{LH}ile elde edilen modeller en iyi korelasyonu vermiştir.

Basınç dayanımı, eğilme dayanımı, eğilmede tokluk ve basmada yarma dayanımı özelliklerini tarhribatsız yoldan betonun olgunluk ilişkisi kullanılarak elde etmek için ise dört değişik mukavemet-olgunluk denklemi (lineer hiperbolik, parabolik hiperbolik, logaritmik ve eksponansiyel) kullanılmıştır. Tüm denklemlerin de korelasyon değerleri kabul edilebilir seviyede çıkmıştır.

Bu çalışmada toplam olarak 320 yeni olgunluk ilişkisi elde edilmiştir. Tüm modellerin (denklemlerin) geçerlilikleri de ayrıca çalışılmıştır.

Bunlara ek olarak modelleme çalışmalarında kullanılması için tüm betonların sıcaklık seyri ve sıfır noktası sıcaklık değerleri de bulunmuştur. Sıcaklık seyirlerine bakıldığı zaman çelik elyaf oranı arttıkça ilk 24 saatte sıcaklığın arttığı da gözlemlenmiştir.

Anahtar Kelimeler: Olgunluk metodu, aktivasyon enerjisi, çelik elyaf, basınç dayanımı, eğilme dayanımı, basmada yarma dayanımı, eğilme tokluğu.

DEDICATION

To My Family

ACKNOWLEDGMENT

I would like to thanks my express deepest appreciation Prof. Dr. Özgür Eren, who gave me the opportunity to study on this thesis. Without his guidance in our countless meetings and discussions, I would not have been able to complete my research.

I would like to thanks my express deepest appreciation to my Master supervisor Asst. Dr. Erdinc Soyer. I never forget his great efforts in guiding and encouraging me to start this work.

I would like to express my sincere gratitude to my family for their support and encouragement.

Sincere thanks to Assoc. Prof. Dr. Khaled Marar who took the time to instruct me and gave insightful and constructive comments as well as supervision through my study.

Special Thanks to Mr. Ogün Kılıç for his help and technical guidance. It was not possible to complete experimental tests on time without the help of Mr. Ogün Kılıç.

I wish to express my special thanks for all the members of the Civil Engineering Department at Eastern Mediterranean University.

I would like to thanks all my friends in North Cyprus, for their friendship and hospitality.

TABLE OF CONTENTS

LIST OF TABLES

LIST OF FIGURES

LIST OF SYMBOLS

E	Apparent Activation Energy, J/mol.
k_T	Rate Constant.
M	Maturity.
R	Universal Gas Constant.
T	Elapsed Time (hours or days).
t_0	Age at the Start of Strength Development,
t_e	The Equivalent Age at the Reference Temperature.
T	Average Concrete Temperature, °C.
T_0	Datum Temperature, °C.
T_r	Absolute Reference Temperature, Kelvin.
Q	Slope of Best-fit of Rate constant
S_u	Ultimate Strength, MPa.
Δt	Time Interval at Temperature T.
τ	Time Constant.
α	Shape Parameters.
V_f	Volume Fractions of Fibers.

LIST OF ABBREVIATIONS

FRC	Fiber Reinforced Concrete.
SFRC	Steel Fiber Reinforced Concrete.
L-D	Load Deflection curve.
LH	Linear Hyperbolic.
PH	Parabolic Hyperbolic.
EXP	Exponential.
LH_{eq}	Equivalent Age by Linear Hyperbolic Method .
PH_{eq}	Equivalent Age by Parabolic Hyperbolic Method.
EXP_{eq}	Equivalent Age by Exponential Method.
MI	Maturity Index.
S_{LH}	Linear Hyperbolic Strength- Maturity Equation.
S_{PH}	Parabolic Hyperbolic Strength-Maturity Equation.
S_{LOG}	Logarithmic Strength-Maturity Equation.
S_{EXP}	Exponential Strength-Maturity Equation.

Chapter 1

INTRODUCTION

1.1 General

Concrete is the most widely used construction material all over the world. One of the most important characteristics of concrete is its high capacity in carrying compressive loads. Concrete structures are generally designed according to 28 days compressive strength value of the concrete. However, concrete is a brittle material which has a low tensile strength and a low strain capacity. In order to address this problem, the use of fiber reinforced concrete (FRC) has been employed over the past 40 years (Bentur et al., 2007). Fiber reinforced concrete is a concrete that is made of hydraulic cement, aggregates and discontinuous discrete fibers. The fibers are usually produced from steel, glass and organic polymers (synthetic fibers) (ACI 544.1R_96, 1977). Steel-fiber reinforced concrete is the most common form of FRC and has been used in flat slabs, pavement(s) and tunnel lining (Bentur et al., 2007). The addition of steel fibers to concrete significantly improves the tensile properties of concrete. The ACI committee of fiber reinforced concrete (ACI 544.4R_88, 1988) reported that the flexural strength of fiber reinforced concrete is 50% to 70% higher than that of unreinforced concrete and that the compressive strength of concrete is up to 15% higher compared to plain concrete. Eren et al. (1999) found that the addition of steel fiber increased compressive strength and splitting tensile strength by 28% and 129%, respectively, compared to plain concrete.

However, at construction sites, the rate of strength development is as important as the 28-day compressive strength of concrete. Especially, an early-age strength development becomes very crucial in the safe and economical application of some critical processes such as stripping of forms, post-tensioning etc. during the construction. If the forms are removed before the concrete elements gain sufficient strength, there is a high possibility that some cracks would develop in the structure (Eren, 2009).

This undesired situation, eventually, leads to loss of strength in the structure. Consequently, some parts or whole of the structure may collapse which will, in the end, cause a hazard to both human life, the environment, and materials. On the other hand, if the forms are stripped too late so those concrete elements gained a strength value above what is sufficient, then the construction will not be completed within the desired budget and time limits. In today's rapidly changing and improving business environments, being fast and economical are mandatory to catch up with the rapidly growing world. In order to finish a construction utility safely and economically; engineers should develop reliable methods to predict the strength gain of concrete at the construction site. In-place strength development of concrete can be estimated by the following methods:

1. Testing the standard specimens prepared from the same concrete batch and cured at the site conditions: This method does not reflect the actual element size and geometry or the effectiveness of placing and compacting.
2. Testing the actual structure members by nondestructive test methods: Nondestructive test methods may not give accurate results since these methods predict the compressive strength of concrete indirectly from

some characteristics such as surface hardness, density etc. Especially at early ages, the accuracy and the reliability of these methods decrease.

3. Estimating the compressive strength of concrete from its temperature history known as "maturity method": By using maturity method, mathematical formulas for predicting the strength development of concrete can be derived in order to estimate the concrete's strength at any age.

In 1978, there was a terrifying construction failure in Willow Island and this resulted in the death of 51 workers. The ensuing investigations to find out the reasons for the failure discovered that the insufficient strength gain of concrete to support the construction loads was the most likely reason for the failure (Carino N.J. and Lew, H.S., 2001).

The concrete which the scaffolding was carrying was anchored only at the first day and the temperature was less than 10°C during the very first day. After this accident, National Bureau of Standards (NBS) started to work on the in-place strength prediction from the temperature history of concrete. As a result of these researches, in 1987 ASTM published a standard titled "Standard Practice for Estimating Concrete Strength by Maturity Method, ASTM CI074" (ASTM C1074, 2004).

1.2 Problem Statement

Many research studies have focused on prediction of the compressive strength of concrete using the maturity method during the last decade. This study tries to solve the problems as follow:

1. There is no any valid literature for evaluating steel fiber reinforced concrete by maturity method.

2. The number of the maturity researches which evaluate the compressive strength and give other information about other mechanical properties of concrete by maturity method are very limited and there has been no research found for evaluating the flexural toughness by maturity method.
3. Apparent activation energy has been obtained according to ASTM (1074) by Linear Hyperbolic function. The information about the evaluation of activation energy by parabolic hyperbolic and exponential function is very limited.
4. In order to predict the strength of concrete by Nurse-Saul maturity function, most of the researchers used the logarithmic equation; the information gathered about using other strength-maturity equations are very limited.

1.3 Goals

The main objective of this research is to provide new equation(s) for predicting some mechanical properties of steel fiber reinforced concrete using the maturity method under isothermal curing conditions and to determine the activation energy for fiber reinforced concrete by the four different methods. In this research, mechanical properties of fiber reinforced concrete at different curing conditions were evaluated and then predicted by several maturity equations.

1.4 Aim of the Research

The concept of maturity has been applied to increase the temperature from hydration of pozzolanic reactions of cement and other binders, fiber cannot react with cementitious components and however, the steel fiber can slightly increase the hydration temperature due to heat transfer by the steel components. Rather, the fiber changes some mechanical properties of concrete, such as compressive strength,

flexural strength, flexural toughness and splitting tensile strength. Therefore, predicting the strength of fiber reinforced concrete requires a different approach compared with normal concrete. Unfortunately, no information has been found or archived regarding the prediction of the strength and apparent activation energy of steel-fiber reinforced concrete using the maturity method.

The main purpose of this research is to devise mathematical formulas to estimate the compressive strength, flexural strength, flexural toughness and splitting tensile strength of fiber reinforced concrete from the combined effects of time and temperature, which is known as "*maturity method*", on five different volume fractions of fiber. The followings were the main investigation points of this research:

1. To provide a concise literature survey about maturity methods for estimating some of the mechanical properties of steel fiber reinforced concrete.
2. To evaluate the different maturity models for steel fiber reinforced concrete and to find the validity of these models.
3. Determination of the activation energy for steel fiber reinforced concrete by different methods.
4. To study the effects of different curing temperature (8°C, 22°C, and 32°C) on compressive strength, flexural strength, flexural toughness and splitting tensile strength of five different volume fractions of fibers (0%, 0.5%, 1%, 1.5% and 2%) at various ages (1, 3, 7, 10, 14, 28 and 56) days were evaluated.

1.4 Methodology

1. Determining the maturity relation for some mechanical properties of normal and steel fiber reinforced concrete by two methods (Nurse-Saul and Arrhenius).
2. Determining the apparent activation energy for steel fiber reinforced concrete.
3. Determining the apparent activation energy by alternative methods.
4. Predicting the strength gain of normal and fiber reinforced concrete with different maturity models.
5. Analyzing the maturity models and finding the best models for each mechanical properties of steel fiber reinforced concrete.
6. Evaluating the effects of curing temperature on different proportion of steel fiber reinforced concrete.
7. Evaluating the effects of steel fiber on the temperature history of concrete.

Chapter 2

LITERETURE REVIEW

2.1 Maturity Concept

Time and temperature are two factors that mainly influenced on the degree of cement hydration. As a result, the two factors are also affected on the strength development of concrete (Mindess and Young., 1981). The combination of effects of time and temperature on concrete is possible to be evaluated by maturity concept. Maturity is defined as a function of time and temperature.

Maturity function was defined by Saul for the first time as the integral of concrete temperature beyond a datum temperature over the age of concrete (Saul, 1951). This idea can be schematically expressed by Figure 1.

According to Figure 1, the maturity at age t* is the area under the time-temperature curve. After the first maturity function proposed by Saul (Saul, 1951), another function was defined by taking into account the rate of reaction depending upon the Arrhenius law (Freisleben and Pedersen, 1977). This function is more complex but it shows the behaviour of concrete according to temperature better than the previous function (Carino and Lew, 2001).

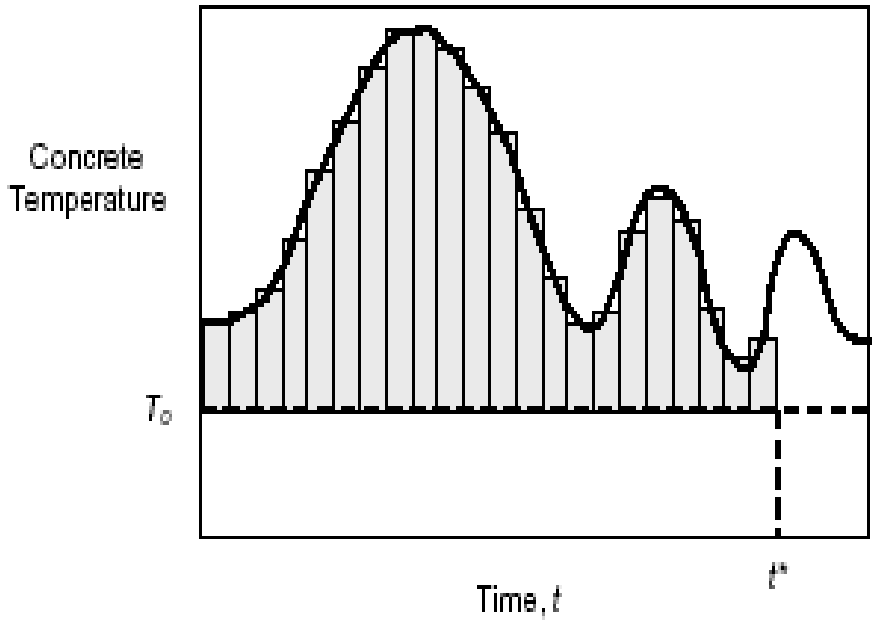

Figure 1: The concept of maturity according to Saul

2.2 Maturity Method

Maturity method is on approach to estimating the strength of concrete by combination of time and temperature. Maturity method relies on measuring the temperature histories of concrete to calculate the maturity index and then predicted the strength development of concrete by this index (Galobardes, 2015).

According to maturity method, the concretes made up of the same mix compositions have approximately the same strength when they are at the same maturity level (Saul, 1951). Depending on this assumption, if the maturity of a special concrete mix is calculated, the strength of concrete at any age can be predicted.

2.3 Maturity Functions

The maturity concept was first brought to the academic literature during the researches about the accelerated curing methods of concrete due to the need for taking the effects of time and temperature on the development of concrete strength

into account. The maturity method can be said to have originated from the papers written on the issue of steam curing which were published in late 1940s and early 1950s (Nurse, 1949; Saul, 1951; McIntosh, 1959).

The maturity concept was first brought to the academic literature during the researches about the accelerated curing methods of concrete due to the need for taking the effects of time and temperature on the development of concrete strength into account. The maturity method can be said to have originated from the papers written on the issue of steam curing which were published in late 1940s and early 1950s (Nurse, 1949 ; Saul, 1951; McIntosh, 1959).

Several functions have been proposed to define the relationships between time and temperature on concrete strength by several researchers. The first function, which is still widely used due to its simplicity, is known as Nurse-Saul maturity function (Nurse, 1949; Saul, 1951). According to Saul, the product of time and temperature could be used to estimate the strength of concrete. This idea was modelled with the following formula:

$$M = \sum_{0}^{t} (T - T_0)\Delta t \qquad (1)$$

Where M represents the Maturity (°C-days), T is the Average temperature during the time interval (°C), T_o is the datum temperature (°C), t is the elapsed time (in days), and Δt is the time interval (in days).

Datum temperature can be defined as the temperature below which concrete is assumed not to be able to gain strength. The most widely used datum temperature having the value of -10°C was suggested by Bergstrom (Bergstrom, S.G., 1953).

However, this value of datum temperature should not be generalized since it may change as the compositions and the type of ingredients of concrete change. In ASTM C 1074, a procedure for determining the datum temperature experimentally is given (ASTM C 1074).

Nurse-Saul maturity function has linear relationship between the initial rate of strength gain and the temperature. However, when curing temperatures vary over a wide range, this linear relation might not be valid. Bergstrom concluded that the Nurse-Saul maturity function could be applied to the concretes cured at normal temperatures (Bergstrom, 1953).

Nurse-Saul method has some deficiencies, this method at low temperature and early age, estimates the strength of concrete very low and also, at later age when concrete subjected to high temperature, the strength predicted by this function is very high (McIntosh, 1956).

Alexander and Taplin (1962) studied the effects of Nurse-Saul maturity function on concrete and cement pastes at three different curing temperatures (5°C, 21°C and 42°C). They found that the effects of temperature on strength gain of concrete by Nurse-Saul maturity function is underestimated at early ages and overestimated at later ages.

To overcome the deficiencies of Nurse-Saul maturity function, a new function based upon the Arrhenius law was proposed in 1977 (Freislebenand Pedersen, 1977). This new function was more complex than that of Nurse-Saul and is known as the Arrhenius function, given as:

$$M = \int_0^t \mathrm{A}e^{-(\frac{E}{\mathrm{RT}})}\, dt \qquad (2)$$

Where,M is the maturity, A is constant, E is the apparent activation energy, (J/mol), R is the gas constant, (8.314 J/mol °K) and T is the temperature (°K).

Using Equation (2) and Rastrup's equivalent age concept (1954) as a basis, the following equation for equivalent age was proposed (Freisleben and Pedersen, 1977):

$$t_e = \sum_0^t e^{-\frac{E}{R}\left(\frac{1}{T}-\frac{1}{T_r}\right)}\Delta t \qquad (3)$$

Where, t_e is the equivalent age at the reference temperature, Tr is the reference temperature (in °K), T is the average temperature of the concrete during the time interval Δt (in °K), E is the apparent activation energy, (in J/mol), and R is the gas constant, (8.314 J/mol-°K).

Equivalent age is the curing age at a constant standard temperature (T_r) that results in the same maturity and the same strength as cured under the actual temperature history (Carino and Lew, 2001). The reference temperature is usually taken as 23°C in North America, while it is taken as 20 °C in Europe (Carino and Lew, 2001).

The maturity function based on the Arrhenius equation reflects the behaviour of concrete better than the Nurse-Saul equation (Carino and Lew, 2001). However, this method also has some shortcomings. It is obvious that the value of the apparent activation energy used in the Arrhenius function or the equivalent age calculation is very important in the application of the procedure. The accuracy of the results of this method depends on the reliability of the activation energy value. If not defined properly, the reliability of Arrhenius function gets weaker.

As Kjellsen and Detwiller state early-age strength could be accurately estimated by the maturity method of apparent activation energy. However, at higher values of maturity i.e. the maturity above the value corresponding to the 50% of the normal 28-day strength, this method did not give accurate result (Kjellsenand Detwiller, 1993).

Finally, as a result of his researches; Jonasson (1985) concluded that the Arrhenius maturity function properly determined the effect of temperature on the strength up to the half of the 28-day strength of concrete. However, this method at higher strength and higher temperatures are overestimated the effects of temperatures. The apparent activation energy is a key of this method and has to be determined accurately. The researches about the determination of activation energy are still carried on in order to improve the reliability of this method.

2.4 Strength and Maturity Relations

After the maturity function is defined, in order to predict the strength of concrete the strength-maturity relations should be determined.

Bernhardt (1956) assumed that the strength gain rate of concrete at any age is a function of temperature and the current strength. He proposed this idea with the following mathematical expression:

$$dS / dt = f(S)\, k(T) \qquad (4)$$

Where; S: compressive strength, f (S): strength function and k (T): temperatures function.

After integrating and rearranging the Equation (4), the following equation is

obtained:

$$\int dS / f(S) = \int k(T)dt \quad (5)$$

The right-hand side of the Equation (5) is maturity (obtain from time and temperature). This is the main point of strength prediction of concrete by maturity method.

In 1956 Plowman (1956) suggested a logarithmic relation between maturity and the strength. This relationship is modelled with the following formula:

$$S = a + b \log (M) \quad (6)$$

Where S is the compressive strength, M is the maturity index and, a and b are the regression coefficients.

Although Equation (6) is a popular equation due to its simplicity, this function does not predict the strength of concrete correctly at low and high values of maturity (Carino et al, 1983). Plowman's function estimates an unlimited strength with the increasing maturity.

Approximately after two decades, another relationship was constructed between strength and maturity. The relation was demonstrated with a function shown below (Kee, 1971):

$$S = \frac{M}{\frac{1}{A} - \frac{M}{S_u}} \quad (7)$$

Where, S: Strength, M: Maturity, Su: Limiting strength and A: Initial slope of the strength-maturity curve.

Carino and Lew modified the Equation (7), depending on strength-maturity curves as given in Figure 2.2. (Carino and Lew, 1983):

$$S = \frac{\left(M - M_0\right)}{\frac{1}{A} - \left(\frac{M - M_0}{S_u}\right)} \tag{8}$$

Where; M_0: Offset maturity, S, M, A and S_u: Same as stated in Equation (7).

Figure 2 shows the likely shape of the strength–maturity relationship of a concrete or mortar at a given temperature. There are four regions on the curve:

1) Plastic stage: In this stage, the concrete cannot be able to carry load

2) Setting stage: In this stage, concrete transforms from plastic stage to rigid stage

3) Rapid strength gain stage

4) Decreasing strength development rate.

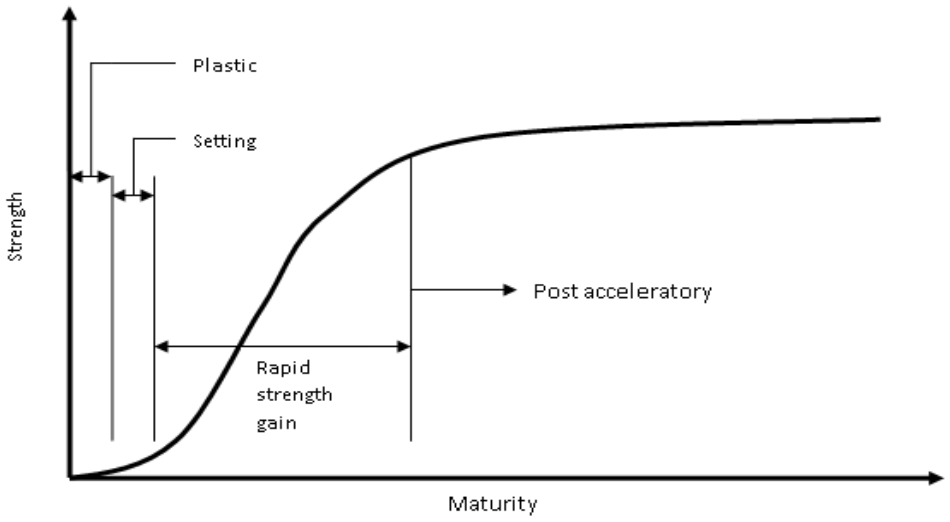

Figure 2: Shape of the strength-maturity relationship.

Finally in 1984 Carino modified the Equation (8) based on, three-parameter hyperbolic function depending on rate constants as follows (Carino, 1984):

$$S = S_u \frac{k_T(t-t_0)}{1+k_T(t-t_0)} \quad (9)$$

Where, S is the Strength, S_u is the Ultimate strength, k_T is the Rate constant at age t, $t_0$is the Age at the start of strength development. The value of S_u, k_T and t_0 were obtained by regression analysis.

Knudsen (1982) performed a parabolic hyperbolic equation as follows:

$$S = S_u \frac{\sqrt{k_T(t-t_0)}}{1+\sqrt{k_T(t-t_0)}} \quad (10)$$

Knudsen (1982) worked on degree of cement hydration rather than concrete strength. He considered reaction of cement grains and particle size distribution of the cement grains. The keys assumptions of Knudsen theory are as follow:

- All cement particles are similar and need to classified according to their size
- The cement particles react independently.
- The particle size distribution and kinetics reaction of each particle describe by an exponential equation.

Knudsen called his results as “dispersion model” because in overall hydration behaviour the cement grains play a dominant role. He demonstrated that parabolic hyperbolic equation is valid for strength development and any other properties that related for cement hydration. He showed the rate constant (k_T) is dependent to particle size distribution of cement grains.

According to Knudsen (1982) assumption the reaction between cement particles is independently significant. When the water cement ratio is lower the distance between cement particles is decreased therefore, the interference of cement particle increased and cause to decrease the rate of hydration. Also, Knudsen noted his assumption is violated at very low water cement ratio. However, Copeland and Kantro (1964) found the effects of interference of cement particles on hydration at early ages with low water cement ratio are not significant. Finally Knudsen concludes that during early age of hydration the rate constant should be independent of the water cement ratio.

Equation (9) is based on linear kinetics; it means that the degree of hydration on cement particles is a linear function due to time and rate constant. Equation (10) is based on parabolic kinetics; it means that the degree of hydration as function of square root due to time and rate constant.

Freisleben and Pedersen (1985) proposed an exponential model for the strength development of concrete under isothermal curing conditions:

$$S = S_u e^{-(\frac{\tau}{t})^{\alpha}} \tag{11}$$

Where, t is the age, $\boldsymbol{\tau}$ is the time constant and α is the shape parameters.

This model is suggested the strength maturity-relations should be similar to relations between maturity and heat of hydration. (Malhotra and Cariono, 2004). In this model, the strength increases gradually during the setting period of concrete, and it is asymptotic to the limiting strength (Carino and Lew, 2001). Figure 3 shows three

curves that obtain from Equation (11) with different values of time constant. Curve 1 and curve 2 have the same value of shape parameters (a = 0.4) but curve 2 has a higher time constant value. Curve 3 has a same value of time constant with curve 1 but has a higher value of shape parameter compare to curve 1 and curve 2. Figure 2.3 shows the significance of time constant for instance when the maturity is equal to time constant the strength (S_∞/e) is equal to 0.37 S_∞. The shape parameter is affected on the shape of the curve. As shape parameter increase the curve has been more pronounced to the S shape (as shown in curve 3).

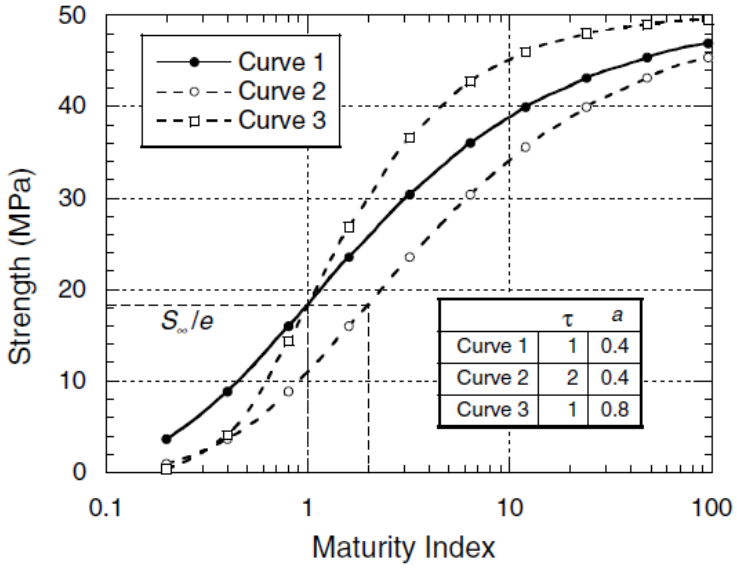

Figure 3: Effects of time constant (**τ**) and shape parameter (α) on the strength maturity relation.

2.5. Apparent Activation Energy

Activation energy is the energy that is needed for a chemical reaction to start. In the case of the concrete, it is the required starting energy of hydration reactions between the cement and the water. As the hydration of cement and water contains several simultaneous and complex chemical reactions, the term "apparent activation energy"

is used for cement hydration. The most challenging part of calculating the equivalent age is the determination of the apparent activation energy, because the value of the apparent activation energy may change from one concrete mix to another. The important factors that affect the apparent activation energy can be summarized as follow (Maage and Helland, 1988):

- Cement composition
- Fineness of cement
- Water/Cement ratio
- Admixtures (if exist)

Although Carino (1984) found that the w/c ratio does not influence the value of the apparent activation energy except for very low ratios, in a more comprehensive study Carino and Tank (1992) concluded that w/c ratio affected the apparent activation energy.

The apparent activation energy can be determined by several ways (Carino, 1984):

1. Curing concrete specimens at several different temperatures and using regression analysis: this procedure is explained in ASTM C1074 (ASTM C 1074, 2004).
2. Using hydration studies of cement pastes: some researchers have done for determining the apparent activation from hydration of cements (Gauthier et al, 1982; Oluokun et al, 1990; Kada-Benamur et al, 2000).
3. Testing mortar specimens instead of concrete specimens: it has been proved that the activation energy values obtained from strength tests of mortar specimens and concrete specimens are similar (Carino et al, 1992; Gauthier et al, 1982; Tank et al, 1991).

Kada-Benameur (2000) determined the apparent activation energy according to degree of hydration of cement particles by using calorimetric technique under isothermal curing conditions. Activation energy was determined at three temperature range (10–20 °C, 20–30 °C, and 30–40 °C). They reported for degree of hydration between ranges of 5-50%, the apparent activation remains constant.

Tank and Carino (1992) used both mortars and concrete to determining the activation energy. The ratio of cement/sand for mortar is equal to cement/coarse aggregate ratio for concretes. They used two w/c ratios (0.55 and 0.6) and three curing temperatures (10°C, 23°C, and 50°C) for both mortars and concretes. In this study, the activation energy of concretes and mortars with same w/c ratios are approximately same.

Many researchers suggested the value of activation energy at certain conditions;Gauthier and Regourd (1982) reported the range of apparent activation energy for ordinary Portland cement between 52-57 kJ/mol. However, the value of apparent activation energy increased 56 kJ/mol when cement blended with 70% blast furnace slag. Chengju (1956) found the range of apparent activation energy should be taken between 30-50 kJ/mol. Carino and Tank (1992) reported the range of activation energy as between 33 kJ/mol to 64kJ/mol. Turcry (2002) reported range of the activation energy for ordinary Portland cement between 29-39 kJ/mol. Han (Han and Han, 2010) obtained the range of apparent activation energy between 20-40 kJ/mol. Lachemi (2007) founded the range of the apparent activation energy are between 18-24 kJ/mol. Clarke (2009) found the values of activation energy are between 40-80 kJ/mol.

However, ASTM C1074 recommended determining the apparent activation energy

experimentally. According to ASTM C1074, the apparent activation energy can be obtained by compressive strength of mortars at three different curing temperatures (maximum, average and minimum) and specified ages. For preparing mortar the concrete should be sieved according to ASTM C403 to separate the coarse aggregates from the mixture.

2.6 Rate Constant Functions

Rate constant is the initial slope of the relative strength versus age curve under isothermal curing condition for strength development of a particular concrete mix (Tank and Carino, 1991). Rate constant function may be used to describe the combined effects of time and temperature on concrete for strength development of concrete. (Tank and Carino, 1991). Rate constant is obtained by regression analysis the strength versus age curve. (Carino and Lew, 2001).

In order, to find the relationship between rate constant and temperature, Carino and Tank (Tank and Carino, 1991) test the three different equations (Linear, hyperbolic and exponential) at curing temperatures of 10 °C, 23 °C and 40°C. As results they found the linear equation cannot provide accurate results. However, hyperbolic and exponential provide the good correlation between rate constant and temperature.

2.5.1 Rate Constant Calculation

According to the literature (Carino and Lew; 2001): there are three methods available for determining activation energy of calculating rate constant: linear hyperbolic, parabolic hyperbolic and exponential. These methods are explain as follows:

2.5.1.1 Linear Hyperbolic Method

It is one of most common method that has been recommended by ASTM C1074.The rate constant can be calculated by regression analysis of the compressive strength of mortars by Equation (9) which obtained by Carino and it is described at section 2.4. Linear hyperbolic is a very popular method for determining the activation energy and also, this method has been recommended by ASTM C1074 standard. Carino (1984) used the mortar strength to determine the activation energy, he found the value of activation energy as between 42.7- 44.6 (kJ/mol). Barnett et al. (2005) determined the activation energy for the concrete with different levels of ground granulated blast-furnace slag (ggbs). They found apparent activation energy for that obtained for normal Portland cement was 34 (kJ/mol), however, the apparent activation energy is approximately increased linearly by increasing the level of ggbs. For mortal with level of 70% ggbs, the apparent activation energy was 60 kJ/mol. (Brooks et al., 2007) found apparent activation for ordinary Portland cement (type I) is 45 kJ/mol, for mortar that containing class C fly ash the apparent activation energy was 35.5 kJ/mol, for class F fly ash the value of apparent activation energy was 36.3 kJ/mol and for GGBF slag was 36.2 kJ/mol.

2.5.1.2 Parabolic Hyperbolic Method

This method has been used Equation (10) which assumed by Knudsen to calculate the rate constant. However, except Knudsen (1983) study, there is no any literature that has been attempt for determining apparent activation energy with this method.

2.5.1.3 Exponential Method

That method was suggested by Hansen and Pedersen (1985), Equation (11) is used to calculate the rate constant. Number of researchers used exponential equation for determining the apparent activation energy. Brooks found the value of apparent

activation energy for ordinary Portland cement is 40.7 kJ/mol, when used class C fly ash in the mortar the value of apparent activation energy was 44 kJ/mol, when use class F fly ash the value of activation energy was 45 kJ/mol and when use ggbs the value of apparent activation energy was 41 kJ/mol.

2.6 Previous Literatures

During the last decade many researches were done for estimating strength of concrete by maturity method. Zhang et al. (2008) applied the maturity method for predict some mechanical properties of high performance concrete over time. In this study maturity method was applied for compressive strength, splitting tensile strength, modulus of elasticity and degree of heat of hydration. They used 7 different mixes at curing temperatures of 10 °C, 20 °C and 40 °C. In this research the main findings about activation energy are:

1) Different properties of concrete may have different activation energy for given concrete.
2) Different concrete may have different activation energy for given properties.
3) Different development stage of properties may have different activation energy.

Han and Han (2010) estimated setting time of concrete which subjected to various dosages super retarding admixture (SRA) by maturity method. They used 0%, 0.15%, 0.3%, 0.45% and 0.6% SRA (by weight of cement) at three different curing temperatures (5 °C, 20 °C and 35 °C). In this study the initial and final setting time of concrete which containing various dosage of SRA were measured. They found in this research that by increasing dosage of SRA and decreasing the curing temperature, initial and final setting time was considerably delayed. The ranges of the apparent activation energy were 20-40 kJ/mol, which lower than conventional

concretes. All predicted models that obtained by initial and final setting time of all mixtures by maturity method had a good correlation with experimental results.

Soutsos et al. (2013) prepared a series of laboratory tests for lightweight self-compacting concrete that incorporated high volumes of pulverise fuel ash (PFA), ground granulated blast furnace slag (GGBS) and limestone powder (LSP). They manufactured 100 mm concrete cubes and cured under isothermal conditions (20 °C, 30 °C, 40 °C and 50 °C) and also adiabatic conditions. The compressive strength results at isothermal curing were used for determining apparent activation energies. The range of the apparent activation energies was between 20- 42 (kJ/mol). The results show that, activation energies of lightweight concrete are similar to normal aggregate concrete. The datum temperature that was obtained in this study is not reliable, so, they used value of -11 °C as datum temperature. Maturity relations by equivalent age method were establishing to predict compressive strength under isothermal and adiabatic curing conditions. They used linear hyperbolic equation to predict compressive strength of all samples. The results show that temperature histories of mixtures that recorded from adiabatic curing are higher than normal in-situ constructions and temperature raise in adiabatic curing much earlier than in-situ concrete cast. The temperature histories of concrete with 100% (PC) of normal aggregate have 10 °C different with lightweight aggregate one.

Boubekeur et al. (2014) prepared two sets of mortars with additions of several minerals (10% limestone powder, 20% natural pozzolan and 30% blast furnace slag). First set was cured in steam room with constant temperature (20 °C, 30 °C, 40 °C and 50 °C) and second set was cured under variable temperatures. Compressive strength test was done at ages of 1, 3, 7, 28 and 90 days. At early age, the

compressive strength was increased linearly by increasing temperature at all mixes. The mixture which included limestone powder has higher compressive strength compare to other mixes (ordinary Portland cement, natural pozzoalana and blast furnace slag) all ages. At later ages due to activation of pozzolanicity of natural pozzolana and hydraulicity of blast furnace slag the compressive strength increased compare to the mortar that included ordinary Portland cement. Maturity method had been used to predict compressive strength of all mixes. Both equivalent age method and Nurse-Saul method had been used in this study. They founded a critical value of maturity method as 350 °C day, beyond this value the relations between strength and maturity are not linear and cannot be explained by the model. Logarithmic equation can be used to predict strength by maturity method at later ages. If cement type and early age strength are known, the later age strength (lower than M = 350 days) can be easily determined by strength-maturity relations.

Ferreira et al. (2015) applied maturity method to alkali-activated binders. This study was evaluated for four different alkali activated mortars and four different alkali activated concrete. The influence of OPC was also evaluated in this study, compressive strength were analysed for all mixes at ages of 8,18, 28 and 42 days at curing temperatures of 50 °C, 70 °C and 90 °C. Furthermore, maturity method was applied for preparing precast alkali-activated pacade panels. They evaluated both equivalent age and Nurse-Saul maturity method for all mixes. They found in this study that the range of datum temperature was 44 °C to 55 °C. The experimental values have good approximation with both Nurse-Saul and Arrhenius maturity methods when, datum temperature is lower than 50 °C. The errors obtained from predicted strength at early ages and long-term ages were lower than 20% and 10% respectively.

Nokken (2015) used the electrical conductivity to determine maturity relations and activation energy of concrete. He measured electrical conductivity of ten different mixes at three different temperatures (7 °C, 23 °C and 39 °C) for a period of 28 days. In addition, in this study apparent activation energy was determined by four methods of calculating rate constant. Nokken found that the electrical conductivity with time decreased for all mixtures when regardless of exposure temperature due to pore structure development. Activation energies were determined by four methods: direct method, linear hyperbolic method, parabolic hyperbolic method and exponential method. For direct method they adjusted conductivity at 28 days and plotted versus the inverse of the absolute temperature. However, one of the disadvantages of direct method, is measuring the property at a specific point in time and lead to prepare incomplete information about test. For the other three methods the electrical conductivity was measured at each 3 hours from 1 day up to 7 days. The activation energy that has been found in the study by linear hyperbolic method was generally higher than the reported results by previous literatures because in previous literatures the effects of pore solution were not take an account. The results that have been obtained by exponential method were much less than the available results in previous studies.

Yikici and Chen (2015) applied the maturity method to estimate in-place strength of very large cube concrete block (1.8 m) with four different mix- design. Cylinder specimens with dimensions of 150×300 mm were used for strength test at laboratory. The activation energy of four different mix design for using equivalent age method is also determined in laboratory. In addition, core samples from concrete block were tested at ages of 4, 28 and 56 days and compare with the predicted strength results that obtained by maturity method. The strength maturity relations of all mixes were

obtained by linear hyperbolic equation. The results show that temperature histories at the centre of the cube are significantly higher than top and bottom surface of the cube. Core strength that obtains from top surface of the block is significantly lower than bottom surface of the cube. As comparing the results of in-place strength and core strength, at the top surface of the cube the predicted in-place strength is higher than core strength. However, the core strength at mid-section and bottom surface of cube was 15% higher than predicted in-place strength.

2.7 Application of Maturity Method

The maturity method has a many applications in concrete constructions. Maturity has been used to estimate in-place strength of concrete to early removal of form works and assure the safety of structures. In addition, the maturity method is a tool for planning the time schedule for construction activities (Carino and Lew, 2001). Furthermore, the maturity method has been used to estimate early-age strength of post-tensioning concrete to early removal of tendons without any damage to the post-tensioning anchorage zone concrete (Sofi et al, 2012 and Nixon et al. 2008).

Maturity method can be used to terminate the cold weather protection of concrete. In cold weather the structure cure is slower or cure is faster if heat of hydration of concrete rise up in the forms. Without maturity method samples should be tested periodically to control the strength of concrete. Also, maturity can be save structure from freeze damage. (Galcier, 2008).

Maturity method can be used for early open road ways and cause to reduce traffics. Using maturity method in pavement started from the late of 1980s and early of 1990s. At these times the Strategic Highway Research Program (SHRP) published

some reports that applied maturity method for constructing pavement (Roy et al. 1993 and Bickley, 1993). However, in recent years there are many transportation institutes in United States applied maturity method in pavement (Ahmad et al., 2006, Wade et al. 2008, Hosten et al. 2011 and Henault, 2012). In 2007 the West Virginia Division of Highways (WVDOH) reported in the United State of America, twenty-five out of thirty-six states applied maturity method for estimating early age compressive strength for early remove of formwork or open the pavement to traffic (Yikici and Chen, 2015).

Maturity method has been useful for laboratory work with different specimen sizes. A good example is maturity method can establish a good correlation between in-place test method and cylinder strength (Carino and Lew, 2001).

Carino and Lew (Carino and Lew, 2001) applied the maturity for high strength concrete. They used two w/c ratios (0.26 and 0.32). The results of maturity method can be applied for high strength concrete. After Carino some other researchers applied maturity method for high strength concrete (Myers, 2000 and Pinto and Hover, 1996). They concluded that maturity method can be applicable for using in high strength concrete, However, using maturity method in high strength concrete have some limitations (Carino and Lew, 2001).

Waller et al. (Waller et al., 2004) had been successfully used method to control cracking of concrete at early ages. This technique can be applied to predict successfully the compressive strength, modulus of elasticity, tensile strength and thermal coefficient that needed to control risk of cracking with some numerical tools such as finite element programs.

Chapter 3

EXPERIMENTAL PROGRAMS

3.1 Materials

3.1.1 Cement

Blast-furnace slag cement CEM II/B-M (S-L) 32.5 R was used for this study. The initial and final setting of the cement was 225 and 345 minutes, respectively.

3.1.2 Fiber

Hooked-end steel fibers of 60 mm in length and aspect ratio (l/d: length-diameter ratio) of 65 were used.

3.1.3 Aggregates

Limestone crushed rock aggregate obtained from a crushing plant located at Beşparmak mountains was used. Two different particle sizes of crushed stones were used as aggregates for preparing the concrete mixtures. Proper combinations of two different sizes of aggregate groups were used while designing the concrete mixes. These aggregate groups had the maximum particle sizes of (5 mm) and (10 mm), for the fine and coarse aggregates respectively.

Relative density on saturated and surface dry basis and on dry basis, apparent specific gravity and water absorption capacity of each aggregate group was determined before designing the mix proportions of concretes.

Some of the physical and mechanical properties of the aggregates used in this investigation are as given in Table 1. Aggregates are combined in proper percentages according to the results of sieve analysis tests. While proportioning the aggregates, the particle size distribution was kept within the standard limits of British Standards Institution. The gradation of combined aggregates is as given in Figure 4.

Table 1: Physical and mechanical properties of limestone crushed aggregates.

Property of Aggregate	**Fine (05 mm)**	**Coarse (10 mm)**
Relative Density (SSD)	2.68	2.68
Relative Density (Dry)	2.62	2.65
Absorption (% of dry mass)	1.20	1.01
Apparent Specific gravity	2.80	2.73

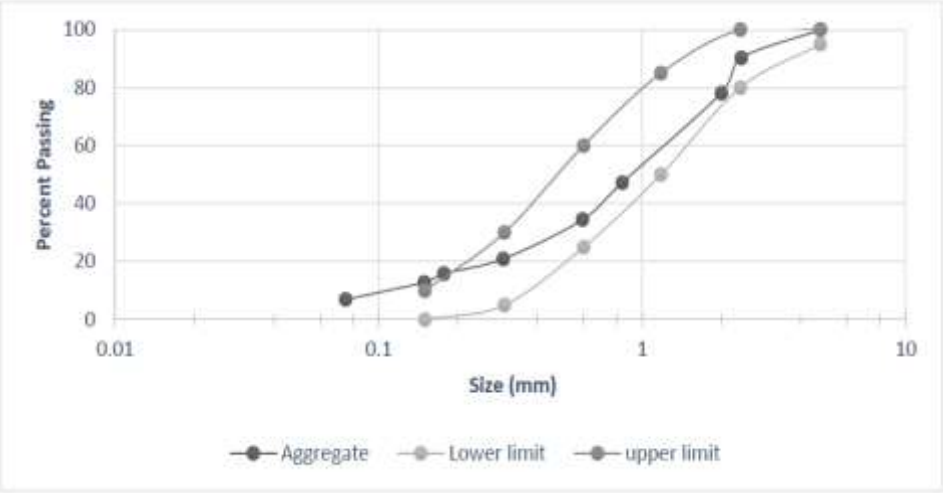

Figure 4: Sieve analyses & grading of combined aggregates.

3.1.4 Water

Tap water (drinking) available in the Materials of Construction Laboratory was used as mixing water for the preparation f concrete mixtures.

3.1.5 Admixture

To achieve the desired workability, a polycarboxylic ether based superplasticizer (Glenium 27) was employed. The dosage of superplasticizer used was 0.7% by weight of cement.

3.2Testing Plan

The procedure for determining the strength of concrete by maturity method is described in Figure 5. In order to achieve this goal, the first step is the preparation of samples, the mix design proportion and the mixing procedures are explainedin section 3.2.1. The second step is to embed the sensors into the concrete and record their temperature histories. The third step is to determine the activation energies and datum temperatures, thefourth step is testing the hardened concrete while the fifth step is calculating the equivalent age and maturity index and the last step involves the prediction of the strength of concrete by regression analysis.

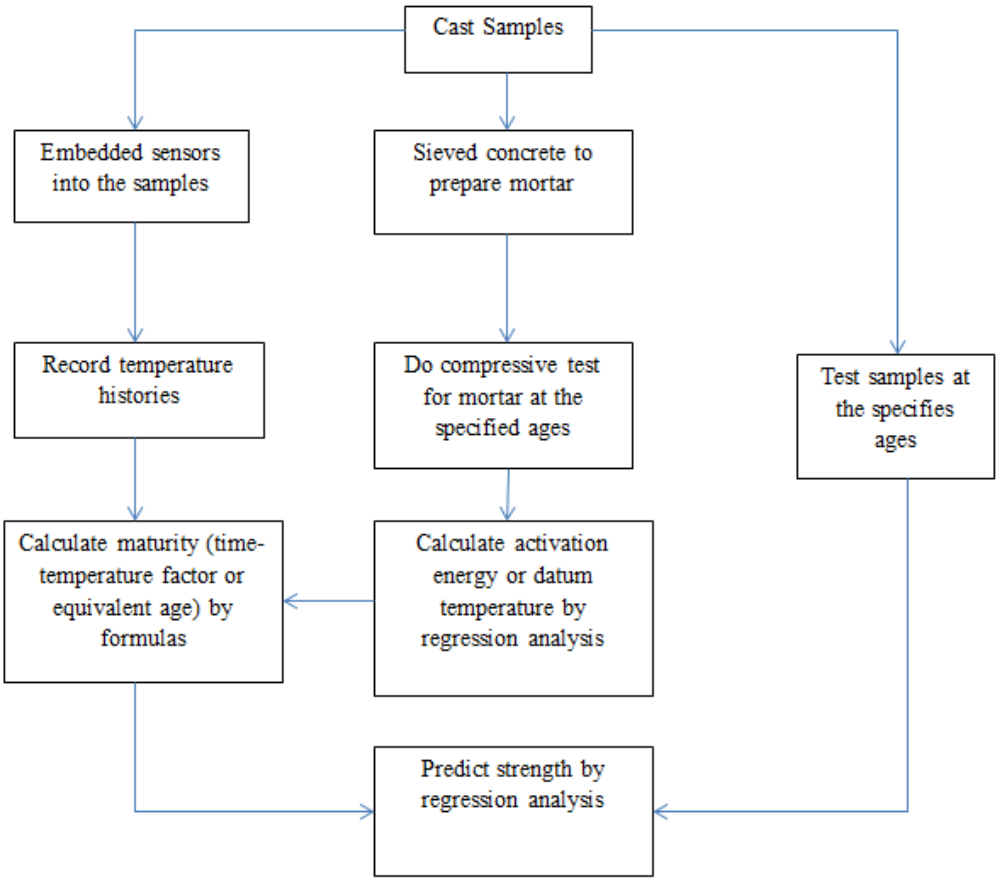

Figure 5: Maturity procedure.

3.2.1 Mix Design Proportions

Mix design proportioning was performed by using weight-batching method. Five different mixes were performed for this study, namely, SP0, SP1, SP2, SP3 and SP4. The proportions of each of the mixes are presented in Table 2.

Table 2: Mix Proportions.

Series	Fiber Dosage kg/m^3	w/c	Cement kg/m^3	Water kg/m^3	Fine kg/m^3	Coarse kg/m^3	SP kg/m^3	Vebe Time sec
SP0	0	0.43	581	250	670	810	4.07	1.03
SP1	39.25	0.43	581	250	670	810	4.07	1.24
SP2	78.5	0.43	581	250	670	810	4.07	1.67
SP3	117.75	0.43	581	250	670	810	4.07	1.98

3.2.2 Mixing Procedure

After weighing the materials according to the mix design, they were placed into a laboratory pan mixer with a capacity of 0.018 m^3. The mixing procedure was started by dry mixing the fine and coarse aggregates with fibers for 3 minutes to avoid fiber balling during mixing. Next, cement was added to the mixture and then mixed for 2 minutes. Furthermore, water blended with superplasticizer was added to the mixture. The mixing time for all mixtures was 3 minutes.

3.2.3 Properties of Fresh Concrete

3.2.3.1 Vebe Test

The workability of fresh concrete of each mix was measured by Vebe test according to BS 1881, Part 104. Generally, the workability of concrete decreased with increasing volume fractions of fibers (Lomond and James, 2006). Table 3.2 shows the results of Vebe test for 0%, 0.5 %, 1%, 1.5% and 2% volume fractions of fibers. The results show that when volume fractions of fibers increased the Vebe time was increased. The highest Vebe time result is 1.98 seconds is obtain for concrete with 2% volume fractions of fibers, it is increased 48% compare to plain concrete.

3.2.3.2 Compaction Method

Vibrating table was used with frequency of 3000 rpm for compaction of fresh mixes. The compaction time for all concrete mixes was 1 minute.

3.2.3.3 Curing Regimes

Three different curing temperatures (8°C, 22°C and 32°C) were performed for this study. Specimens were kept in the mould after casting for one day in the moist curing room. After 24 hours, specimens were removed from the moulds and kept in water curing tank for the test at specified ages.

3.2.3 Recording Temperature Histories

In order to record the temperature histories after molding, samples were sealed and immediately after casting, were put into the curing tank, then thermocouple sensors were embedded into the concrete as shown in Figure 6. The thermocouple was connected to the maturity meter. The maturity meter recorded the temperatures after every 30 minutes.

Figure 6: Recording temperature histories.

3.2.4. Determination of Apparent Activation Energy

The apparent activation energy was obtained according to ASTM 1074 (2011) from the compression test of mortar. For preparing the mortar, the concrete should be sieved according to ASTM C403 (2008) separate the coarse aggregate from the mixture. However, sieving concrete with fiber can be very difficult and may not be possible because fiber cannot pass through the sieve. Therefore, the mortar was prepared in a separate batch with the same ratio of fine aggregate to cement with the ratio of coarse aggregate to cement of concrete according to ASTM 1074 (2011). In

addition, the water-cement ratio and the amount admixture of mortars was kept the same as those of the concrete mixtures. The mix proportions of the mortar are presented in Table 3. Compressive strength test was done on 100 mm cubes at the 1, 2, 4, 8, 16, 32 and 64 days for curing temperatures of 8°C, 22°C and 32°C.

Table 3: Mix proportion of mortars.

Series	Fiber Dosage kg/m^3	w/c	Cement kg/m^3	Water kg/m^3	Fine kg/m^3	SP kg/m^3
SP0	0	0.43	581	250	810	4.07
SP1	39.25	0.43	581	250	810	4.07
SP2	78.5	0.43	581	250	810	4.07
SP3	117.75	0.43	581	250	810	4.07
SP4	157	0.43	581	250	810	4.07

3.2.5 Testing of Hardened Concrete

3.2.5.1 Compressive Strength

For each mixture, 150 mm cubic samples were tested for the compressive strength at curing temperatures of 8°C, 22°C and 32°C. The samples were tested at 1, 3, 7, 10, 14, 28 and 56 days of water curing.

3.2.5.2 Flexural Strength

Prism beam with dimensions of 100 mm × 100 mm × 500 mm were tested for flexural strength according to the ASTM C78 (2015) standard. The flexural strength test was performed for each mixture at curing temperatures of 8°C, 22°C and 32°C, at 1, 3, 7, 10, 14, 28 and 56 days.

3.2.5.3 Flexural Toughness

For the performed experimental study, the closed-looped servo-control hydraulic machine was used. The specimens were tested for flexure (as shown in Figure 3.4) by using four point loading arrangement according to ASTM C1609 (2013). The distance between two supports was adjusted 450 mm and the distance between top loading points was 150 mm and the rate of loading during the test was 0.002 mm/s. The test was continued up to 3 mm deflection according to ASTM C1609. The flexural toughness test was performed for each mixture at curing temperatures of 8°C, 22°C, and 32°C, at 3, 7, 14, 28 and 56 days.

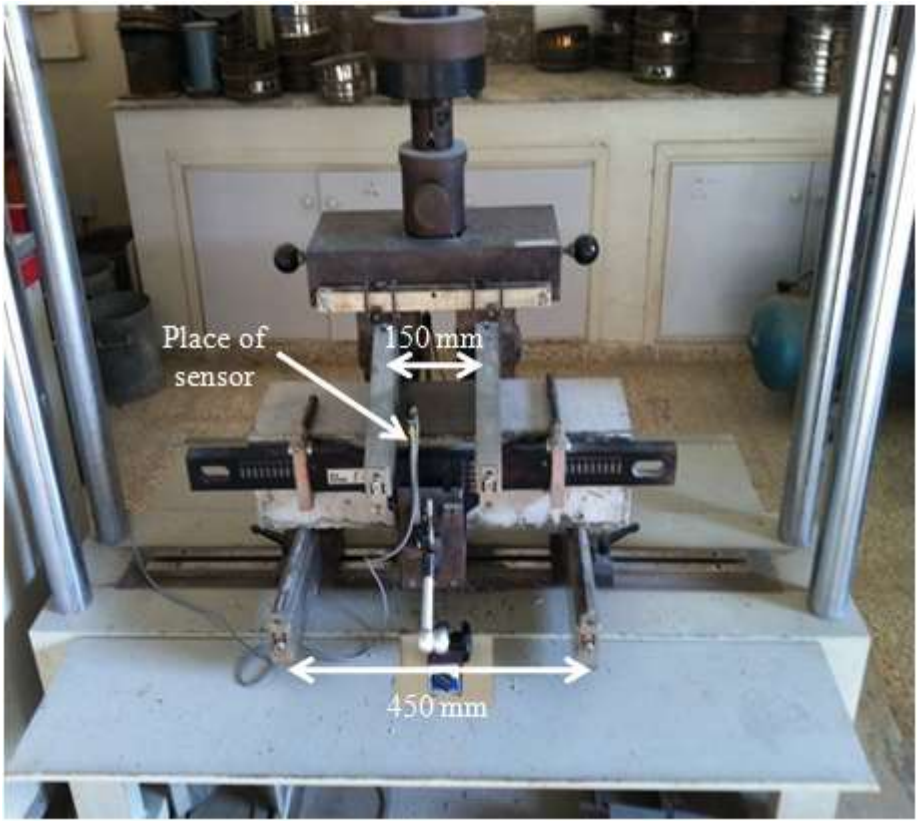

Figure 7: Flexural toughness test set up.

3.2.5.4 Splitting Tensile Strength

For each mixture, cylinder samples with the size of 100×200 (D×L) were tested for splitting tensile at 8 °C, 22 °C and 32 °C curing temperatures. The samples were tested at 1, 3, 7, 10, 14, 28 and 56 days.

Chapter 4

EXPERIMENTAL RESULTS

4.1 Compressive Strength

The compressive strength was performed for five different volumes of fiber fractions, they are (0, 0.5, 1, 1.5 and 2%) with three different curing temperatures of (8°C, 22°C, and 32°C), at the ages of 1, 3, 7, 10, 14, 28 and 56 days. The results of compressive strength for all samples were presented in Appendix.

4.1.1 Effects of Volume Fractions of Fibers on Compressive Strength

Generally, the compressive strength usually increased by increasing the volume fractions of fibers. Because due to the fact that at an increased volume fraction of fibers, the distance between fibers reduced and caused propagates a faster load transferring to be faster and is supported by adjacent fibers (Marar et al. 2011).

The specimen with the maximum increase in compressive strength is the SP4 mix, at the age of 56 days it increased up to 13, 14, 11% at curing temperatures of 8°C, 22°C, and 32°C respectively, when compared to SP0 mixes. The minimum increase in compressive strength is at an early age, which is usually the first day for SP1 mixes with 2, 3 and 10 % increase, at curing temperatures of 8°C, 22°C, and 32°C respectively.

4.1.2 Effects of Curing Temperature on Compressive Strength

An increase in the temperature leads to a faster hydration process (Neville, 2002).

The concretes specimen which was cured at 32°C had a higher compressive strength at early ages (up to 10 days) but at later ages (14, 28 and 56 days) the crossovereffects (Verbeck and Helmuth, 1968) occurred and compressive strength at 32°C curing temperatures decreased compared to 22 °C with the same volume fraction of fibers. However, at 56 days the compressive strength of concrete that cured at 32 °C had the same value with the concrete specimen which had cured at 8 °C. The compressive strength of the SP4 mixes that were 3 days old which cured at 32 °C were 10 and 20% higher than same mixes that cured at 8 °C and 22 °C respectively.

For specimen SP0, the compressive strength at 28 days increased to 12% and 15% at curing temperatures of 22 °C and 32 °C compared to 8 °C curing temperature respectively. SP1 shows 13% and 15% increase in compressive strength at 28 days when the curing temperature is about 22^{o}C and 32^{o}C of concrete that cured at 8 °C respectively. SP2 has a 12% and 16% increase for curing temperatures of 22 °C and 32 °C compared to 8 °C respectively. SP3 showed that at 28 days the compressive strength for curing temperatures of 22 °C and 32 °C increased 9% and 14% respectively when compared to 8 °C. SP4 shows a 14% increase in compressive strength for 22 °C at 28 days compared to 8 °C but this increase will only be 7% for concrete that cured at 32 °C.

4.2 Flexural Strength

The flexural strength was performed for five different volume fractions of fibers (0%, 0.5%, 1%, 1.5% and 2%) at three different curing temperatures (8°C, 22°C, and

32°C) at 1, 3, 7, 10, 14, 28 and 56 days. The flexural strength results of all samples were presented in Appendix

4.2.1 Effects of Volume Fractions of Fiber on Flexural Strength

The flexural strength results indicate that, by increasing the volume fraction of fibers, the flexural strength increased at all ages and for all the curing temperatures. This is because the fibers increased the ductility of the matrix; this ductile behavior of fiber reinforced concrete at a tension zone changed the normal elastic distribution of stress and strain over the depth of the member. This change in stress distribution is essentially plastic in the tension zone and elastic in the compression zone and which leads to cause a shift in the neutral axis towards the compression zone. Therefore, the tension tensile strength was increased by adding fibers (ACI 544.1R_96, 1997).

The maximum increase was found for the SP4 mixture, with an increase of 40, 39 and 38% when compared to plain concrete at 28 days with a temperature range of 8°C, 22°C, and 32°C, respectively. The minimum increase was found for SP1 mixture with an of increase 5%, and 6% compared to plain concrete at day 1 for 8°C, 22°C, and 32°C, respectively.

4.2.2 Effects of Curing Temperature on Flexural Strength

Similar to the compressive strength, increasing the curing temperature lead to an increase in the flexural strength up to 56 days. The flexural strength of concrete cured at 32°C has a higher tensile value at early ages compared to other curing temperatures of (8°C and 22°C) however, at 28 days, approximately the same tensile strength value of concrete was obtained for specimens cured both of 22°C and 32°C for all volume fractions of fibers. This means that the high curing temperature does

not have destructive effects on the flexural strength at later ages.

For SP0 the flexural strength after 28 days increased between 8% and 10% at curing temperature of 22 °C and 32 °C compared to an 8 °C curing temperature respectively. SP1 shows flexural strength at 28 days for 22 °C and 32 °C curing temperature and has a 7% and 11% increase compared to concrete that cured at 8 °C respectively. SP2 increased 12% for both curing temperature of 22 °C and 32 °C when compared to 8 °C temperature respectively. SP3 shows at 28 days the flexural strength for curing temperatures of 22 °C and 32 °C increase 10 and 12% respectively compared to 8 °C. SP4 shows 5% increase in flexural strength for 22 °C at 28 days compared to 8 °C. But this increase will be 7% for concrete that cured at 32 °C.

4.3Flexural Toughness

The flexural toughness is calculated from the area under the load - deflection (L-D) curve according to ASTM C 1609. The L-D curves of SP0, SP1, SP2, SP3, and SP4 at the ages of 3, 7, 14, 28 and 56 days and at curing temperature of 8 °C 22 °C and 32 °C are shown in Appendix. All samples have a similar relation at different ages and different curing temperatures. The relation of the L-D curve in SP0 was linear. When the load was raised up to the peak, the sample collapsed due to the brittle behavior of plain concrete. SP1 and SP2 have a strain-softening relationship due to the low fiber content, while the relationship of SP3 and SP4 had a strain-hardening behavior. The relationship of L-D curves is same at all ages and all curing temperatures. The results show that only the volume fractions of fiber can change the behavior of L-D curves.

4.3.1 Effects of Volume Fractions of Fibers on Flexural Toughness

The results of the flexural toughness of all mixes at all ages at three different curing temperatures are presented in Appendix. The results indicate that the flexural toughness increased by increasing the volume fraction of fibers at all ages and the curing temperatures.

Generally, thevolume fraction of steel fibers increased the toughness and influenced on bridging the tensile cracks. Because cracking of the concrete occurred before reaching its ultimate load, a decrease can be seen in the ascending part of the load-deflection curves. Upon reaching the ultimate load the internal cracks begin to interconnect, therefore, the overall stiffness of the specimen reduced. The presence of steel fibers perpendicular to the direction of the applied load can cause a reduction in the lateral deformations because of their stiffness effect; therefore, the toughness of steel fiber reinforced concrete increased (Marar et al. 2011).

The maximum increase in the flexural toughness was obtained for SP4 mixture. It increased 51, 49 and 48 times at the age of 3 compared to plain concrete for curing temperatures of 8 °C, 22 °C, and 32 °C respectively. However, at the age of 56 days, the flexural toughness of SP4 mixture increased 34, 34 and 32 times compare to plain concrete at curing temperatures of 8 °C, 22 °C, and 32 °, respectively.

4.3.2 Effects of Curing Temperature on Flexural Toughness

As shown in Figure 4.4 the flexural toughness of mixtures cured at the 32 °C have higher absorption energy at early ages (3 and 7 days) because high temperature accelerates hydration process (Neville 2003) but at later age, there is little difference between samples cured at 22 °C and 32 °C. However, at the age the of 56 days the

toughness values of concrete cured at temperature 22 °C and 32 °C are approximately same.

For SP0 the flexural strength at age of 28 days increases 8 and 10% at curing temperature of at 22 °C and 32 °C compared to concrete that was cured at 8 °C curing temperature respectively. SP1 shows flexural toughness at 28 days for 22 °C and 32 °C curing temperature that has increase 4 and 11% compared to concrete that cured at 8 °C respectively. SP2 has increased 17 and 31 % for both curing temperature of 22 °C and 32 °C when compared to 8 °C respectively. SP3 shows at 28 days the flexural toughness for curing temperatures of 22 °C and 32 °C increased 20% and 23% 45 respectively when compared to 8 °C. SP4 shows 4% increase in flexural toughness for 22 °C at 28 days compared to 8 °C. But this increase will be 11% for concrete that is cured at 32 °C.

4.4 Splitting Tensile Strength

The splitting strength was performed for all concrete mixtures at three different curing temperatures (8°C, 22°C, and 32°C) at 1, 3, 7, 10, 14, 28 and 56 days.

4.2.1 Effects of Volume Fractions of Fiber on Splitting Tensile Strength

The volume fractions of fiber have the same relationship on the splitting tensile strength with flexural strength. This is the same as some other properties of concrete, the splitting tensile strength increased by increasing the volume fractions of fibers.

The maximum increase is for the SP4 mixture which increased 53, 49 and 48% when compared to plain concrete (SP0) at an age of 28 days for curing temperatures of 8°C, 22°C, and 32°C respectively

4.2.2 Effects of Curing Temperature on Splitting Tensile Strength

Similar to some other properties of concrete, that mentioned in previous sections by increasing the curing temperature leads to an increase in the splitting tensile strength at early ages. Splitting tensile strength that is cured at 32°C has a higher tensile value at early ages when compared to other curing temperatures (8°C and 22°C); At 56 days, an approximate tensile value which was similar was obtained for all volume fractions of fibers as concrete cured at 22 °C and 32 °C.

For SP0 the flexural strength at an age of 28 days increased 21 and 24% at curing temperature of at 22 °C and 32 °C when compared to an 8 °C curing temperature. SP1 shows the flexural strength at 28 days for 22 °C and 32 °C curing temperature has a 14% and 19% increase when compared to concrete that cured at 8 °C respectively. SP2 has increased 35% and 41% for curing temperature of 22 °C and 32 °C compared to 8 °C respectively. SP3 shows that at 28 days the flexural strength for curing temperatures of 22 °C and 32 °C increased 13% and 16% respectively when compared to 8 °C. SP4 shows a 13% increase in flexural strength for 22 °C at 28 days when compared to 8 °C. But this increase will be 17% for concrete that was cured at 32 °C.

4.4 Apparent Activation Energy

In order to calculate apparent activation energy the mortar mixtures were prepared to compressive strength. Table 4 present the results of compressive strength of mortars.

Table 4: Compressive strength of mortars.

Age	Experimental Compressive Strength (MPa)						
(Days)	**1**	**2**	**4**	**8**	**16**	**32**	**64**
				8 °C			
SP0	8.89	15.45	19.9	26.8	36.83	43.46	47.23
SP1	9.19	15.58	20.16	29.15	38.25	44.4	48.21
SP2	9.66	16.47	21.6	30.51	39.95	45.7	48.54
SP3	10.3	19.26	23.31	32.54	40.46	45.95	50.66
SP4	10.82	20.97	24.21	33.81	44.03	48,25	51.62
				22 °C			
SP0	9.27	18.64	24.7	31.85	40.6	48.1	48.3
SP1	10.4	19.38	25.22	33.09	41.1	48.5	49.11
SP2	10.42	20.96	27.24	34.05	44.2	49.45	50.7
SP3	11.24	23.96	27.51	37.37	44.1	52.6	53.43
SP4	11.4	25.2	28.55	38.8	45.12	53.3	54.62
				32 °C			
SP0	10.34	21.33	26.84	33.85	43.15	48	47.7
SP1	11.27	22.28	27.77	36.55	45.05	49.55	48.32
SP2	11.61	23.91	28.64	37	46.25	50.35	49.46
SP3	12.16	25.7	29.6	39.5	47.6	51.9	52.35
SP4	12.68	26.81	30.15	40.8	48.45	52.5	53.45

After testing the compressive strength of the mortars, regression analysis was performed to determine the rate constant (k_T). In order, to calculate the rate constant regression analysis were done by three methods (linear hyperbolic, parabolic hyperbolic and exponential) according to Equations 9, 10 and 11, the values of rate constant are presented in Table 5. To calculate the activation energy according to ASTM C1074 (2011), one should plot Ln (k_T) versus $1/T_{abs}$, where T_{abs} is the absolute curing temperature of the water tank. Three values of k_T that were obtained from three different curing temperatures (8°C, 22°C, and 32°C) and determined from the line of best-fit for k_T values are shown in Figure 8. The rate constant values of these three curing temperatures are presented in Table5. The apparent activation energy was determined by dividing the negative slope of the line of the best-fit (Q) by the gas constant (R: 8.314 J/mol-°K).

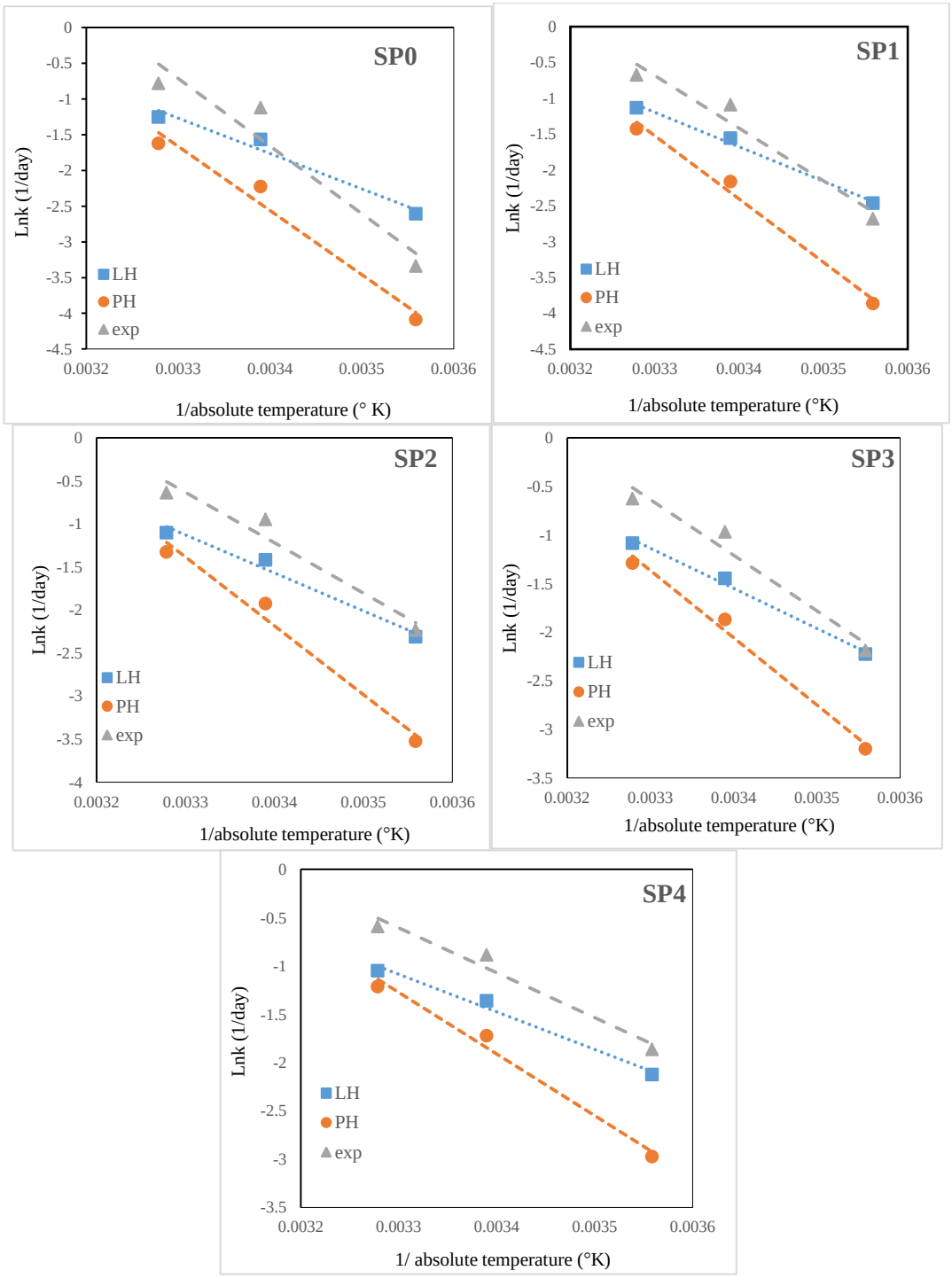

Figure 8: Ln k versus absolute temperature.

Table 5: Rate constant (k_T) values of mortars mixtures.

Series	LH			PH			EXP		
	8°C	22°C	32°C	8°C	22°C	32°C	8°C	22°C	32°C
SP0	0.074	0.209	0.286	0.017	0.108	0.197	0.036	0.326	0.458
SP1	0.085	0.211	0.322	0.021	0.115	0.240	0.069	0.336	0.509
SP2	0.099	0.242	0.332	0.029	0.146	0.266	0.107	0.387	0.528
SP3	0.108	0.235	0.338	0.041	0.154	0.276	0.112	0.380	0.535
SP4	0.120	0.257	0.350	0.051	0.179	0.297	0.155	0.413	0.554

In fact, activation energy is the energy that is required for starting hydration. This value is not activation energy of reactions; rather, it is the apparent activation energy and is obtained from the compressive strength of the mortar (Ferreira et al. 2015). The addition of fiber slightly increases the compressive strength. Increasing the compressive strength decreases the Q value and causes a decrease in the apparent activation energy (Kamkar and Eren, 2017). Table 6 presents the value of the activation energy and rate constant values of five different volume fractions of fibers (0, 0.5, 1, 1.5 and 2%) that were obtained by linear hyperbolic (LH), parabolic hyperbolic (PH) and exponential (EXP) methods. The range of apparent activation energy in this study was between 32 and 79 kJ/mol. The results show that the apparent activation energy decreased by increasing the volume fraction of fibers with all three methods.

Figure 9 presents the values of activation energy versus volume fractions of fibers of linear hyperbolic, parabolic hyperbolic and exponential methods. The highest values of the apparent activation energy were obtained for SP0 mixture (without fibers) in all three methods. It was approximately 21, 31 and 51% higher than concrete with a 2% volume fraction for linear hyperbolic, parabolic hyperbolic and exponential methods respectively.

By comparing the values of activation energies that were obtained by LH, PH and EXP methods, the LH method has the lowest values of activation energy in all volume fractions of fibers. For a plain concrete, the activation energy values of PH and EXP were 46 and 48% higher than LH method. At 0.5% volume fractions of fibers the apparent activation energy was 45 and 35% higher than the LH method respectively. Comparing the values of apparent activation energy in concrete with

1% volume fractions of fibers show PH and EXP methods were 45 and 25% higher than LH method respectively. In 1.5% volume fractions of fibers PH and EXP methods were 40 and 28% higher than LH respectively. At 2% volume fractions of fibers PH method were 39% higher than LH method, however, EXP method was 16% higher than the LH method.

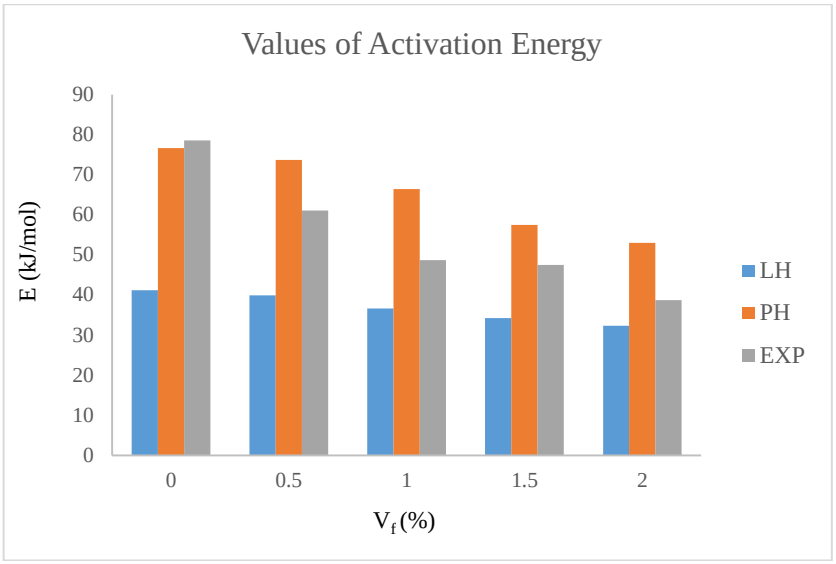

Figure 9: Values of activation energy for LH, PH and EXP methods.

.

Table 6: Activation energy with LH, PH and EXP methods.

Series	LH		PH		EXP	
	Q (K^{-1})	E (kJ/mol)	Q (K^{-1})	E (kJ/mol)	Q (K^{-1})	E (kJ/mol)
SP0	4948	41.15	8971.6	76.61	9446	78.55
SP1	4797.3	39.89	8811	73.72	7344.2	61.07
SP2	4406.5	36.64	7982.7	66.38	5855.6	48.7
SP3	4118.5	34.25	6911.5	57.48	5713.6	47.51
SP4	3886.7	32.32	6376.3	53.03	4652.3	38.69

4.5 Datum Temperature

For determining the datum temperature we need to first plot the K_T values (y-axis) versus curing temperatures (x-axis), then determine the best-fit line of the k_T values as shown in Figure 10. Datum temperature can be obtained from the intercept of

best-fit line with curing temperature axis. Table 7 presents the datum temperature values of five different volume fractions of fibers (0, 0.5, 1, 1.5 and 2%) that were obtained by linear hyperbolic (LH), parabolic hyperbolic (PH) and exponential (EXP) methods. The results show that the value of datum temperature for all mixes and all methods are approximately zero.

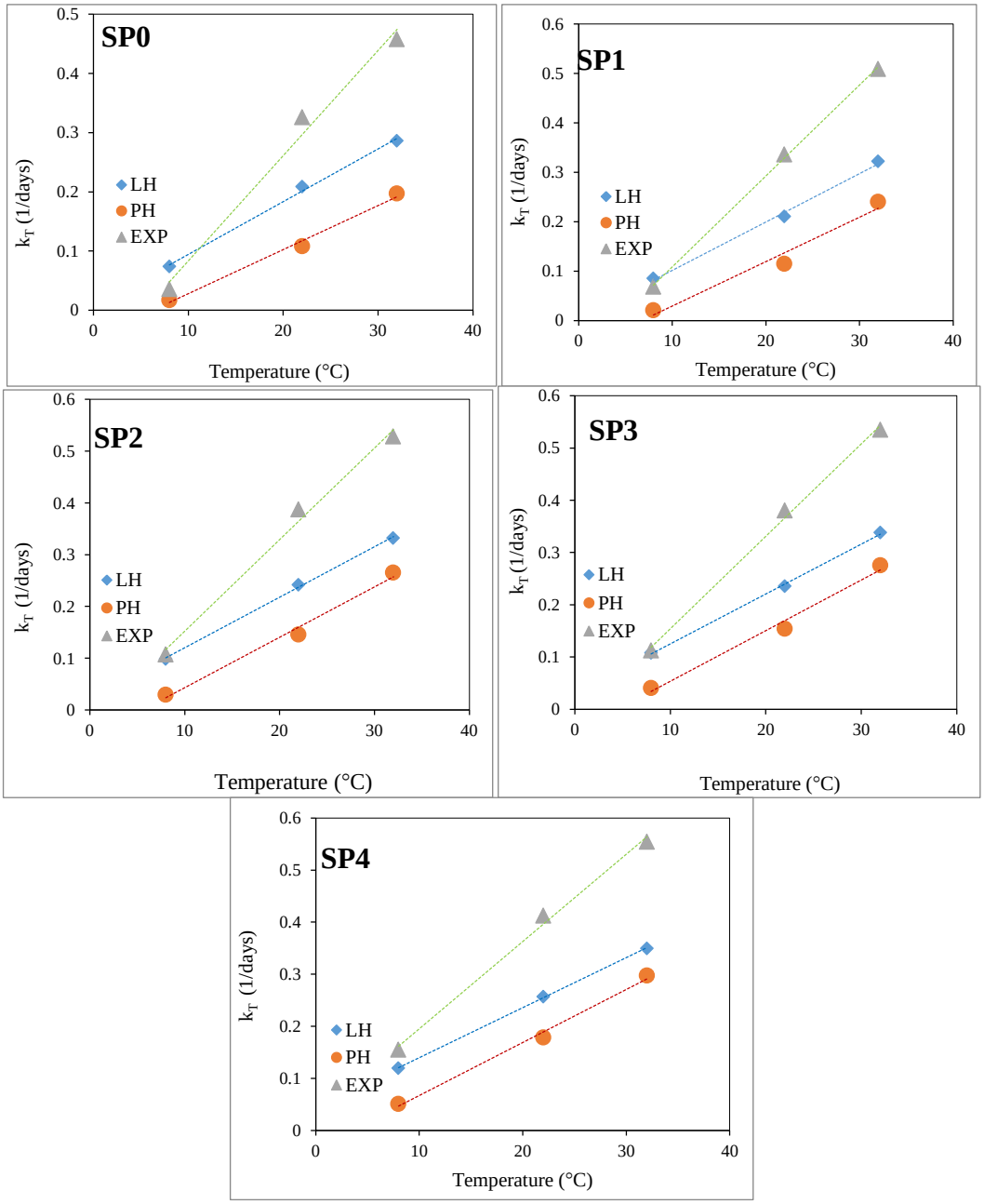

Figure 4.8: k_T versus curing temperature

Table 7: Values of datum temperatures.

Series	LH	PH	EXP
	T_0 (°C)		
SP0	0.005	-0.046	-0.094
SP1	0.003	-0.06	-0.075
SP2	-0.054	0.022	-0.025
SP3	0.039	-0.043	-0.023
SP4	0.043	-0.034	0.027

4.6 Temperature Histories

Figure 10 shows the temperature histories of five different volume fractions of fibers (0, 0.5, 1, 1.5 and 2% by volume of concrete) at different curing temperatures (8, 22 and 32°C). From this figure, it can be seen that at early stages, the temperature rises to a maximum due to the high heat of hydration mechanisms. As hydration proceeds, the temperature drops down to a temperature of the environment.The temperature histories at early ages (first 24 hours) slightly increased by increasing volume fraction of fibers, due to transferring the heat of hydration by steel fibers. However, after 24 hours, the temperature histories of all volume fractions of fibers at all curing temperatures are approximately the same as plain concrete. At curing temperatures of 22 °C and 32 °C, the maximum temperature histories occur during 1000 minutes (16 hours). However, the maximum temperature histories at curing temperature of 8 °C occur during 3000 minutes (80 hours). The maximum curing temperature at 32 °C wasincreased by 3.1, 4.9, 6.3 and 8% for 0.5, 1, 1.5 and 2% volume fractions of fibers respectively when compared to plain concrete. At a curing temperature of 22 °C, the maximum temperature histories were increased 0.7, 2.6, 4 and 6.3% for 0.5, 1, 1.5 and 2% volume fractions of fibers respectively when compared to plain

concrete. At curing temperature of 8 °C, the maximum increase in temperature histories for 0.5, 1, 1.5 and 2% volume fractions fibers were 3.1, 6.8, 9.5 and 13.3% compared to plain concrete respectively.

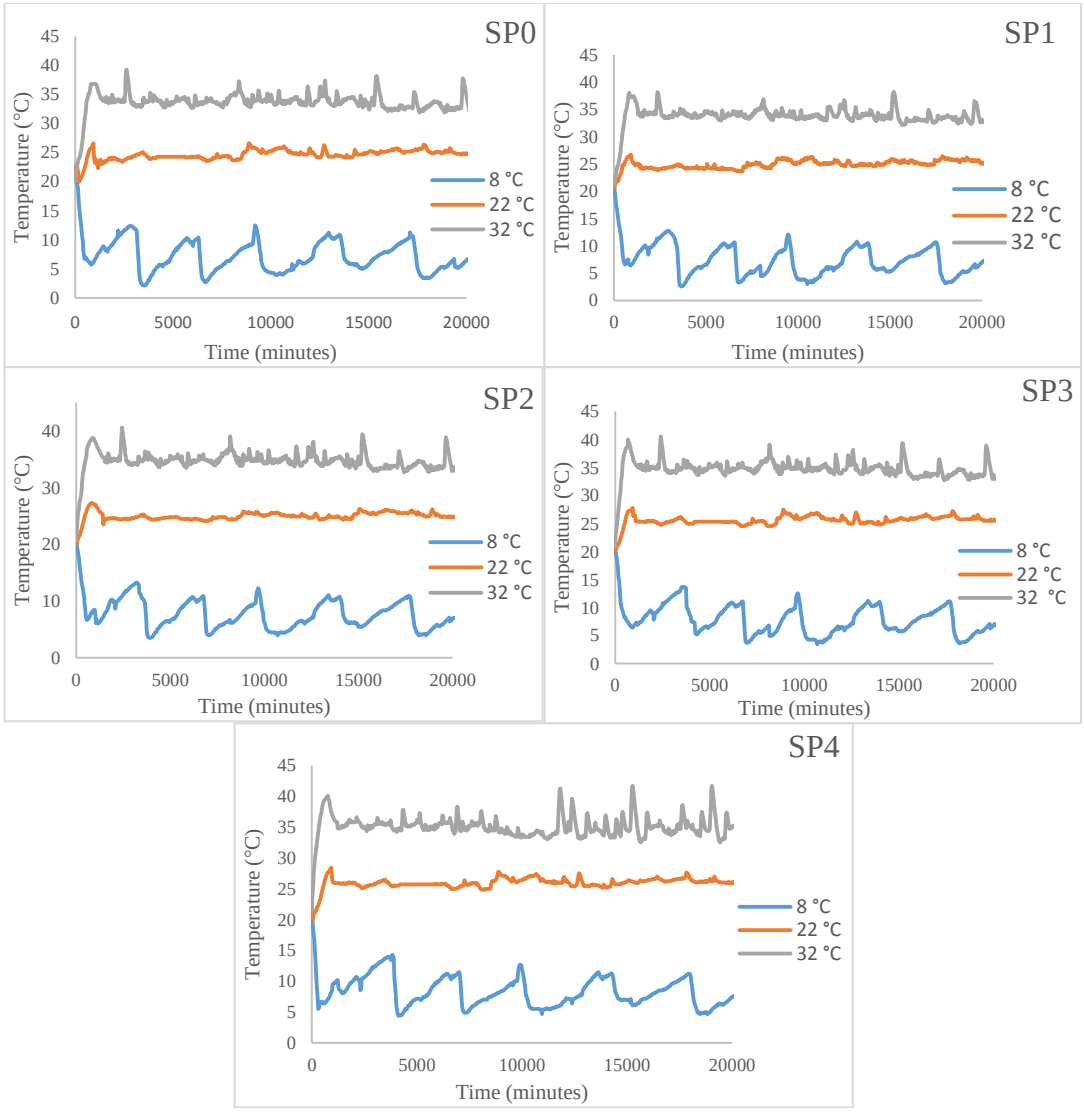

Figure 10: Temperature histories of SP0, SP1, SP2, SP3 and SP4.

4.7 Maturity Calculation

Two methods have been used to calculate maturity (Nurse-Saul and Arrhenius). The maturity index and equivalent age has been calculated by Nurse-Saul and Arrhenius methods according to Equations (1) and (3), respectively. Three equivalent ages from

different activations energies namely, LH_{eq}, PH_{eq} and EXP_{eq} were calculated for five volume fractions of fibers (0, 0.5, 1, 1.5 and 2% by volume of concrete) at ages of 1, 3, 7, 10, 14, 28 and 56 days and at a curing temperature of 8 °C, 22 °C, and 32 °C. The specific temperature for calculating equivalent age was 20°C (293 K). The results obtained from LH, PH and EXP methods were summarized in Appendix.

Maturity index was obtained from Nurse- Saul method for all mixes at the ages of 1, 3, 7, 10, 14, 28 and 56 days and at curing temperature of 8 °C, 22 °C, and 32 °C. The results of maturity index were presented in Appendix.

Chapter 5

PREDICTED MATURITY MODELS

5.1 Compressive Strength Models

After the calculation of the equivalent age and maturity index, the compressive strength was predicted. In order to, investigate the sensitivity of the strength development, four equations have been used which is the linear hyperbolic equation (S_{LH}), parabolic hyperbolic (S_{PH}), logarithmic (S_{LOG}) and exponential (S_{EXP}) equations 9, 10, 6 and 11, in order to help predict the compressive strength by both maturity index and equivalent age. To predict the compressive strength three equivalent ages (LH_{eq}, PH_{eq} and EXP_{eq}) were obtained for all the volume fractions of fibers in all the different curing temperatures. The results show that all of these equations have a good correlation with the experimental results, exhibiting a correlation coefficient (R^2) between 0.881 and 0.948 for all the predicted models in all mixes. In addition, maturity index was obtained for all mixes and used to predict compressive strength with equations (S_{LH}, S_{PH}, $S_{LOG,}$ and S_{EXP}).

5.1.1 Compressive Strength Development for Linear Hyperbolic Equivalent Age (LH_{eq})

Figure 11 presents the experimental and predicted compressive strength of SP0, SP1, SP2, SP3, and SP4 that were obtained by linear hyperbolic equivalent age (LH_{eq}) with four models (S_{LH}, S_{PH}, S_{LOG} and S_{EXP}). The regressions, which are parameters of all these four models, were shown in Table 8. The range of correlation coefficient (R^2) was between 0.881 and 0.948. All the models have a good correlation with

experimental results. However, the accuracy of linear hyperbolic and exponential equations is slightly higher than parabolic, hyperbolic and logarithmic equations. Logarithmic equation (S_{LOG}) has the lowest (R^2) in all mixes.

For SP0 mixes the rates of correlation coefficient are 0.922, 0.891, 0.875 and 0.918 for linear hyperbolic, parabolic hyperbolic, logarithmic and exponential equations respectively. For SP1, the rates of correlation coefficient are 0.941, 0.905, 0.887 and 0.938 for linear hyperbolic, parabolic hyperbolic, logarithmic and exponential equations respectively. For SP2 mixes the rates of R^2 are 0.944, 0.9, 0.881 and 0.942 for S_{LH}, S_{PH}, S_{LOG} and S_{EXP} equations respectively. The values of R^2 of SP3 for S_{LH}, S_{PH},S_{LOG} and S_{EXP} equations are 0.943, 0.899, 0.881 and 0.943 respectively. For the SP4 mix, the values of the correlation coefficient for S_{LH}, S_{PH} are 0.948 and 0.906 respectively, however, this value for S_{LOG} and S_{EXP} are 0.889 and 0.946 respectively.

Table 8: Regression parameters of compressive strength for LHeq.

V_f	equation	Regression parameters							
		S_u	k_T	T_0	τ	α	a	b	R^2
SP0	Linear hyperbolic	53.703	0.238	0.019					0.963
	Parabolic hyperbolic	71.21	0.11	0.488					0.952
	Plowman						13.173	9.546	0.957
	exponential	57.31			2.6	0.647			0.964
SP1	Linear hyperbolic	55.911	0.259	0.167					0.965
	Parabolic hyperbolic	74.22	0.117	0.527					0.945
	Plowman						13.668	10.132	0.95
	exponential	55.911			2.508	0.716			0.965
SP2	Linear hyperbolic	58.297	0.249	0.194					0.95
	Parabolic hyperbolic	77.875	0.527	0.536					0.93
	Plowman						13.673	10.653	0.935
	exponential	60.139			2.62	0.743			0.949
SP3	Linear hyperbolic	59.592	0.26	0.26					0.954
	Parabolic hyperbolic	79.74	0.112	0.548					0.937
	Plowman						13.984	11.011	0.970
	exponential	60.612			2.574	0.79			0.954
SP4	Linear hyperbolic	61.656	0.274	0.331					0.942
	Parabolic hyperbolic	81.959	0.12	0.563					0.936
	Plowman						14.6	11.451	0.935
	exponential	66.554			2.524	0.849			0.952

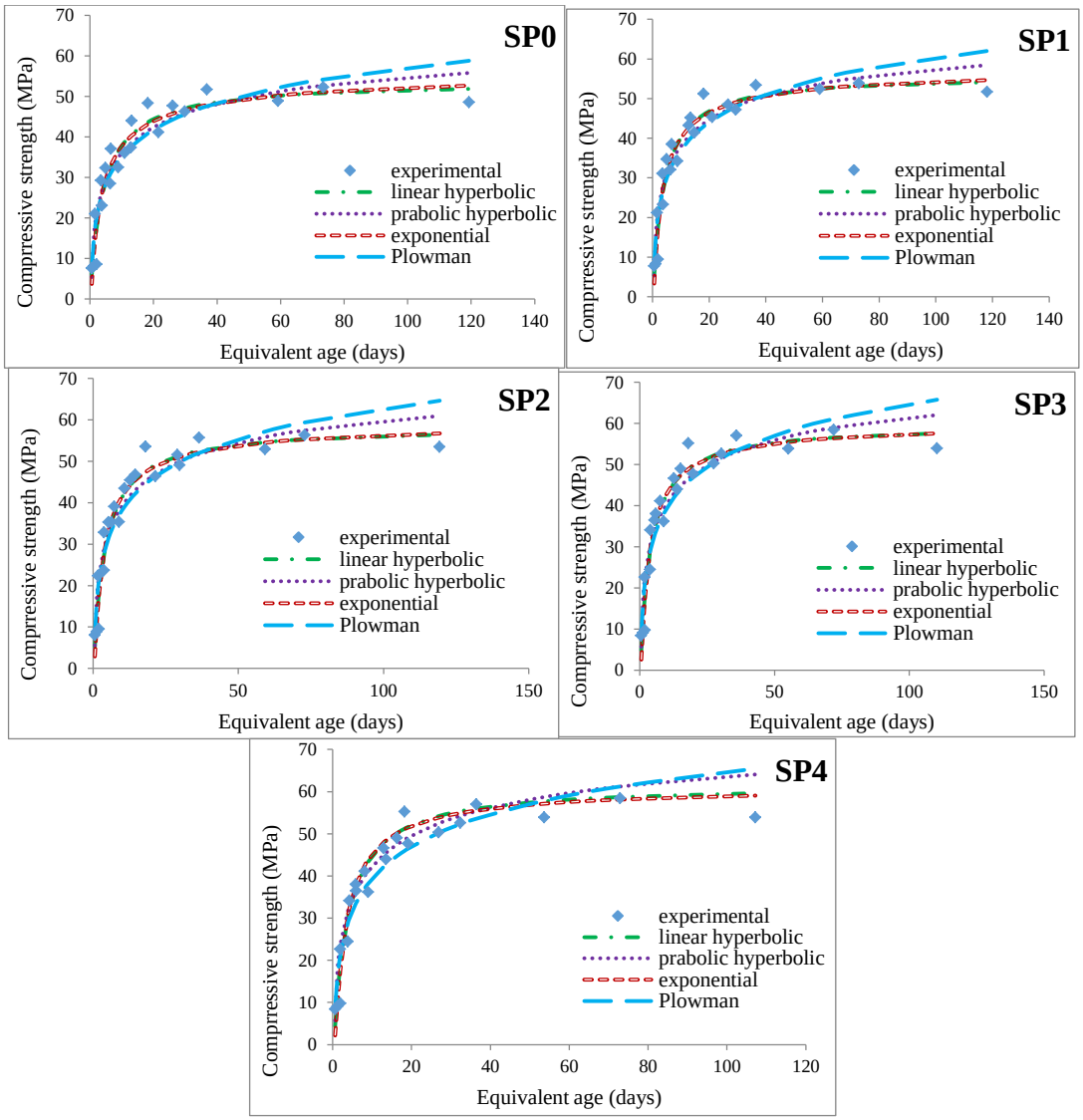

Figure 11: Predicted Compressive strength by LHeq method.

5.1.2 Compressive Strength Development for Parabolic Hyperbolic Equivalent Age (PH_{eq})

Figure 12 presents the experimental and predicted compressive strength of SP0, SP1, SP2, SP3, and SP4 that were obtained by parabolic hyperbolic equivalent age with four models (S_{LH}, S_{PH}, S_{LOG} and S_{EXP}). The regressions, which are parameters of all these four models, were shown in table 9. The range of correlation coefficient (R^2) was between 0.702 and 0.957. Similar as LH_{eq}, all the models have a good correlation with experimental results. However, the R^2 that was obtained for SP0,

SP1, and SP2 mixes are slightly lower than that of the SP3 and SP4 mixes. The accuracy of linear hyperbolic, parabolic hyperbolic and exponential equations are approximately the same. However, the accuracy ofthe logarithmic equation (S_{LOG}) is slightly lower than other equations.

For SP0 mixes the rates of correlation coefficient are 0.711, 0.721, 0.702 and 0.715 for linear hyperbolic, parabolic hyperbolic, logarithmic and exponential equations respectively. For SP1 the rates of correlation coefficient are 0.745, 0.745, 0.722 and 0.749 for linear hyperbolic, parabolic hyperbolic, logarithmic and exponential equations respectively. For SP2 mixes the rates of R^2 are 0.777, 0.761, 0.737 and 0.77 for S_{LH}, S_{PH}, S_{LOG} and S_{EXP} equations respectively. The values of R^2 of SP3 for S_{LH}, S_{PH}, S_{LOG} and S_{EXP} equations are 0.830, 0.803, 0.774 and 0.824 respectively. For SP4 mix the values of the correlation coefficient for S_{LH}, S_{PH} are 0.824 and 0.857 respectively, however, this value for S_{LOG} and S_{EXP} are 0.8020 and 0.849 respectively.

Table 9: Regression parameters of compressive strength for PHeq.

V_f	equation	Regression parameters							
		S_u	k_T	T_0	τ	α	a	b	R^2
SP0	Linear hyperbolic	50.313	0.248	-					0.963
	Parabolic hyperbolic	60.32	0.211	0.273					0.952
	Plowman						17.876	7.126	0.957
	exponential	59.5			1.952	0.421			0.964
SP1	Linear hyperbolic	53.242	0.26	-					0.965
	Parabolic hyperbolic	64.331	0.203	0.273					0.945
	Plowman						18.437	7.727	0.95
	exponential	60.771			1.919	0.472			0.965
SP2	Linear hyperbolic	56	0.239	-					0.95
	Parabolic hyperbolic	64.331	0.17	0.329					0.93
	Plowman						17.983	8.393	0.935
	exponential	62.548			2.163	0.513			0.949
SP3	Linear hyperbolic	57.678	0.261	-					0.954
	Parabolic hyperbolic	72.109	0.161	0.482					0.937
	Plowman						16.892	9.344	0.970
	exponential	61.326			2.257	0.636			0.954
SP4	Linear hyperbolic	61.162	0.263	-					0.942
	Parabolic hyperbolic	76.217	0.147	0.39					0.936
	Plowman						17.468	9.838	0.935
	exponential	62.326			2.315	0.709			0.952

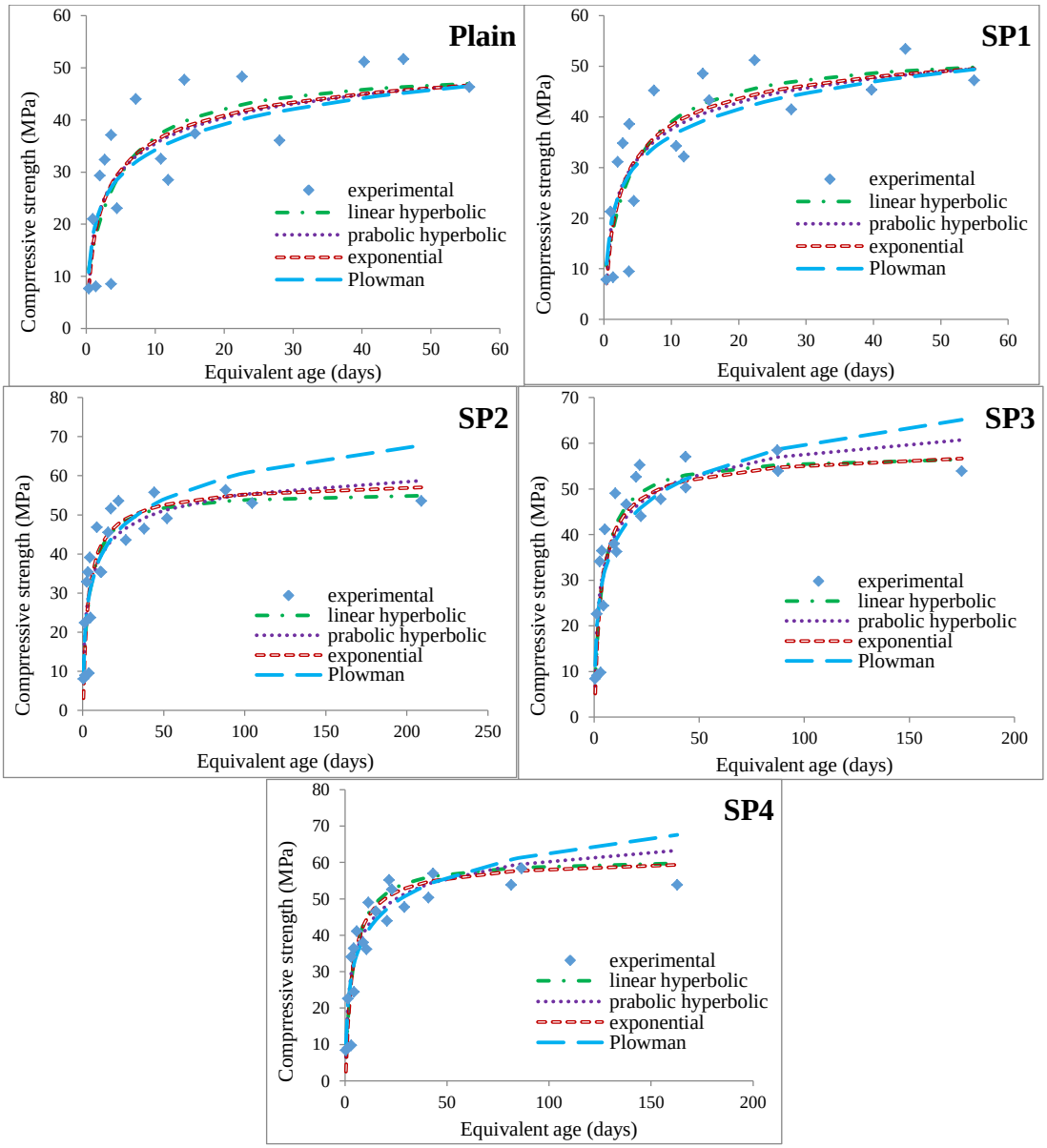

Figure 12: Predicted Compressive strength by PHeq method.

5.1.3 Compressive Strength Development for Exponential Equivalent Age (EXP_{eq})

Figure 13 presents the experimental and predicted compressive strength of SP0, SP1, SP2, SP3, and SP4 that is obtained by exponential equivalent age with four modes (S_{LH}, S_{PH}, S_{LOG} and S_{EXP}). The regressions, which are parameters of all these four models, were shown in table 10. The ranges of correlation coefficient (R^2) for all the models were between 0.671 and 0.895. For other equivalent ages, (LH_{eq} and PH_{eq}),

all the models have a good correlation with experimental results. However, the R^2 that was obtained for SP0 is lower than that of the other mixes, while the R^2 that was obtained for other mixes had a good correlation with experimental results in all strength development equations. The range of the R^2 for all strength developed in this method (EXP_{eq}) is approximately the same.

For SP0 mixes the rates of correlation coefficient are 0.678, 0.686, 0.671 and 0.685 for linear hyperbolic, parabolic hyperbolic, logarithmic and exponential equations respectively. For SP1 the rates of correlation coefficient are 0.833, 0.812, 0.789 and 0.828 for linear hyperbolic, parabolic hyperbolic, logarithmic and exponential equations respectively. For SP2 mixes the rates of R^2 are 0.885, 0.851, 0.831 and 0.878 for S_{LH}, S_{PH}, S_{LOG} and S_{EXP} equations respectively. The values of R^2 of SP3 for S_{LH}, S_{PH}, S_{LOG} and S_{EXP} equations are 0.885, 0.844, 0.821 and 0.88 respectively. For SP4 mix the values of the correlation coefficient for S_{LH}, S_{PH} are 0.892 and 0.834 respectively, however, the values for S_{LOG} and S_{EXP} are 0.806 and 0.895 respectively.

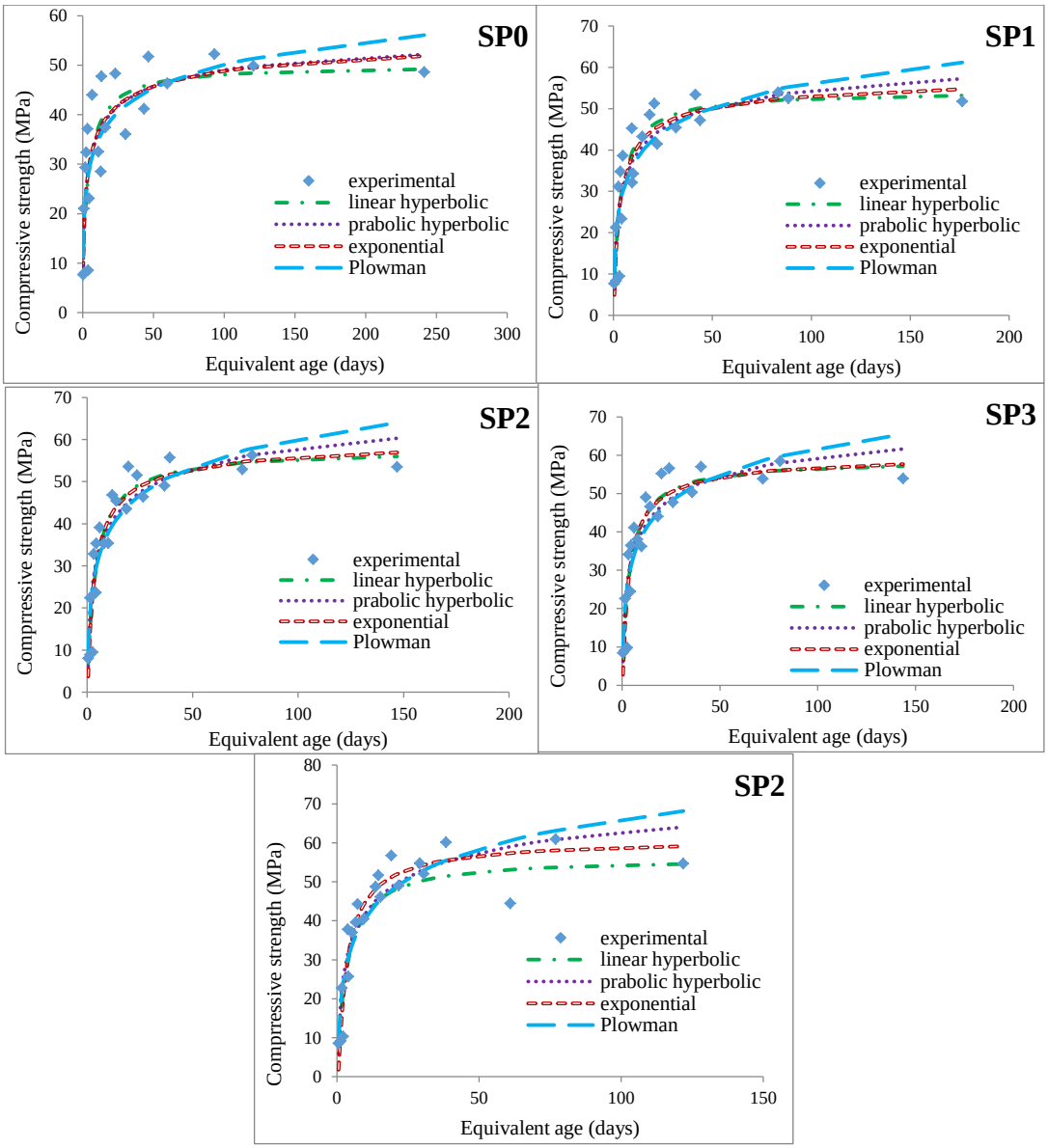

Figure 13: Predicted Compressive strength by EXPeq method.

Table 10 : Regression parameters of compressive strength for EXPeq.

V_f	equation	Regression parameters							
		S_u	k_T	T_0	τ	α	a	b	R^2
SP0	Linear hyperbolic	50.012	0.245	-					0.963
	Parabolic hyperbolic	59.177	0.231	0.248					0.952
	Plowman						18.437	6.86	0.957
	exponential	60.072			1.88	0.395			0.964
SP1	Linear hyperbolic	54.26	0.263	-					0.965
	Parabolic hyperbolic	68.052	0.16	0.373					0.945
	Plowman						16.644	8.61	0.95
	exponential	59.35			2.162	0.571			0.965
SP2	Linear hyperbolic	57.572	0.241	-					0.95
	Parabolic hyperbolic	74.313	0.126	0.445					0.93
	Plowman						15.364	9.75	0.935
	exponential	61.131			2.488	0.648			0.949
SP3	Linear hyperbolic	58.705	0.255	0.052					0.954
	Parabolic hyperbolic	75.982	0.129	0.439					0.937
	Plowman						15.753	10.02	0.970
	exponential	60.936			2.44	0.711			0.954
SP4	Linear hyperbolic	61.264	0.268	0.246					0.942
	Parabolic hyperbolic	80.55	0.124	0.45					0.936
	Plowman						15.376	10.991	0.935
	exponential	61.496			2.5	0.833			0.952

5.1.4 Comparison of Strength Development between LH_{eq}, PH_{eq} and EXP_{eq}

By comparing the predicted compressive strength models between different equivalent ages ($LH_{eq,}$ PH_{eq} and EXP_{eq}), the eq_{LH} has higher R^2 values in all mixes with values of approximately 0.9. The R^2 values of exponential equivalent age are lower than LH_{eq}, but it is higher than PH_{eq}, with values of approximately 0.8 and the lowest values of R^2 are for the PH_{eq} with an approximate value of 0.7.

5.1.5 Compressive Strength Development for Maturity Index (MI)

Maturity index (MI) is calculated to predict the compressive strength. Four equations (S_{LH}, S_{PH} S_{LOG} and S_{EXP}) are used to predict the compressive strength by maturity index for all mixes. Figure 14 presents the experimental and predicted compressive strength of SP0, SP1, SP2, SP3, and SP4 that are obtained by maturity indexThe regressions, which are parameters of all these four models, were shown in Table 11. The ranges of correlation coefficient (R^2) are between 0.906 and 0.97. The results show that all the models have a very good correlation with experimental results. In

this method, the R^2 values of all models are similar to each other. However, the accuracy of S_{LOG} is slightly lower than that of other equations.

For SP0 mixes the rates of correlation coefficient are 0.968, 0.943, 0.931 and 0.966 for linear hyperbolic, parabolic hyperbolic, logarithmic and exponential equations respectively. For SP1 the rates of correlation coefficient are 0.97, 0.935, 0.915 and 0.968 for linear hyperbolic, parabolic hyperbolic, logarithmic and exponential equations respectively. For SP2 mixes the rates of R^2 are 0.967, 0.932, 0.916 and 0.966 for S_{LH}, S_{PH} S_{LOG} and S_{EXP} equations respectively. The values of R^2 for SP3 are 0.962, 0.924, 0.906 and 0.961 respectively, for S_{LH}, S_{PH}, S_{LOG} and S_{EXP} equations respectively. For SP4 mix the values of the correlation coefficient for S_{LH}, S_{PH} are 0.961 and 0.924 respectively, however, this value for S_{LOG} and S_{EXP} are 0.97 and 0.96 respectively.

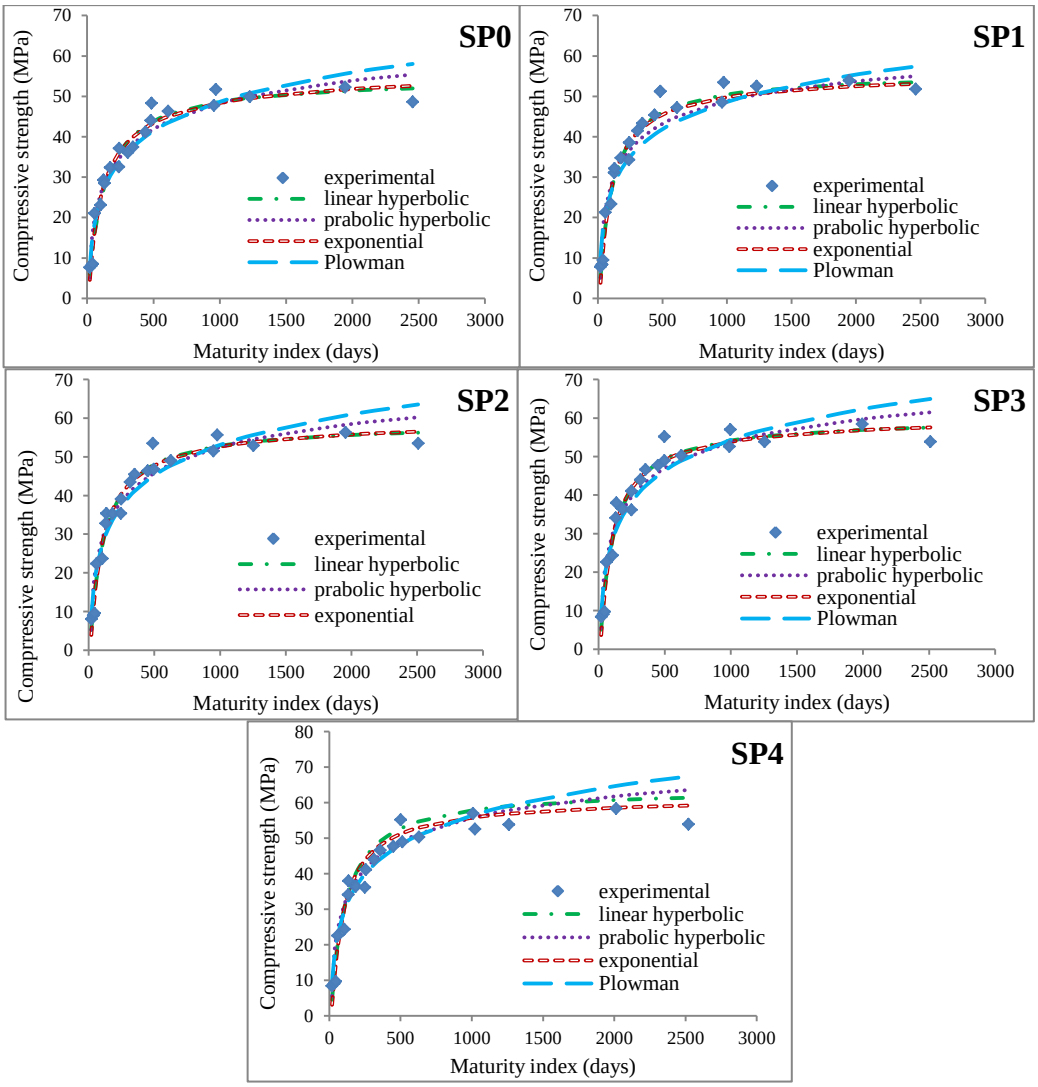

Figure 14: Predicted Compressive strength by MI method.

Table 11 : Regression parameters of compressive strength for MI.

V_f	equation	Regression parameters							
		S_u	k_T	T_0	τ	α	a	b	R^2
SP0	Linear hyperbolic	54.53	0.008	4.758					0.963
	Parabolic hyperbolic	74.714	0.003	17.94					0.952
	Plowman						-23.53	10.448	0.957
	exponential	58.272			79.57	0.664			0.964
SP1	Linear hyperbolic	55.3	0.01	8.956					0.965
	Parabolic hyperbolic	70.348	0.005	18.37					0.945
	Plowman						-18.64	9.737	0.95
	exponential	56.586			70.13	0.773			0.965
SP2	Linear hyperbolic	58.724	0.009	8.983					0.95
	Parabolic hyperbolic	80.044	0.004	18.4					0.93
	Plowman						-25.477	11.375	0.935
	exponential	60.704			75.13	0.753			0.949
SP3	Linear hyperbolic	59.867	0.009	9.592					0.954
	Parabolic hyperbolic	81.183	0.004	18.03					0.937
	Plowman						-25.428	11.547	0.970
	exponential	61.358			73.13	0.778			0.954
SP4	Linear hyperbolic	61.751	0.01	11.21					0.942
	Parabolic hyperbolic	83.19	0.004	17.95					0.936
	Plowman						-25.9	11.913	0.935
	exponential	62.271			71.11	0.836			0.952

5.1.6 Validation of Compressive Strength Models

To assess the accuracy of the predicted compressive strengths of each model, the additional lines are provided with ranges of ±10 and ±20% errors for the different volume fractions of the fibers.

5.1.6.1 Validation of Compressive Strength Models for LH_{eq}

The results show that the percentage of errors on day 1 is very high because of the shorter curing period; however, at later ages, the ranges of errors were between 0 and ±20%, as observed in Figures 15, 16, 17, 18 and 19. During the day 1 age, the parabolic hyperbolic equation (S_{PH}) has a higher error when compared to other equations in all mixes. However, at later ages (28 and 56 days) the errors of logarithmic equation (S_{LOG}) in all mixes are higher than the other equations.

Figure 15 observes the correlation between experimental compressive strength and the predicted compressive strength of SP0 with linear hyperbolic, parabolic

hyperbolic, logarithmic and exponential equations. The maximum percentage of errors which occursat 1 day were -100.5%, -141.1%, 130.9% and 130.8% for S_{LH}, S_{PH}, S_{LOG} and S_{EXP} equations respectively. However, at 56 days, the percentage of errors values were -6.7%, -14.8%, -21% and -8.4% for S_{LH}, S_{PH}, S_{LOG} and S_{EXP} equations respectively.

Figure 16 shows a correlation between predicted and measured compressive strength with four equations (S_{LH}, S_{PH}, $S_{LOG,}$ and S_{EXP}) for the SP1 mixture. The maximum percentages of errors at 1 day were -90.2%, -130.1%, -118.7% and 90% for S_{LH}, S_{PH}, S_{LOG} and S_{EXP} equations respectively. However, at 56 days the percentages of errors were -4.6%, -13%, -19.8% and -5.6% for S_{LH}, S_{PH}, S_{LOG} and S_{EXP} equations respectively.

Figure 17 shows the predicted and measured compressive strength of SP2. The maximum percentages of errors at 1 day are -88.6%, -132.7%, -120.3% and 84.6% for S_{LH}, S_{PH}, S_{LOG} and S_{EXP} equations respectively. However, at 56 days the percentages of errors are -5.4%, -13.9%, -20.8% and -6% for S_{LH}, S_{PH}, S_{LOG} and S_{EXP} equations respectively.

Figure 18 presents the estimated and measured compressive strength of SP3 mixture with four different equations. The maximum percentage of errors at 1 day were -88.3%, -134% for S_{LH}, S_{PH} equations respectively, and on the sameday, the maximum percentage of error were -120.5% and 81.1% for S_{LOG} and S_{EXP} equations respectively. However, at 56 days the percentages of errors are -6.8%, -15.1%, -22% and -6.8% for S_{LH}, S_{PH}, S_{LOG} and S_{EXP} equations respectively.

Figure 19 presents estimated and measured compressive strength of SP4 mixture with four different equations. The maximum percentages of errors at 1 day were -96.2%, -145.5% for S_{LH} and S_{PH} equations respectively, and on the same day, the percentage of errors were -120.5% and 84.1% for S_{LOG} and S_{EXP} equations respectively. However, at 56 days the maximum percentages of errors for S_{LH} and S_{PH} were -10.6%, -18.9%, respectively, and for S_{LOG} and S_{EXP} is -21.5% and -9.6% respectively.

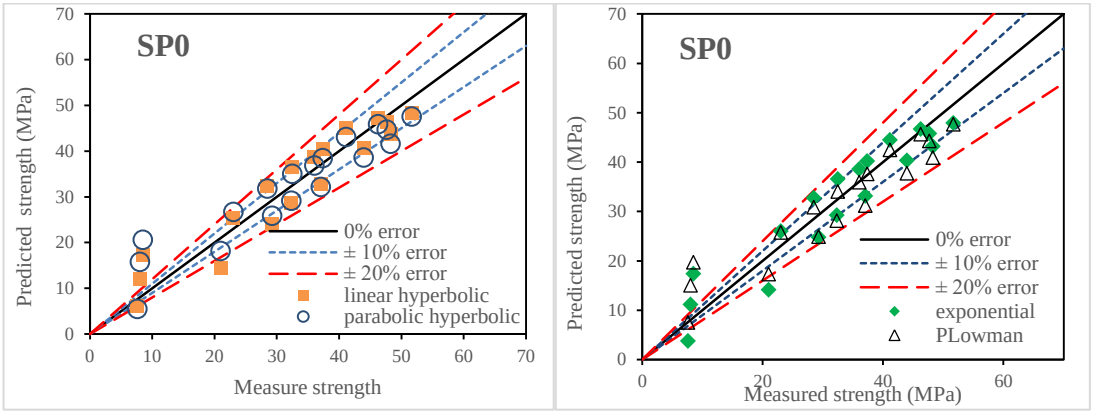

Figure 15: Measured predicted compressive strength LHeq method for SP0: (a) linear and parabolic hyperbolic model and (b) exponential and Plowman model.

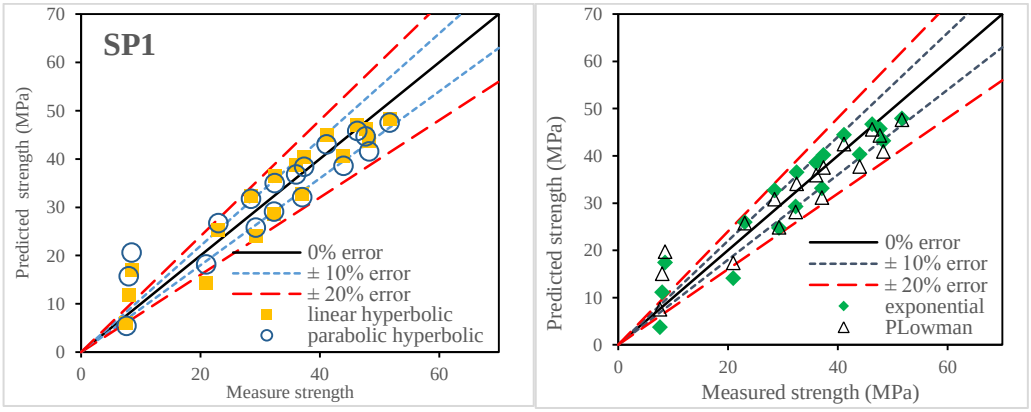

Figure 16: : Measured versus predicted compressive strength LHeq method for SP1: (a) linear and parabolic hyperbolic model and (b) exponential and Plowman model.

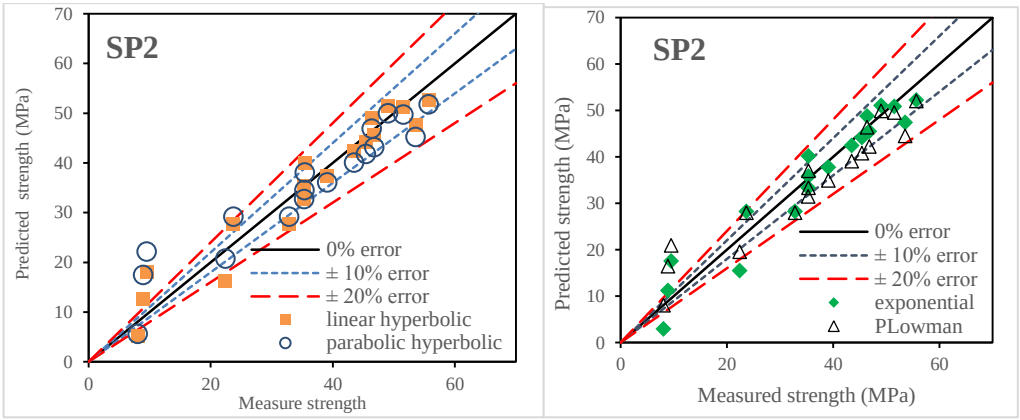

Figure 17: Measured versus predicted compressive strength LHeq method for SP2: (a) linear and parabolic hyperbolic model and (b) exponential and Plowman model.

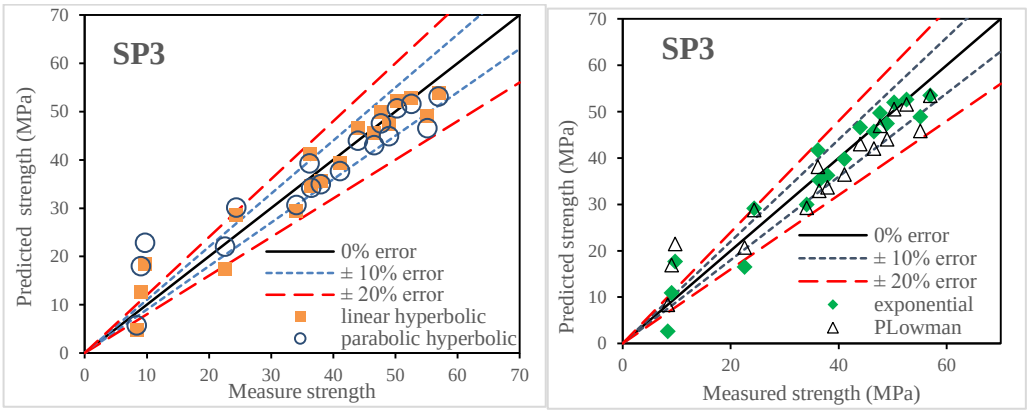

Figure 18: Measured versus predicted compressive strength LHeq method for SP3: (a) linear and parabolic hyperbolic model and (b) exponential and Plowman model.

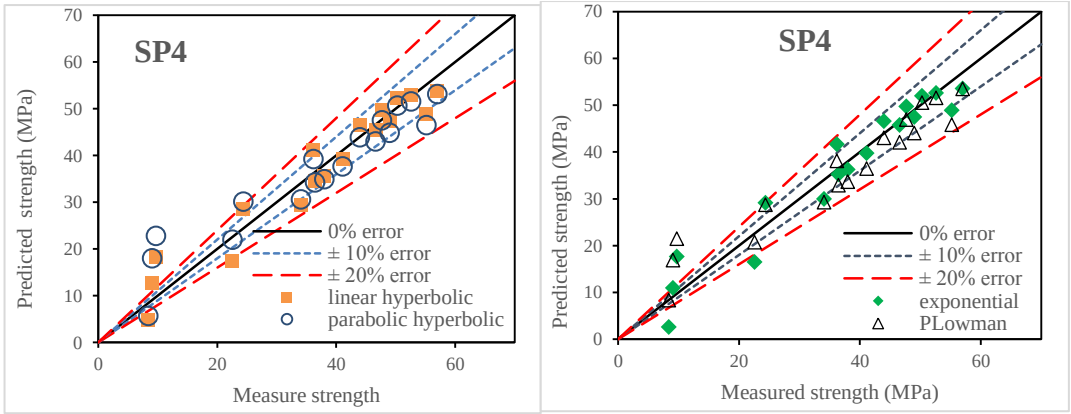

Figure 19: Measured versus predicted compressive strength by LHeq method for SP4: (a) linear and parabolic hyperbolic model and (b) exponential and Plowman model.

5.1.6.2 Validation of Compressive Strength Models for PH_{eq}

Same as eq_{LH} the results show that the percentage of errors on day 1 were very high; however, at later ages, the range of errors were between 0 and ±20%, as observed in Figures 20, 21, 22, 23 and 24. During the period of the first day, the maximum percentage of error was for Logarithmic (S_{LOG}) equation in all mixes. However, the errors of parabolic hyperbolic equation (S_{PH}) in all mixes were higher than errors of S_{LH} and S_{EXP} equations. However, at later ages (28 and 56 days) the errors of logarithmic equation (S_{LOG}) in all mixes were higher than other equations.

Figure 20 observes the correlation between experimental compressive strength and predicted compressive strength of SP0 with linear hyperbolic, parabolic hyperbolic, logarithmic and exponential equations. The maximum percentages of errors at day 1 were -121.7%, -146.2%, 152.5% and 115.6% for S_{LH}, S_{PH}, S_{LOG} and S_{EXP} equations respectively. However, at 56 days the percentages of errors were -1.7%, -8.3%, -16.1% and -16.7% for S_{LH}, S_{PH}, S_{LOG} and S_{EXP} equations respectively.

Figure 21 shows a correlation between predicted and measured compressive strength with four equations (S_{LH}, S_{PH}, $S_{LOG,}$ and S_{EXP}) for the SP1 mixture. The maximum percentages of errors at 1 day were -117.2%, -148.2%, -152.9% and 128.9% for S_{LH}, S_{PH}, S_{LOG} and S_{EXP} equations respectively. However, at 56 days the percentages of errors were -1.1%, -8.2%, -16.2% and -5.6% for S_{LH}, S_{PH}, S_{LOG} and S_{EXP} equations respectively.

Figure 22 shows the predicted and measured compressive strength of SP2. The maximum percentages of errors at 1 day were -118.4%, -149.8%, -154.3% and 113.9% for S_{LH}, S_{PH}, S_{LOG} and S_{EXP} equations respectively. However, at 56 days the

percentages of errors were -1.1%, -4.9%, -20.6% and -4.1% for S_{LH}, S_{PH}, S_{LOG} and S_{EXP} equations respectively.

Figure 23 presents estimated and measured compressive strength for SP3 mixture with four different equations. The maximum percentages of errors at day 1 were -84%, -127.7% for S_{LH}, S_{PH} equations respectively, and at the sameday, the maximum percentage of errors were -126.6% and 79.8% for S_{LOG} and S_{EXP} equations respectively. However, at 56 days the percentages of errors were -4.7%, -12.7%, -20.9% and -5.1% for S_{LH}, S_{PH}, S_{LOG} and S_{EXP} equations respectively.

Figure 24 presents estimated and measured compressive strength of SP4 mixture with four different equations. The maximum percentages of errors at 1 day were -87.4%, -138.9% for S_{LH}, S_{PH} equations respectively, and at the sameday, the percentage of errors were -133.6% and 71.7% for S_{LOG} and S_{EXP} equations respectively. However, at 56 days the percentages of errors for S_{LH} and S_{PH} were -10.9%, -17.4%, respectively, and for S_{LOG} and S_{EXP} is -21.4% and -10.1% respectively.

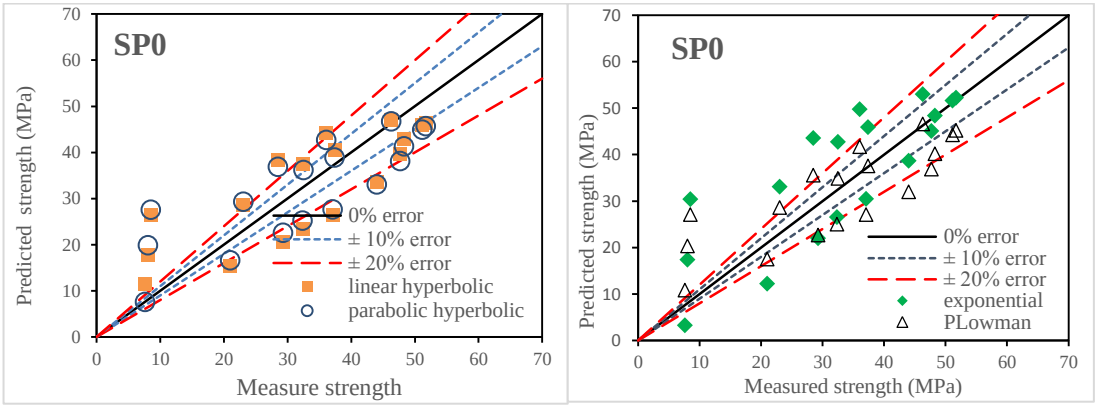

Figure 20: Measured versus predicted compressive strength by PHeq method for SP0: (a) linear and parabolic hyperbolic model and (b) exponential and Plowman model.

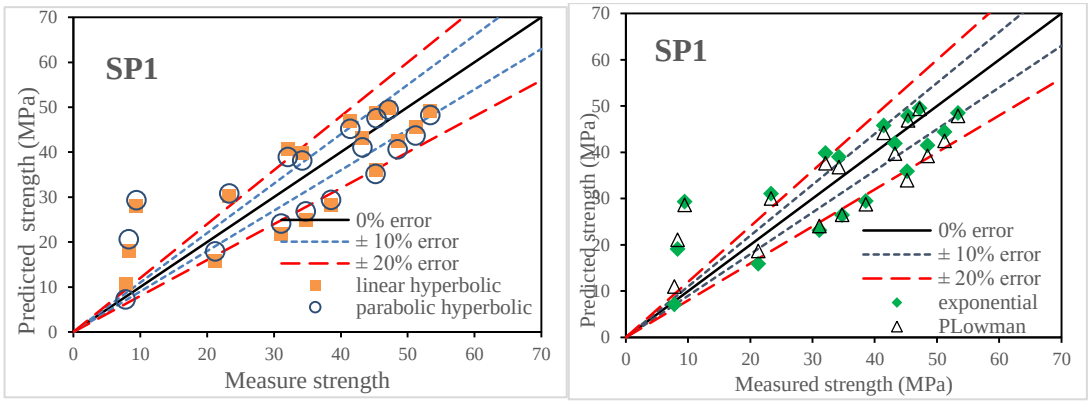

Figure 21: Measured versus predicted compressive strength by PHeq method for SP1: (a) linear and parabolic hyperbolic model and (b) exponential and Plowman model.

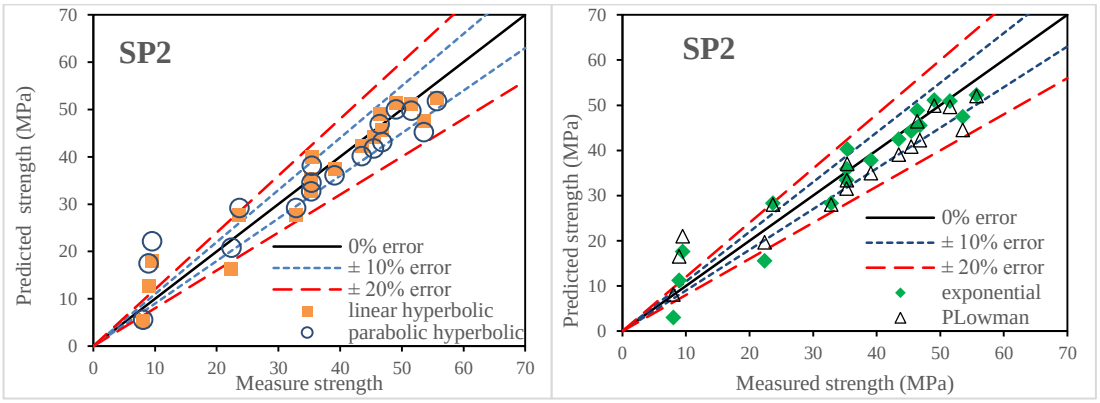

Figure 22: Measured versus predicted compressive strength by PHeq method for SP2: (a) linear and parabolic hyperbolic model and (b) exponential and Plowman model.

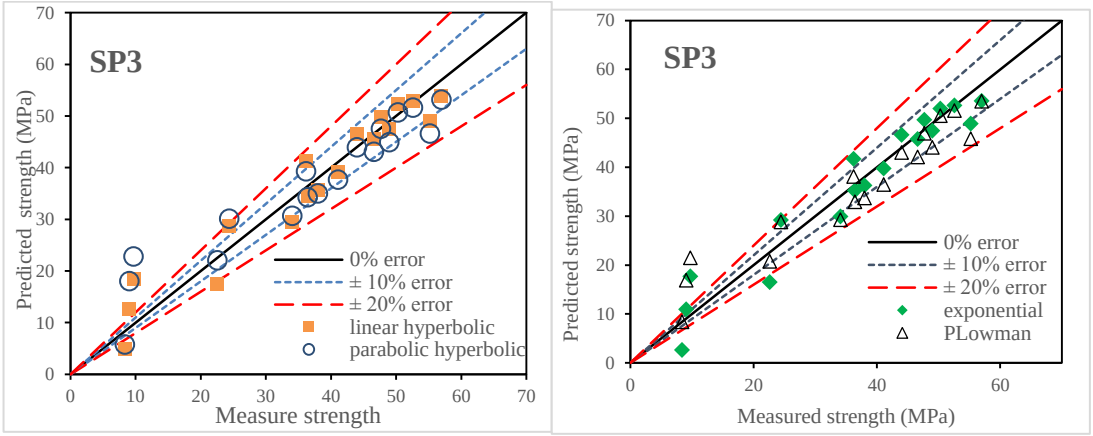

Figure 23: Measured versus predicted compressive strength by PHeq method for SP3: (a) linear and parabolic hyperbolic model and (b) exponential and Plowman model.

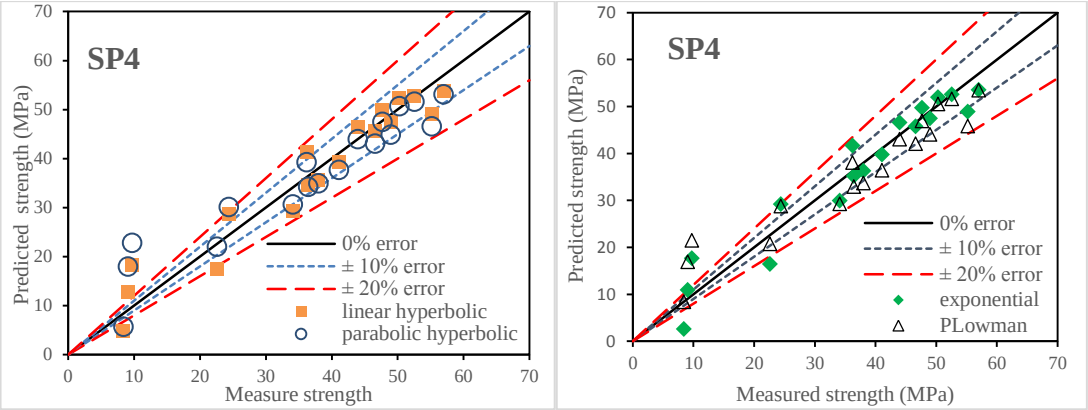

Figure 24: Measured versus predicted compressive strength by PHeq method for SP4: (a) linear and parabolic hyperbolic model and (b) exponential and Plowman model.

5.1.5.3 Validation of Compressive Strength Models for EXP_{eq}

The results show that the percentage of errors are the same as other methods at day 1 is very high; however, at later ages, the range of errors is between 0 and ±20%, as observed in Figures 25, 26, 27, 28 and 29. During the first day, the parabolic hyperbolic equation (S_{PH}) and logarithmic have a higher errors when compared to linear hyperbolic and exponential equations in all mixes. However, the errors of linear hyperbolic and Exponential equations in the first day are approximately the same. The errors of logarithmic equation (S_{LOG}) at later ages are higher than other equations. However, at later ages, the linear hyperbolic equation has a minimum error compared to other equations.

Figure 25 observes the correlation between experimental compressive strength and the predicted compressive strength of SP0 with linear hyperbolic, parabolic hyperbolic, logarithmic and exponential equations. The maximum percentages of errors at day 1 were -131%, -153%, -160.1% and -145.7% for S_{LH}, S_{PH}, S_{LOG} and S_{EXP} equations respectively. However, at the 56th day, the percentages of errors were -1.2%, -7.4%, -15.4% and -6.7% for S_{LH}, S_{PH}, S_{LOG} and S_{EXP} equations respectively.

Figure 26 shows a correlation between the predicted and measured compressive strength with four equations (S_{LH}, S_{PH}, $S_{LOG,}$ and S_{EXP}) for the SP1 mixture. The maximum percentages of errors at day 1 were -168%, -181.2%, -174.4% and -171.6% for S_{LH}, S_{PH}, S_{LOG} and S_{EXP} equations respectively. However, at 56 days, the percentages of errors were -2.8%, -10.6%, -18.2% and -5.8% for S_{LH}, S_{PH}, S_{LOG} and S_{EXP} equations respectively.

Figure 27 shows the predicted and measured compressive strength of SP2. The maximum percentages of errors at day 1 were -138%, -169%, -160.7% and -145% for S_{LH}, S_{PH}, S_{LOG} and S_{EXP} equations respectively. However, at 56 days, the percentages of errors were -4.7%, -12.7%, -19.7% and -6.4% for S_{LH}, S_{PH}, S_{LOG} and S_{EXP} equations respectively.

Figure 28 presents the estimated and measured compressive strength of SP3 mixture with four different equations. The maximum percentage of error at day 1 were -142.3%, -168.9% for S_{LH}, S_{PH} equations respectively, and on the sameday, the maximum percentage of error are -159.5% and -139.5% for S_{LOG} and S_{EXP} equations respectively. However, at 56 days, the percentages of errors were -6%, -14.3%, -21.6% and -7% for S_{LH}, S_{PH}, S_{LOG} and S_{EXP} equations respectively.

Figure 29 presents an estimated and measured compressive strength of SP4 mixture with four different equations. The maximum percentage of error at day 1 is -114.6%, -150% for S_{LH}, S_{PH} equations respectively, and at the sameday, the percentage of error are -137% and -101.4% for S_{LOG} and S_{EXP} equations respectively. However, at 56 days, the maximum percentage of errors for S_{LH} and S_{PH} are 0.1%, -17.2%, respectively, and for S_{LOG} and S_{EXP} are -24.7% and -8.2% respectively.

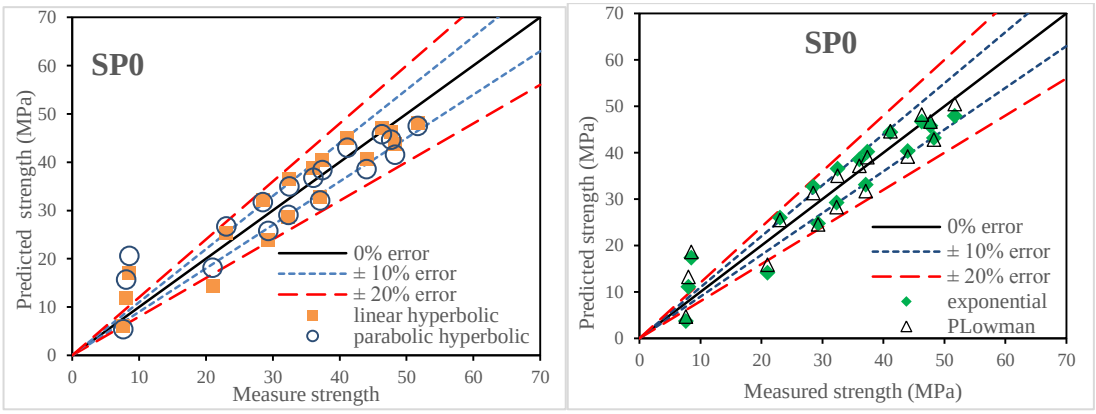

Figure 25: Measured versus predicted compressive strength by EXPeq method for SP4: (a) linear and parabolic hyperbolic model and (b) exponential and Plowman model.

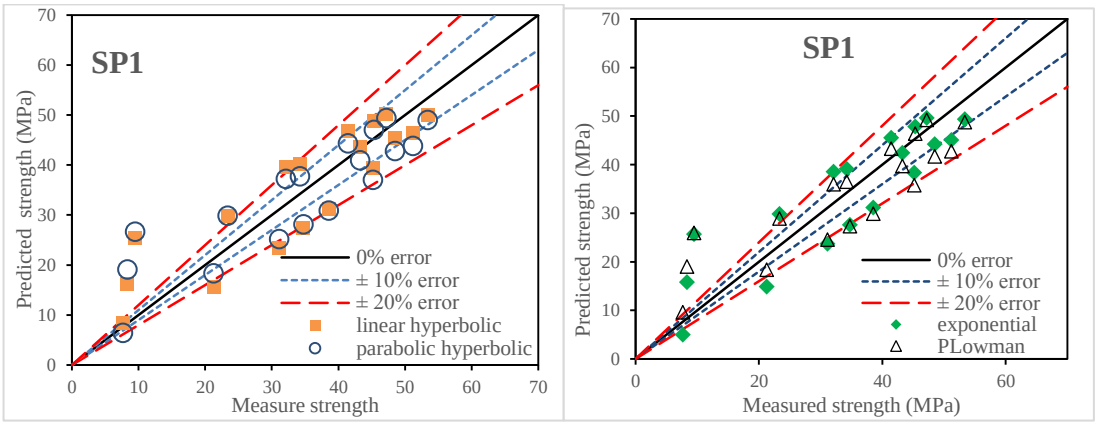

Figure 26: Measured versus predicted compressive strength by EXPeq method forSP1: (a) linear and parabolic hyperbolic model and (b) exponential and Plowman model.

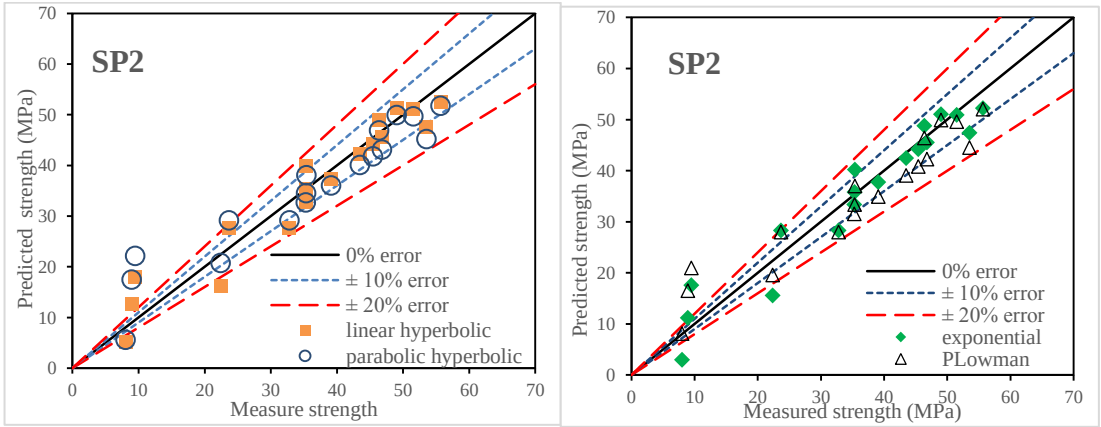

Figure 27: Measured versus predicted compressive strength by EXPeq method for SP2: (a) linear and parabolic hyperbolic model and (b) exponential and Plowman model.

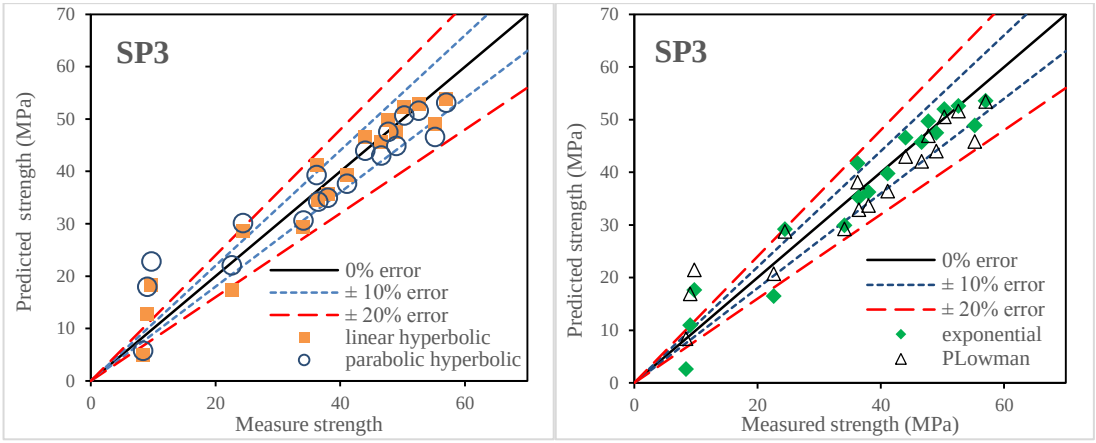

Figure 28: Measured versus predicted compressive strength by EXPeq method for SP3: (a) linear and parabolic hyperbolic model and (b) exponential and Plowman models.

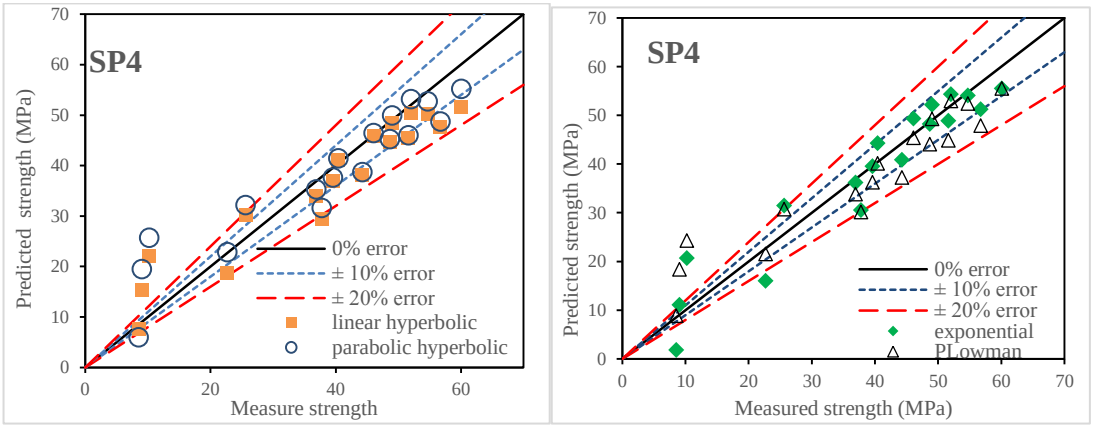

Figure 29: Measured versus predicted compressive strength by EXPeq method for SP4: (a) linear and parabolic hyperbolic model and (b) exponential and Plowman models.

5.1.5.4 Validation of compressive strength models for MI

The results show that the percentages of errors in the first day is very high because of the lower curing period; however, at later ages, the range of errors are between 0 and ±20%, as observed in Figures 30, 31, 32, 33 and 34. During the first day, the parabolic hyperbolic equation (S_{PH}) has a higher error compared to other equations in all mixes. However, at this age (day 1) the exponential equation has minimum error compared to other equations. At later ages (28 and 56 days) the errors of logarithmic equation (S_{LOG}) in all mixes are higher than other equations. However, at 56 days the

S_{LH} and S_{EXP} equations have a lower error when compared to S_{PH} and S_{LOG} equations.

Figure 30 observes the correlation between experimental compressive strength and the predicted compressive strength of SP0 with linear hyperbolic, parabolic hyperbolic, logarithmic and exponential equations. The maximum percentage of error which occurs at day 1 is -49.5%, -93.5%, -81.3% and -47.4% for S_{LH}, S_{PH}, S_{LOG} and S_{EXP} equations respectively. However, at 56 days, the percentages of error values are -6.9%, -14%, -19.4% and -8.2% for S_{LH}, S_{PH}, S_{LOG} and S_{EXP} equations respectively.

Figure 31 shows a correlation between predicted and measured compressive strength with four equations (S_{LH}, S_{PH}, $S_{Log,}$ and S_{EXP}) for the SP1 mixture. The maximum percentages of errors at the first day were -40.2%, -92%, -86.2% and -33.1% for S_{LH}, S_{PH}, S_{LOG} and S_{EXP} equations respectively. However, at 56 days, the percentages of errors were -3.4%, -6.3%, -10.9% and -2.6% for S_{LH}, S_{PH}, S_{LOG} and S_{EXP} equations respectively.

Figure 32 shows the predicted and measured compressive strength of SP2. The maximum percentages of error at 1 day were -50.2%, -99.3%, -85.6% and -44.2% for S_{LH}, S_{PH}, S_{LOG} and S_{EXP} equations respectively. However, at 56 days, the percentages of errors were -5.1%, -12.6%, -18.8% and -5.7% for S_{LH}, S_{PH}, S_{LOG} and S_{EXP} equations respectively.

Figure 33 presents an estimated and measured compressive strength of SP3 mixture with four different equations. The maximum percentages of errors at day 1 were -

852.5%, -102.9% for S_{LH}, S_{PH} equations respectively, and at the sameday, the maximum percentage of errors are -89% and -44.5% for S_{LOG} and S_{EXP} equations respectively. However, at 56 days, the percentages of errors are -6.7%, -14.1%, -20.5% and -6.8% for S_{LH}, S_{PH}, S_{LOG} and S_{EXP} equations respectively.

Figure 34 presents an estimated and measured compressive strength of SP4 mixture with four different equations. The maximum percentages of errors at day 1 is -62.9%, -116.9% for S_{LH}, S_{PH} equations respectively, and on the sameday, the percentages of errors are -101.2% and -49.6% for S_{LOG} and S_{EXP} equations respectively. However, at 56 days, the maximum percentage of errors for S_{LH} and S_{PH}were -13.9%, -18%, respectively, and for S_{LOG} and S_{EXP} were -25.1% and -9.8% respectively.

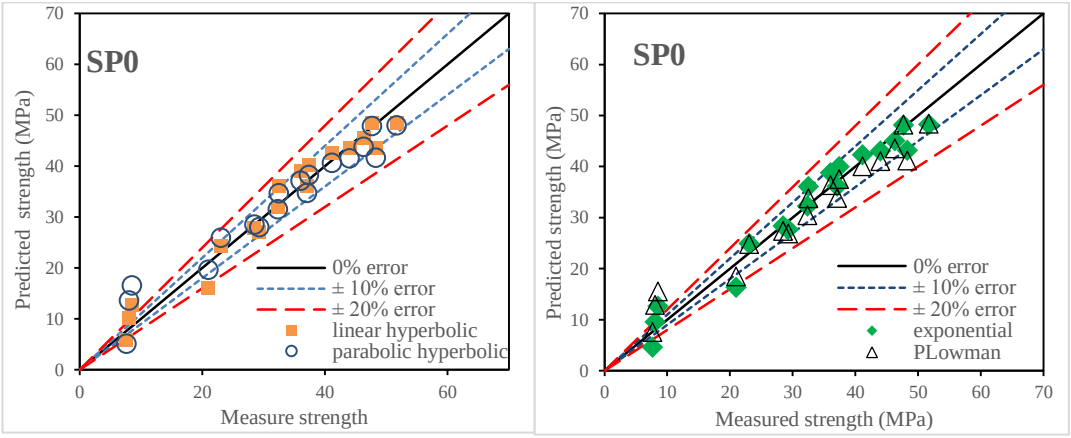

Figure 30: Measured versus predicted compressive strength by MI method for SP0: (a) linear and parabolic hyperbolic model and (b) exponential and Plowman model.

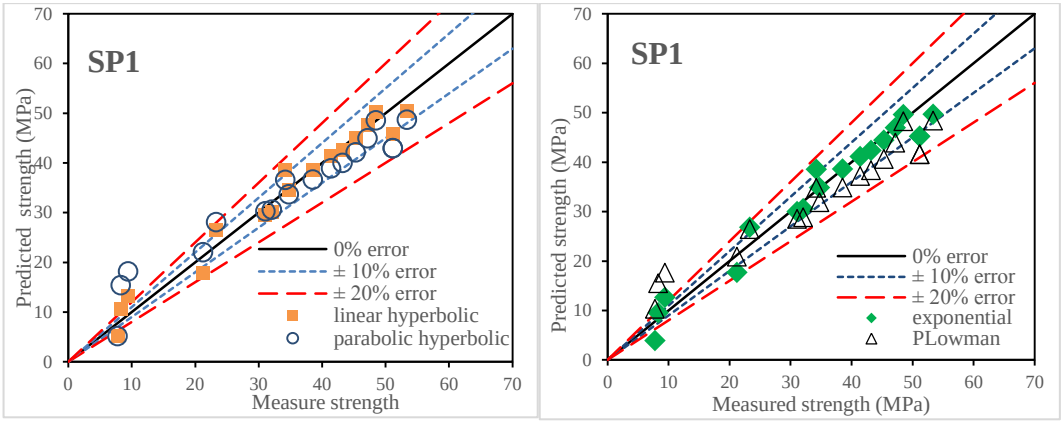

Figure 31: Measured versus predicted compressive strength by MI method for SP1: (a) linear and parabolic hyperbolic model and (b) exponential and Plowman model.

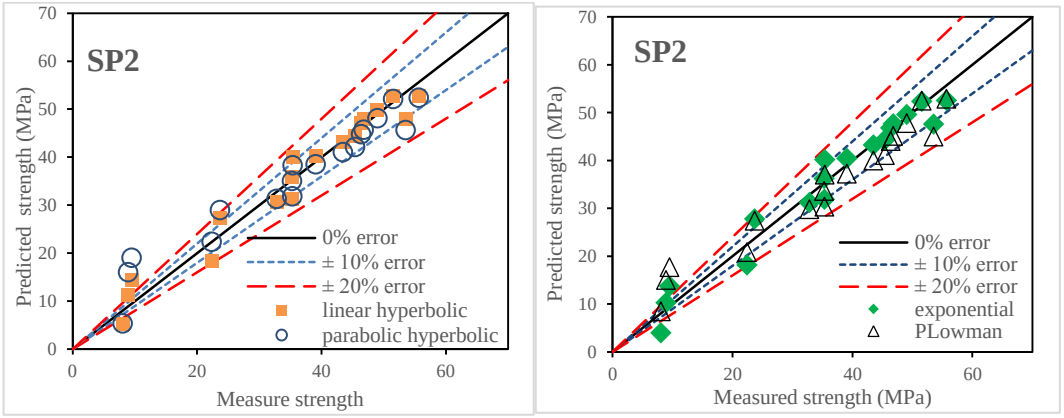

Figure 32: Measured versus predicted compressive strength by MI method for SP2: (a) linear and parabolic hyperbolic model and (b) exponential and Plowman model.

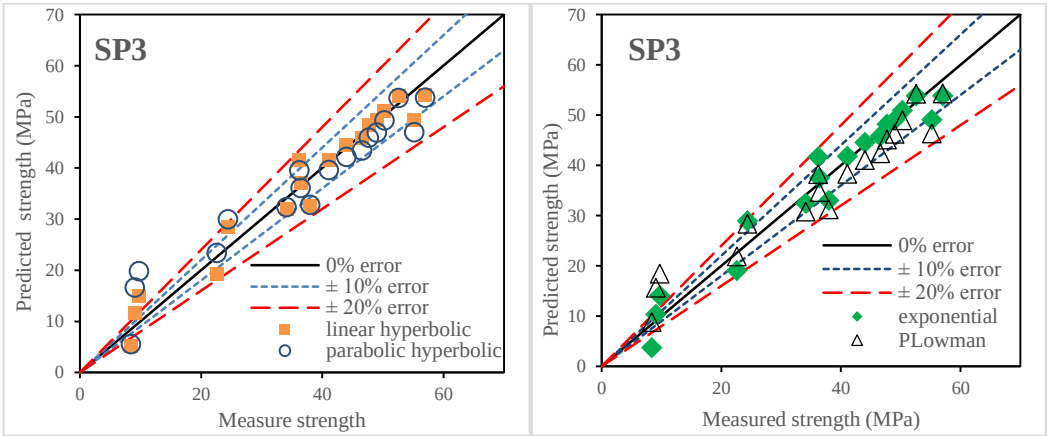

Figure 33: Measured versus predicted compressive strength by MI method for SP3: (a) linear and parabolic hyperbolic model and (b) exponential and Plowman model.

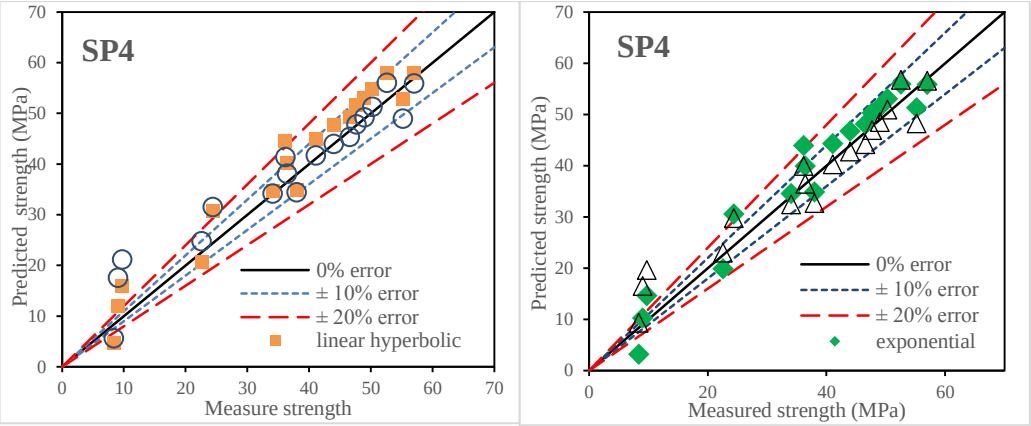

Figure 34: Measured versus predicted compressive strength by MI method for SP4: (a) linear and parabolic hyperbolic model and (b) exponential and Plowman model.

5.2 Flexural Strength Models

A similar study was performed to predict the flexural strength. Flexural strength was predicted for five different mixes (SP0, SP1, SP2, SP3, and SP4). Similar to the compressive strength, four equations were used to predict the flexural strength (S_{LH}, S_{PH}, $S_{LOG,}$ and S_{EXP}). The equivalent age was calculated by three methods (LH_{eq}, PH_{eq}, EXP_{eq}). For all of these models, the flexural strength had a good correlation with the experimental results. The R^2 values were between 0.684 and 0.968. Similar to the compressive strength, maturity index was used to predict the flexural strength by four equations (S_{LH}, S_{PH}, S_{LOG} and S_{EXP}).

5.2.1 Flexural Strength Development for Linear Hyperbolic Equivalent Age (LH_{eq})

Figure 35 presents the experimental and predicted flexural strength of SP0, SP1, SP2, SP3 and SP4 that obtained by linear hyperbolic equivalent age (eq_{LH}) with four models (S_{LH}, S_{PH} S_{LOG} and S_{EXP}). The regressions, which are parameters of all these four models were shown in Table 12. The ranges of correlation coefficient (R^2) were between 0.883 and 0.937. All the models have good correlation with experimental

results. However, the accuracy of linear hyperbolic and exponential equations are slightly higher than parabolic hyperbolic and logarithmic equations. The R^2 values of linear hyperbolic equation and exponential equation are approximately same. Similar to compressive strength the logarithmic equation (S_{LOG}) has the lowest (R^2) is all mixes.

For SP0 mixes the rates of correlation coefficient are 0.917, 0.901, 0.883 and 0.919 for linear hyperbolic, parabolic hyperbolic, logarithmic and exponential equations respectively. For SP1 the rates of correlation coefficient are 0.919, 0.912, 0.893 and 0.921 for linear hyperbolic, parabolic hyperbolic, logarithmic and exponential equations respectively. For SP2 mixes the rates of R^2 are 0.924, 0.905, 0.889 and 0.925 for S_{LH}, S_{PH} S_{LOG} and S_{EXP} equations respectively. The values of R^2 of SP3 for S_{LH}, S_{PH}, S_{LOG} and S_{EXP} equations are 0.934, 0.911, 0.895 and 0.935 respectively. For SP4 mix the values of correlation coefficient for S_{LH}, S_{PH} are 0.937 and 0.911 respectively, however these values for S_{LOG} and S_{EXP} are 0.891 and 0.937 respectively.

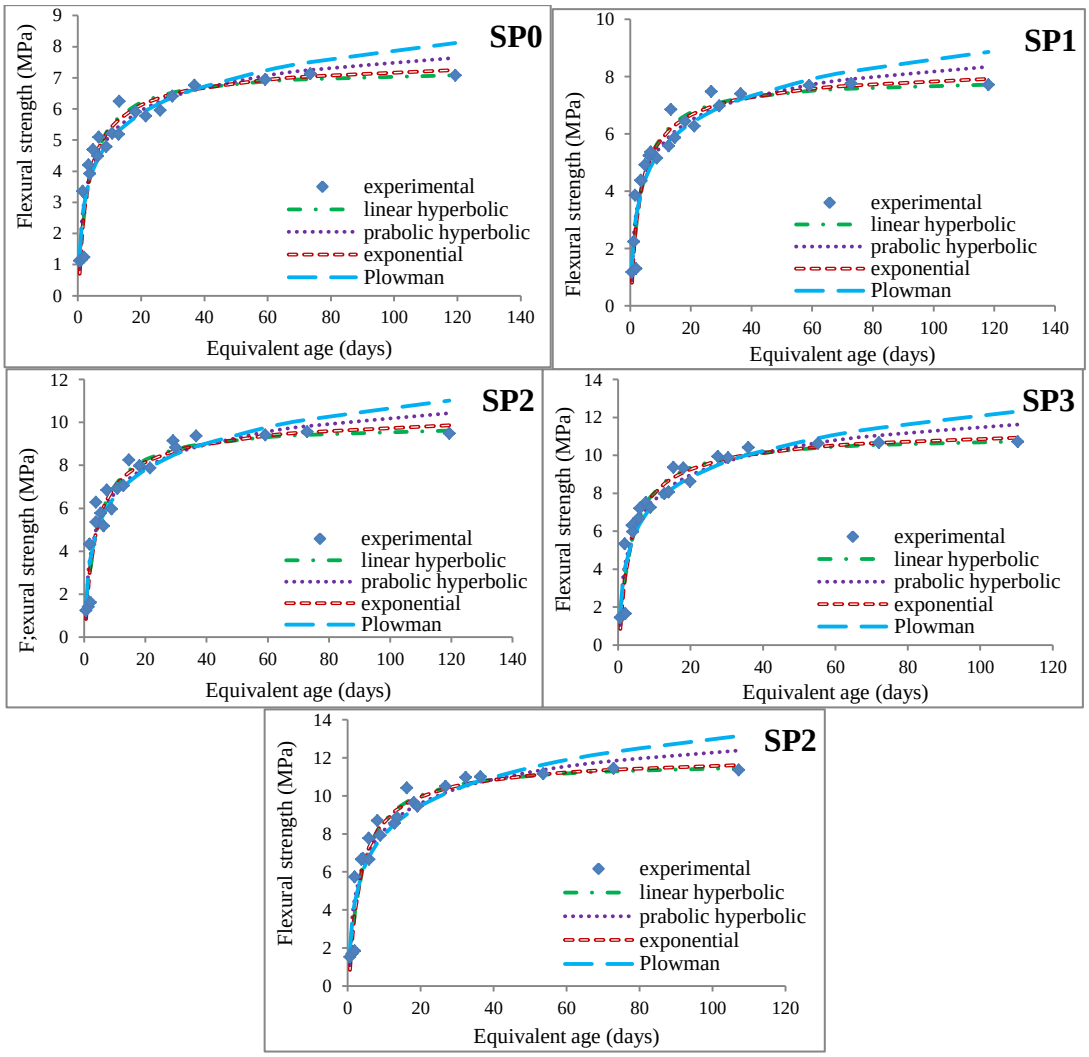

Figure 35: Predicted Flexural strength by LHeq method.

Table 12 : Regression parameters of flexural strength for LH_{eq}.

V_f	equation	Regression parameters							
		S_u	k_T	T_0	τ	α	a	b	R^2
SP0	Linear hyperbolic	7.289	0.284	0.028					0.963
	Parabolic hyperbolic	9.473	0.146	0.483					0.952
	Plowman						2.06	1.266	0.957
	exponential	7.861			2.22	0.631			0.964
SP1	Linear hyperbolic	7.995	0.279	0.049					0.965
	Parabolic hyperbolic	10.404	0.14	0.516					0.945
	Plowman						2.177	1.401	0.95
	exponential	8.627			2.299	0.625			0.965
SP2	Linear hyperbolic	9.949	0.244	0.076					0.95
	Parabolic hyperbolic	13.338	0.108	0.539					0.93
	Plowman						2.388	1.805	0.935
	exponential	10.837			2.664	0.622			0.949
SP3	Linear hyperbolic	11.091	0.272	0.193					0.954
	Parabolic hyperbolic	14.823	0.12	0.551					0.937
	Plowman						2.758	2.032	0.970
	exponential	11.779			2.467	0.683			0.954
SP4	Linear hyperbolic	11.841	0.127	0.245					0.942
	Parabolic hyperbolic	15.753	0.127	0.566					0.936
	Plowman						2.959	2.18	0.935
	exponential	12.412			2.416	0.716			0.952

5.2.2 Flexural Strength Development for Parabolic Hyperbolic Equivalent Age (PH_{eq})

Figure 36 presents the experimental and predicted flexural strength of SP0, SP1, SP2, SP3, and SP4 that are obtained by the parabolic hyperbolic equivalent age (eq_{PH}) with four modes (S_{LH}, S_{PH}, S_{LOG} and S_{EXP}). The regressions, which are parameters of all these four models, were shown in Table 13. The ranges of correlation coefficient (R^2) were between 0.711 and 0.84. Similar to eq_{LH}, all the models have a good correlation with experimental results. However, the R^2 that were obtained for SP0, SP1 and SP2 mixes are slightly lower than SP3 and SP4 mixes. The accuracy of linear hyperbolic, parabolic hyperbolic and exponential equations are approximately same. However, the accuracy ofthe logarithmic equation (S_{LOG}) is slightly lower than other equations.

For SP0 mixes the rates of correlation coefficient are 0.711, 0.728, 0.717 and 0.727 for the linear hyperbolic, parabolic hyperbolic, logarithmic and exponential equations respectively. For SP1 the rates of correlation coefficient are 0.725, 0.732, 0.714 and 0.732 for linear hyperbolic, parabolic hyperbolic, logarithmic and exponential equations respectively. For SP2 mixes the rates of R^2 are 0.718, 0.729, 0.716 and 0.729 for S_{LH}, S_{PH}, S_{LOG} and S_{EXP} equations respectively. The values of R^2 of SP3 for S_{LH}, S_{PH}, S_{LOG} and S_{EXP} equations are 0.821, 0.814, 0.79 and 0.822 respectively. For SP4 mixture, the values of the correlation coefficient for S_{LH}, S_{PH} are 0.82 and 0.84 respectively, however, these values for S_{LOG} and S_{EXP} are 0.799 and 0.836 respectively.

Table 13: Regression parameters of flexural strength for PHeq.

V_f	equation	Regression parameters							
		S_u	k_T	T_0	τ	α	a	b	R^2
SP0	Linear hyperbolic	6.864	0.305	-					0.963
	Parabolic hyperbolic	8.132	0.28	0.272					0.952
	Plowman						2.685	0.945	0.957
	exponential	8.175			1.608	0.412			0.964
SP1	Linear hyperbolic	7.569	0.289	-					0.965
	Parabolic hyperbolic	9.031	0.252	0.287					0.945
	Plowman						2.852	1.062	0.95
	exponential	8.942			1.725	0.425			0.965
SP2	Linear hyperbolic	9.505	0.235	-					0.95
	Parabolic hyperbolic	11.579	0.182	0.329					0.93
	Plowman						3.169	1.4	0.935
	exponential	11.423			2.274	0.42			0.949
SP3	Linear hyperbolic	10.79	0.265	0.189					0.954
	Parabolic hyperbolic	13.468	0.17	0.482					0.937
	Plowman						3.283	1.729	0.970
	exponential	11.966			2.216	0.555			0.954
SP4	Linear hyperbolic	11.596	0.267	-					0.942
	Parabolic hyperbolic	14.665	0.155	0.391					0.936
	Plowman						3.504	1.873	0.935
	exponential	12.64			2.23	0.59			0.952

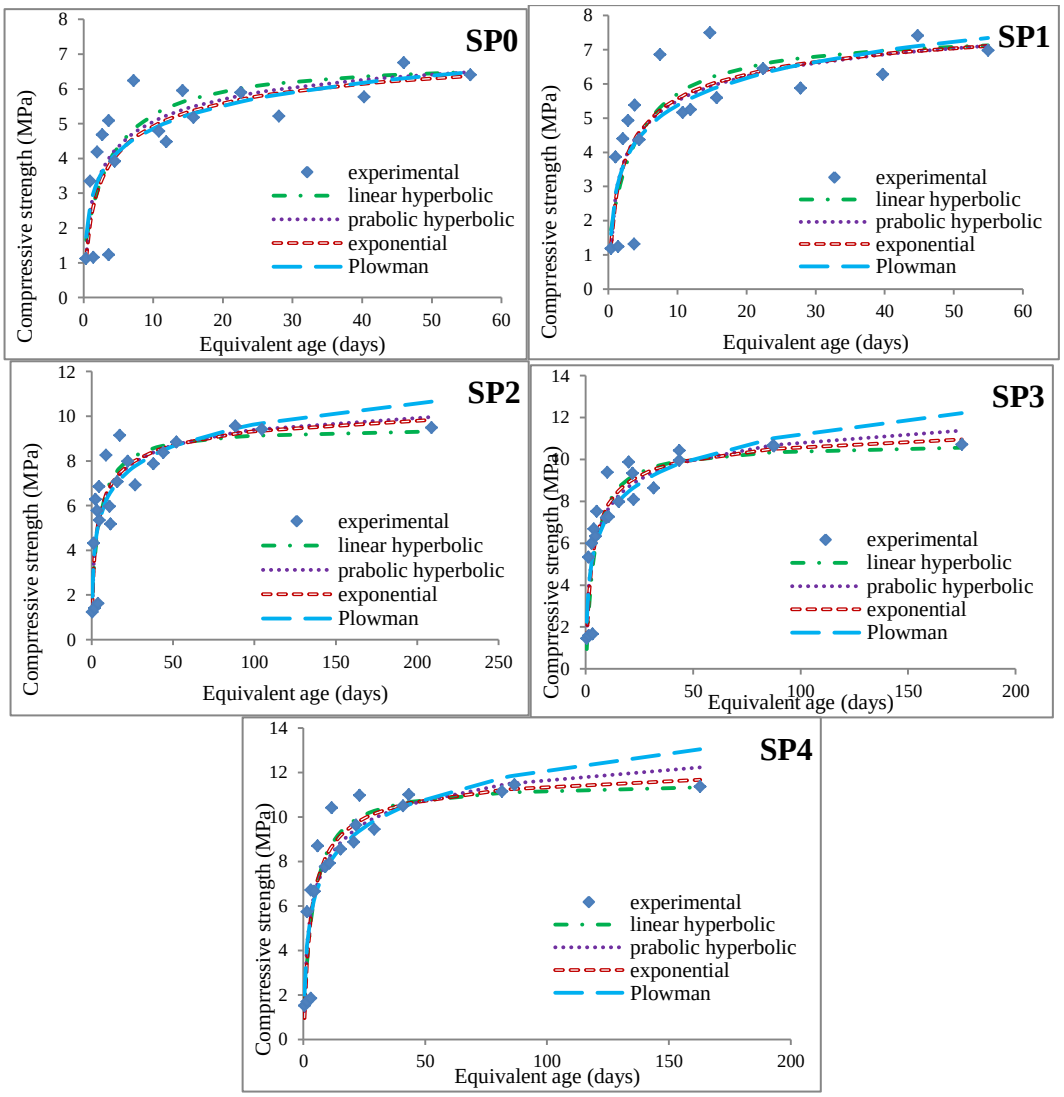

Figure 36: Predicted Flexural strength by PHeq method.

5.2.3 Flexural Strength Development for Exponential Equivalent Age (EXP_{eq})

Figure 37 presents the experimental and predicted compressive strength of SP0, SP1, SP2, SP3 and SP4 that are obtained by exponential equivalent age (eq_{EXP}) with four modes (S_{LH}, S_{PH}, S_{LOG} and S_{EXP}). The regressions, which are parameters of all these four models, were shown in Table 14. The ranges of correlation coefficient (R^2) are between 0.684 and 0.915. Just like the other equivalent ages (LH_{eq} and PH_{eq}), all the models have a good correlation with experimental results. However, the R^2 that was obtained for SP0 is lower than other mixes, but the R^2 which were obtained for other mixes have a good correlation with experimental results in all strength development

equations. The same applies for the compressive strength, the ranges of the R^2 for all strength development equations in this method (EXP_{eq}) are approximately the same.

For SP0 mixes the rates of correlation coefficient are 0.684, 0.705, 0.696 and 0.703 for linear hyperbolic, parabolic hyperbolic, logarithmic and exponential equations respectively. For SP1 the rates of correlation coefficient are 0.807, 0.801, 0.781 and 0.808 for linear hyperbolic, parabolic hyperbolic, logarithmic and exponential equations respectively. For SP2 mixes the rates of R^2 are 0.846, 0.838, 0.823 and 0.848 for S_{LH}, S_{PH}, S_{LOG} and S_{EXP} equations respectively. The values of R^2 of SP3 for S_{LH}, S_{PH}, S_{LOG} and S_{EXP} equations are 0.88, 0.862, 0.844 and 0.879 respectively. For SP4 mix the values of the correlation coefficient for S_{LH}, S_{PH} are 0.915 and 0.898 respectively, however, this value for S_{LOG} and S_{EXP} are 0.868 and 0.914 respectively.

Table 14: Regression parameters of flexural strength for EXPeq.

V_f	equation	Regression parameters							
		S_u	**k_T**	**T_0**	**τ**	**α**	**a**	**b**	**R^2**
SP0	Linear hyperbolic	6.82	0.305	-					0.955
	Parabolic hyperbolic	7.987	0.308	0.249					0.947
	Plowman						2.76	0.91	0.945
	exponential	78.26			1.541	0.385			0.959
SP1	Linear hyperbolic	7.722	0.287	-					0.94
	Parabolic hyperbolic	9.549	0.194	0.359					0.937
	Plowman						2.599	1.187	0.936
	exponential	8.744			1.954	0.509			0.944
SP2	Linear hyperbolic	9.809	0.236	-					0.95
	Parabolic hyperbolic	12.653	0.128	0.445					0.946
	Plowman						2.7	1.641	0.949
	exponential	11.093			2.553	0.534			0.954
SP3	Linear hyperbolic	10.96	0.262	-					0.94
	Parabolic hyperbolic	14.174	0.136	0.441					0.939
	Plowman						3.076	1.852	0.937
	exponential	11.939			2.368	0.605			0.945
SP4	Linear hyperbolic	11.797	0.274	0.148					0.946
	Parabolic hyperbolic	15.494	0.131	0.501					0.944
	Plowman						3.107	2.093	0.935
	exponential	12.434			2.39	0.691			0.947

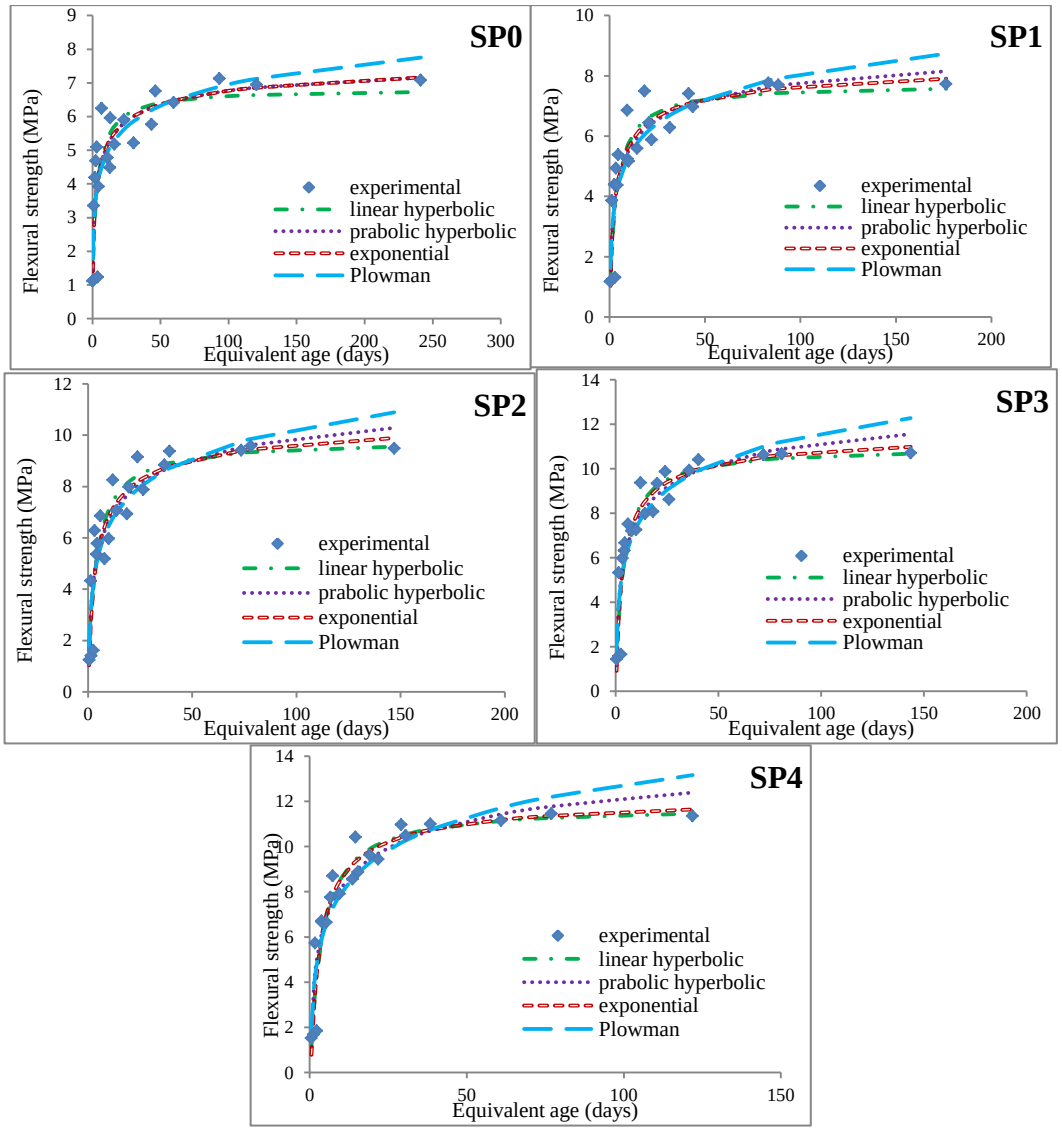

Figure 37: Predicted Flexural strength by EXPeq method.

5.2.4 Comparison of Flexural Strength Development between LH_{eq}, PH_{eq} and EXP_{eq}

As comparing the predicted flexural strength models between different equivalent ages (LH_{eq}, PH_{eq} and EXP_{eq}),similar to compressive strength the LH_{eq} has higher R^2 values in all mixes compare to other equivalent ages. The R^2 values of exponential equivalent age are slightly lower than LH_{eq}. However, the lowest values of R^2 are for parabolic hyperbolic equation.

5.2.5 Flexural Strength Development for Maturity Index (MI)

A similar study was performed to predict the flexural strength. Flexural strength was predicted for five different mixes (SP0, SP1, SP2, SP3, and SP4). For the compressive strength, the flexural strength was predicted by maturity index for five different mixes (SP0, SP1, SP2, SP3, and SP4). Furthermore, four equations (S_{LH}, S_{PH}, $S_{LOG,}$ and S_{EXP}) were used to predict flexural strength by maturity index.

Figure 38 presents the experimental and predicted flexural strength of SP0, SP1, SP2, SP3, and SP4 with four modes (S_{LH}, S_{PH}, S_{LOG} and S_{EXP}). The regressions, which are parameters of all these four models, were shown in Table 15. The ranges of correlation coefficient (R^2) were between 0.711 and 0.921. For the compressive strength, all the models have a good correlation with experimental results. The accuracy of S_{LH} and S_{EXP} are approximately the same and slightly higher than S_{PH} and S_{LOG}. However, the values of R^2 for all four models are very similar to each other.

For SP0 mixes the rates of correlation coefficient are 0.965, 0.953, 0.935 and 0.968 for linear hyperbolic, parabolic hyperbolic, logarithmic and exponential equations respectively. For SP1 the rates of correlation coefficient are 0.953, 0.944, 0.926 and 0.953 for linear hyperbolic, parabolic hyperbolic, logarithmic and exponential equations respectively. For SP2 mixes the rates of R^2 are 0.959, 0.944, 0.931 and 0.962 for S_{LH}, S_{PH}, S_{LOG} and S_{EXP} equations respectively. The values of R^2 for SP3 for S_{LH}, S_{PH}, S_{LOG} and S_{EXP} equations are 0.953, 0.935, 0.917 and 0.956 respectively. For SP4 mix the values of the correlation coefficient for S_{LH}, S_{PH} are 0.953 and 0.931 respectively, however, this value for S_{LOG} and S_{EXP} are 0.91 and 0.955 respectively.

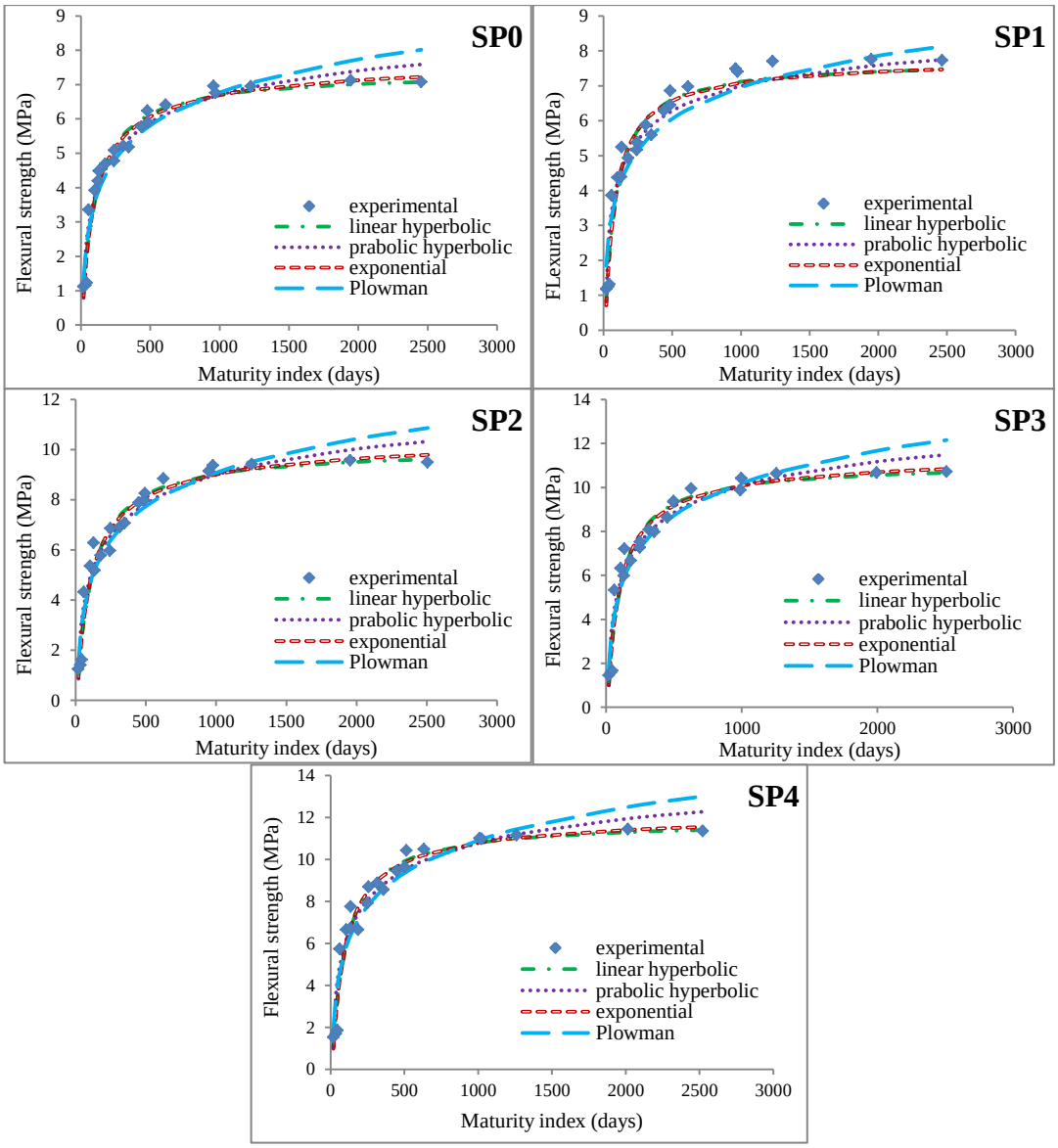

Figure 38: Predicted Flexural strength by MI.

Table 15 : Regression parameters of flexural strength for MI.

V_f	equation	Regression parameters							
		S_u	k_T	T_0	τ	α	a	b	R^2
SP0	Linear hyperbolic	7.362	0.01	5.387					0.963
	Parabolic hyperbolic	9.857	0.004	17.85					0.952
	Plowman						-2.817	1.388	0.957
	exponential	7.943			67.64	0.655			0.964
SP1	Linear hyperbolic	7.712	0.012	9.407					0.965
	Parabolic hyperbolic	9.517	0.008	18.39					0.945
	Plowman						-2.024	1.3	0.95
	exponential	7.849			58.23	0.8			0.965
SP2	Linear hyperbolic	10.037	0.009	6.94					0.95
	Parabolic hyperbolic	13.754	0.004	18.52					0.93
	Plowman						-4.307	1.938	0.935
	exponential	10.81			76.66	0.663			0.949
SP3	Linear hyperbolic	11.079	0.01	8.992					0.954
	Parabolic hyperbolic	14.982	0.004	18.19					0.937
	Plowman						-4.49	2.126	0.970
	exponential	11.724			69.11	0.708			0.954
SP4	Linear hyperbolic	11.832	0.01	9.742					0.942
	Parabolic hyperbolic	15.919	0.004	18.05					0.936
	Plowman						-4.735	2.265	0.935
	exponential	12.384			67.73	0.735			0.952

5.2.6. Validation of Flexural Strength Models

Like compressive strength, in order to assess the accuracy of the predicted flexural strengths of each model, the additional lines are provided with ranges of ±10 and ±20% error for the different volume fractions of the fibers.

5.2.6.1 Validation of Flexural Strength Models for LH_{eq}

Like compressive strength the percentage of errors in 1 day are very high; however, at later ages, the range of errors is between 0 and ±20%, as observed in Figures 39, 40, 41, 42 and 43. At 1 day of age, the parabolic hyperbolic equation (S_{PH}) has a higher error compared to other equations in all mixes; however, the percentage of error on the same day for S_{LOG} equation is higher than S_{LH} and S_{EXP}. At later ages (28 and 56 days) the errors of logarithmic equation (S_{LOG}) in all mixes are higher than other equations. The S_{LH} equation at later ages has the minimum error compared to other equations.

Figure 39 observes the correlation between experimental flexural strength and the predicted flexural strength of SP0 with linear hyperbolic, parabolic hyperbolic, logarithmic and exponential equations. The percentages of errors at day 1 were -117.8%, -145.4%, -137.8% and-118.2 % for S_{LH}, S_{PH}, S_{LOG} and S_{EXP} equations respectively. However, at 56 days the percentage of errors are 0%, -7.9%, -14.6% and -2.4% for S_{LH}, S_{PH}, S_{LOG} and S_{EXP} equations respectively.

Figure 40 shows a correlation between predicted and measured flexural strength with four equations (S_{LH}, S_{PH}, $S_{LOG,}$ and S_{EXP}) for the SP1 mixture. The percentages of error at 1 day were -114.3%, -148.5%, -140.4% and -121.2% for S_{LH}, S_{PH}, S_{LOG} and S_{EXP} equations respectively. However, at 56 days the percentage of errors are 0%, -8%, -14.8% and -2.6% for S_{LH}, S_{PH}, S_{LOG} and S_{EXP} equations respectively.

Figure 41 shows the predicted and measured flexural strength of SP2. The percentages of error at 1 day were -158.6%, -170.4%, -164.5% and -155.7% for S_{LH}, S_{PH}, S_{LOG} and S_{EXP} equations respectively. However, at 56 days the maximum percentages of errors are -0.7%, -8.4%, -14.7% and -4.2% for S_{LH}, S_{PH}, S_{LOG} and S_{EXP} equations respectively.

Figure 42 presents the estimated and measured flexural strength of SP3 mixture with four different equations. The maximum percentage of error at day 1 were -168.2%, -198.7% for S_{LH}, S_{PH} equations respectively, and on the sameday, the maximum percentage of error are -190.4% and -177.7% for S_{LOG} and S_{EXP} equations respectively. However, at 56 days the percentages of errors are -0.4%, -7.9%, -14.6% and -2.5% for S_{LH}, S_{PH}, S_{LOG} and S_{EXP} equations respectively.

Figure 43 presents the estimated and measured flexural strength of SP4 mixture with four different equations. The maximum percentage of error at 1 day were -133.1%, -171.2% for S_{LH}, S_{PH} equations respectively, and on the sameday, the percentage of error are -159.9% and -137.2% for S_{LOG} and S_{EXP} equations respectively. However, at 56 days the maximum percentages of errors for S_{LH} and $S_{PH}$are -0.8%, -9%, respectively, and for S_{LOG} and S_{EXP} are -15.9% and -2.5% respectively.

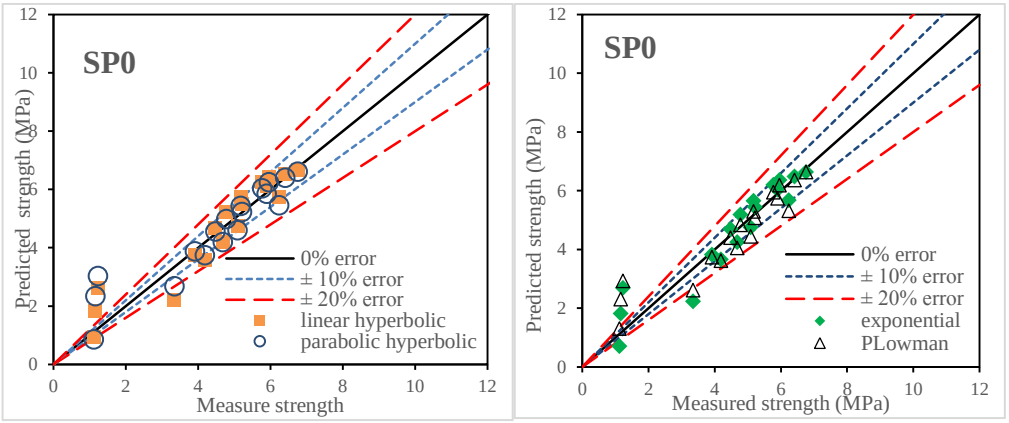

Figure 39: Measured versus predicted flexural strength by LHeq method for SP0: (a) linear and parabolic hyperbolic model and (b) exponential and Plowman model.

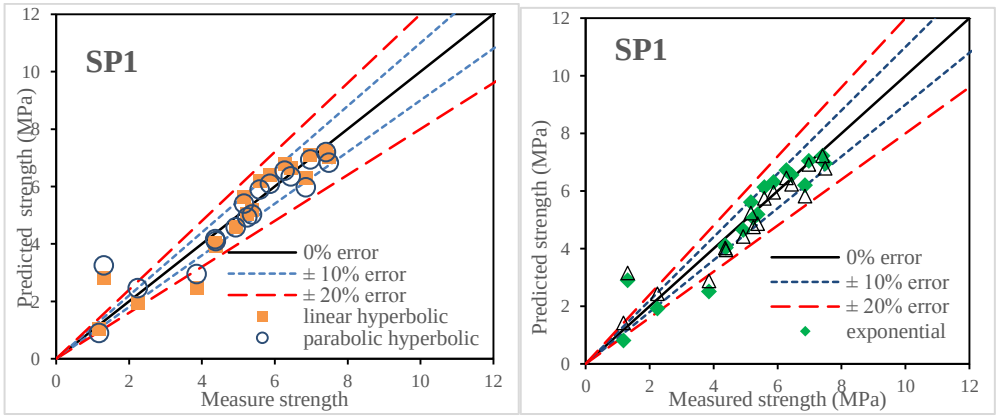

Figure 40: Measured versus predicted flexural strength by LHeq method for SP1: (a) linear and parabolic hyperbolic model and (b) exponential and Plowman model.

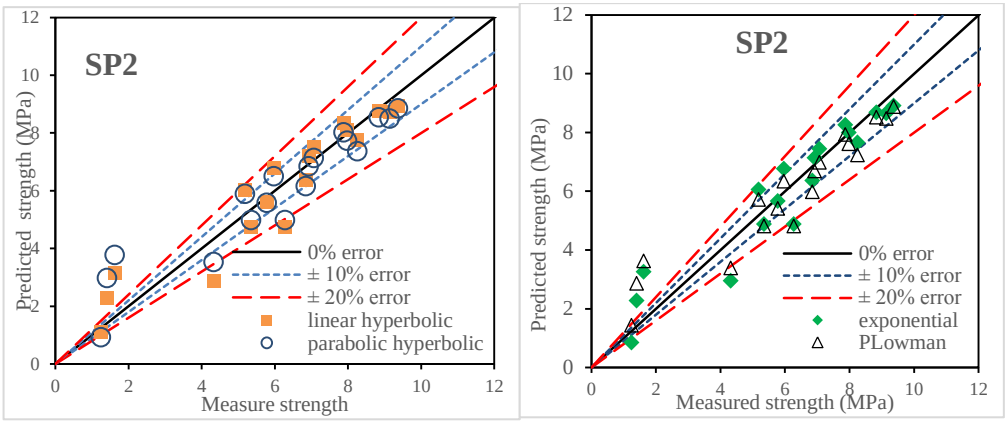

Figure 41: Measured versus predicted flexural strength by LHeq method for SP2: (a) linear and parabolic hyperbolic model and (b) exponential and Plowman model.

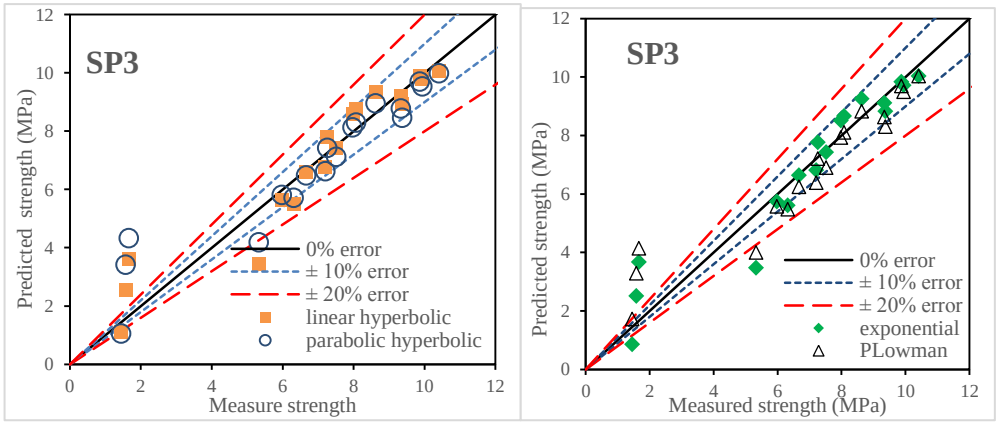

Figure 42: Measured versus predicted flexural strength by LHeq method for SP3: (a) linear and parabolic hyperbolic model and (b) exponential and Plowman model.

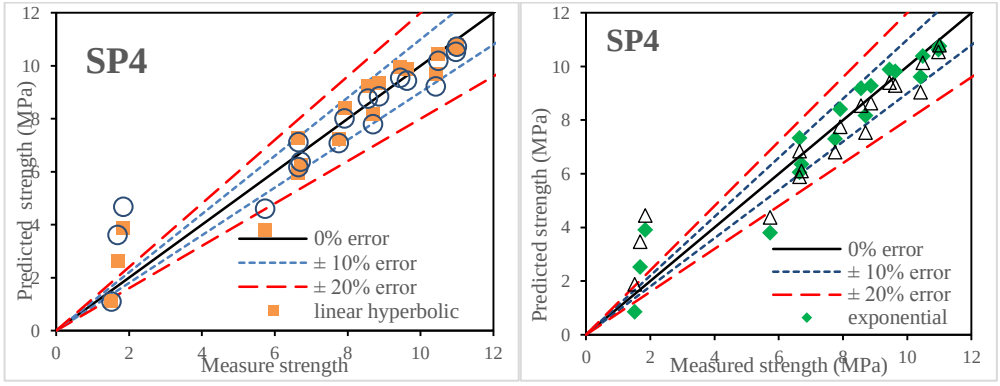

Figure 43: Measured versus predicted flexural strength by LHeq method for SP4: (a) linear and parabolic hyperbolic model and (b) exponential and Plowman model.

5.2.6.2 Validation of Flexural Strength Models for PH_{eq}

The results show that the percentages of errors in day 1 are significantly high. At older ages, the ranges of errors are between 0 and ±20%. However, at 3 days the percentages of error in some data are higher than ±20%. Figs. 44, 45, 5.46, 47 and 48 show the validation of SP0, SP1, SP2, SP3 and SP4 respectively. At 1 day age in all mixes, the maximum error is for parabolic hyperbolic (S_{PH}) equation; however, the linear hyperbolic equation at the same age has a minimum error. At later ages (28 and 56 days) the errors of logarithmic equation in all mixes are higher than other equations. The errors of the parabolic hyperbolic equation at later ages are slightly higher than linear hyperbolic and exponential equation.

Figure 44 observes the correlation between experimental compressive strength and predicted compressive strength of SP0 with linear hyperbolic, parabolic hyperbolic, logarithmic and exponential equations. The maximum percentages of error at 1 day were -216.4%, -223.3%, -217.2% and -208.3% for S_{LH}, S_{PH}, S_{LOG} and S_{EXP} equations respectively. However, at 56 days the percentage of errors are 4.4%, -2%, -10.2% and -0.3% for S_{LH}, S_{PH}, S_{LOG} and S_{EXP} equations respectively.

Figure 45 shows a correlation between predicted and measured compressive strength with four equations (S_{LH}, S_{PH}, $S_{LOG,}$ and S_{EXP}) for the SP1 mixture. The maximum percentages of errors at 1 day were -222.9%, -232.5%, -223.7% and -232.2% for S_{LH}, S_{PH}, S_{LOG} and S_{EXP} equations respectively. However, at 56 days the percentage of errors are 3.5%, -3.1%, -15.9% and -2% for S_{LH}, S_{PH}, S_{LOG} and S_{EXP} equations respectively.

Figure 46 shows the predicted and measured compressive strength of SP2. The maximum percentages of errors at 1 day were -202.1%, -216.2%, -210.7% and 214.5% for S_{LH}, S_{PH}, S_{LOG} and S_{EXP} equations respectively. However, at 56 days the maximum percentage of errors are 3.3%, -0.4%, -4% and 0.4% for S_{LH}, S_{PH}, S_{LOG} and S_{EXP} equations respectively.

Figure 47 presents the estimated and measured compressive strength of SP3 mixture with four different equations. The maximum percentage of error at 1 day were -186.5%, -226.4% for S_{LH}, S_{PH} equations respectively, and on the sameday, the maximum percentage of error are -217.2% and -216.5% for S_{LOG} and S_{EXP} equations respectively. However, at 56 days the percentage of errors are 1.4%, -6.2%, -14% and -2.2% for S_{LH}, S_{PH}, S_{LOG} and S_{EXP} equations respectively.

Figure 48 presents the estimated and measured compressive strength of SP4 mixture with four different equations. The maximum percentage of error at 1 day were -103.5%, -151.3% for S_{LH}, S_{PH} equations respectively, and on the sameday, the percentage of error are -149.3% and -107.2% for S_{LOG} and S_{EXP} equations respectively. However, at 56 days the maximum percentage of errors for S_{LH} and S_{PH} are 0.2%, -7.7%, respectively, and for S_{LOG} and S_{EXP} are -14.9% and -2.8% respectively.

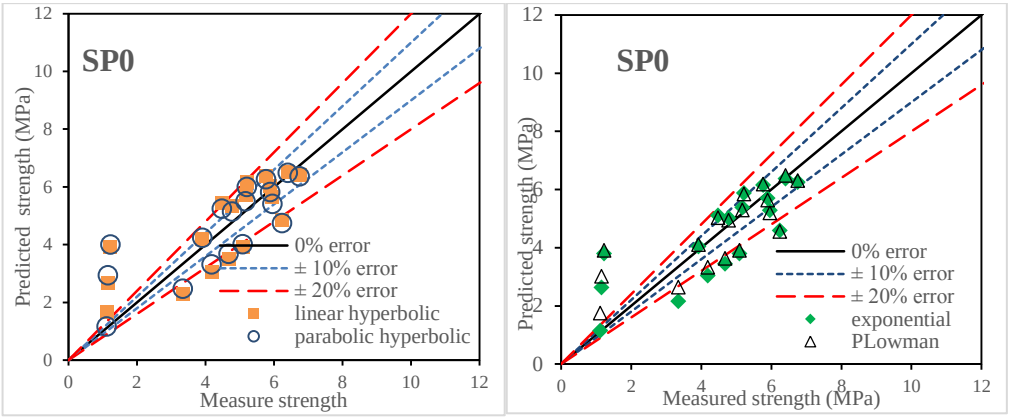

Figure 44: Measured versus predicted flexural strength by PHeq method for SP0: (a) linear and parabolic hyperbolic model and (b) exponential and Plowman model.

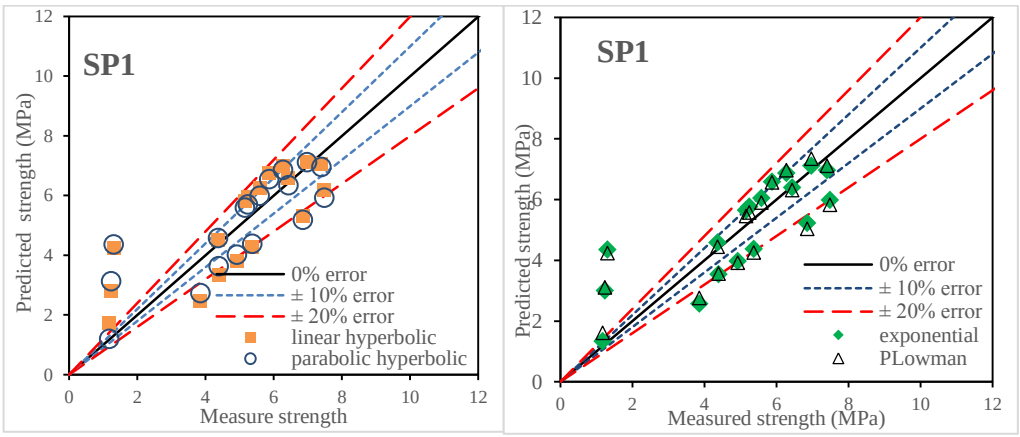

Figure 45: Measured versus predicted flexural strength by PHeq method for SP1: (a) linear and parabolic hyperbolic model and (b) exponential and Plowman model.

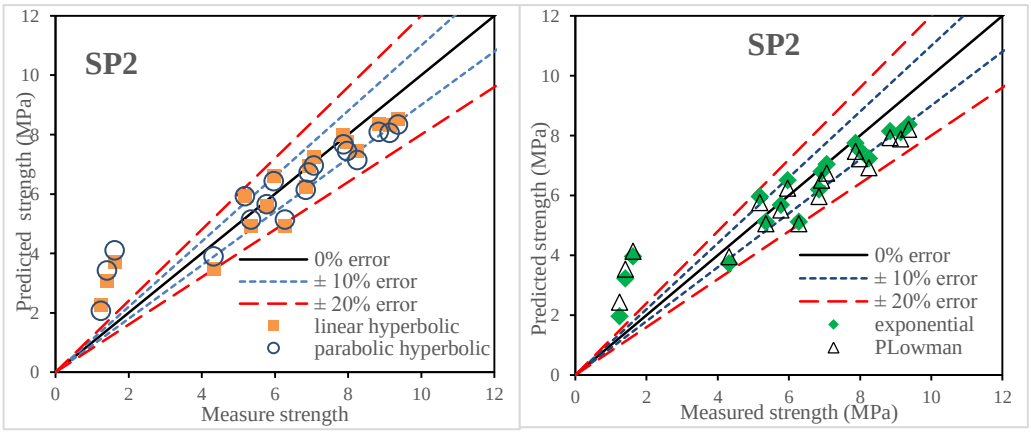

Figure 46: Measured versus predicted flexural strength by PHeq method for SP2: (a) linear and parabolic hyperbolic model and (b) exponential and Plowman model.

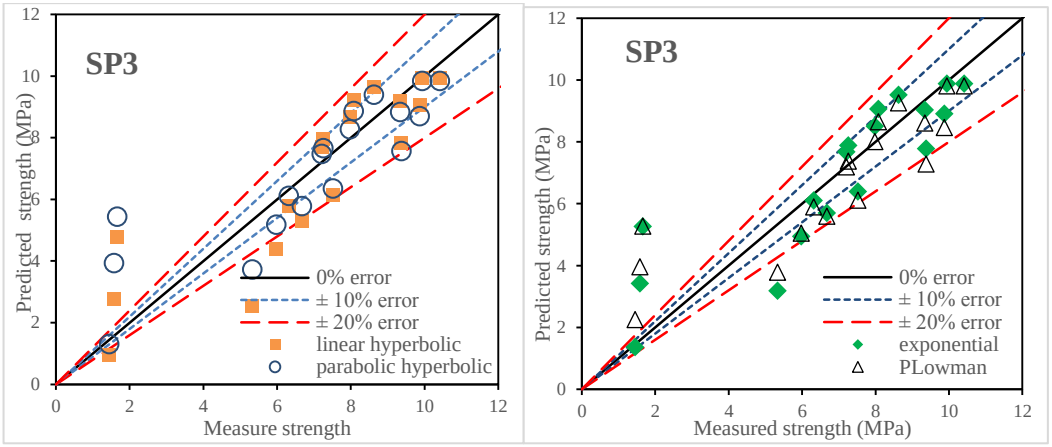

Figure 47: Measured versus predicted flexural strength by PHeq method for SP3: (a) linear and parabolic hyperbolic model and (b) exponential and Plowman model.

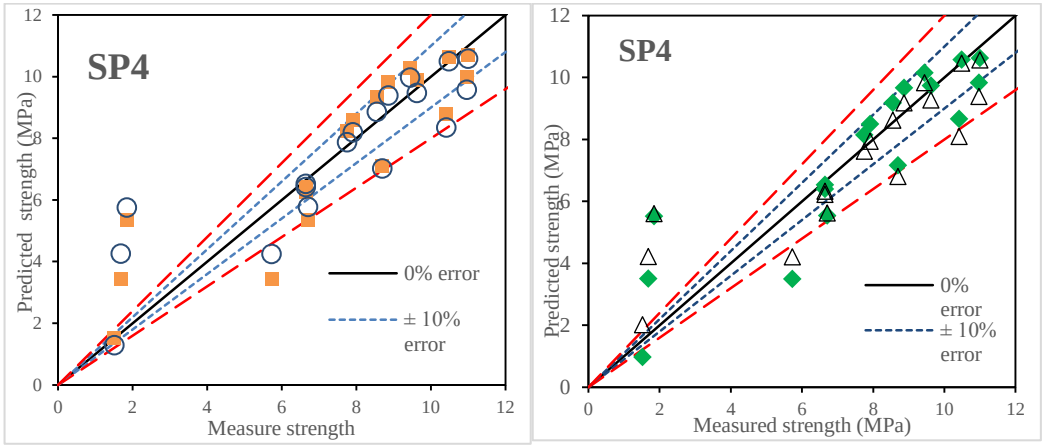

Figure 48: Measured versus predicted flexural strength by PHeq method for SP4: (a) linear and parabolic hyperbolic model and (b) exponential and Plowman model.

5.2.6.3 Validation Flexural Strength Models for EXP_{eq}

Figs 49, 50, 51, 52 and 53 exhibits the measured flexural strength versus estimated flexural strength for SP0, SP1, SP2, SP3 and SP4 mixes respectively. As shown in these figures the percentages of errors at 1 day are significantly high; at other ages, the range of errors is between 0 and ±20%, however the errors of some data at 3 and 7 days are higher than ±20%. At age of 1 day the parabolic hyperbolic equation (S_{PH}) and logarithmic has higher error compare to other equations in all mixes. The errors of linear hyperbolic at 1 day are lower than other equations. The highest error at later

ages is for logarithmic equation (S_{LOG}). However, at later ages linear hyperbolic equation has minimum error compare to other equations.

Figure 49 observe the correlation between experimental compressive strength and predicted compressive strength of SP0 with linear hyperbolic, parabolic hyperbolic, logarithmic and exponential equations. The percentage of error at 1 day were -226.6%,-234.3%, -225.1% and -233.8% for S_{LH}, S_{PH}, S_{LOG} and S_{EXP} equations respectively. However, at 56 days the percentage of errors are 5%, -1.1%, -9.5% and -1.2% for S_{LH}, S_{PH}, S_{LOG} and S_{EXP} equations respectively.

Figure 50 shows correlation between predicted and measured compressive strength with four equations (S_{LH}, S_{PH}, S_{LOG} and S_{EXP}) for SP1 mixture. The percentages of errors at 1 day were -185.4%,-202.6%, -196.4% and -196.8% for S_{LH},S_{PH}, S_{LOG} and S_{EXP} equations respectively. However, at 56 days the percentage of errors are 2%, -5.6%, -13.1% and -2.3% for S_{LH}, S_{PH}, S_{LOG} and S_{EXP} equations respectively.

Figure 51 shows the predicted and measured compressive strength of SP2. The maximum percentages of errors at 1 day were -158.6%, -170.4%, -164.5% and -155.7% for S_{LH}, S_{PH}, S_{LOG} and S_{EXP} equations respectively. However, at 56 days the maximum percentage of errors are -0.7%, -8.4%, -14.7% and -4.2% for S_{LH},S_{PH}, S_{LOG} and S_{EXP} equations respectively.

Figure 52 presents estimated and measured compressive strength of SP3 mixture with four different equations. The maximum percentages of errors at 1 day were -168.2%, -198.7% for S_{LH},S_{PH} equations respectively and at same day the maximum percentage of error are -190.4% and -177.4% for S_{LOG} and S_{EXP} equations

respectively. However, at 56 days the percentage of errors are 4%, -7.9%, -14.6% and -2.5% for S_{LH}, S_{PH}, S_{LOG} and S_{EXP} equations respectively.

Figure 53 presents estimated and measured compressive strength of SP4 mixture with four different equations. The maximum percentage of error at 1 day were -133.1%, -171.2% for S_{LH},S_{PH} equations respectively and at same day the percentage of error are -159.9% and -137.2% for S_{LOG} and S_{EXP} equations respectively. However, at 56 days the maximum percentage of errors for S_{LH} andS_{PH} are -0.8%, -9% respectively, and for S_{LOG} and S_{EXP} are -15.9% and -2.5% respectively.

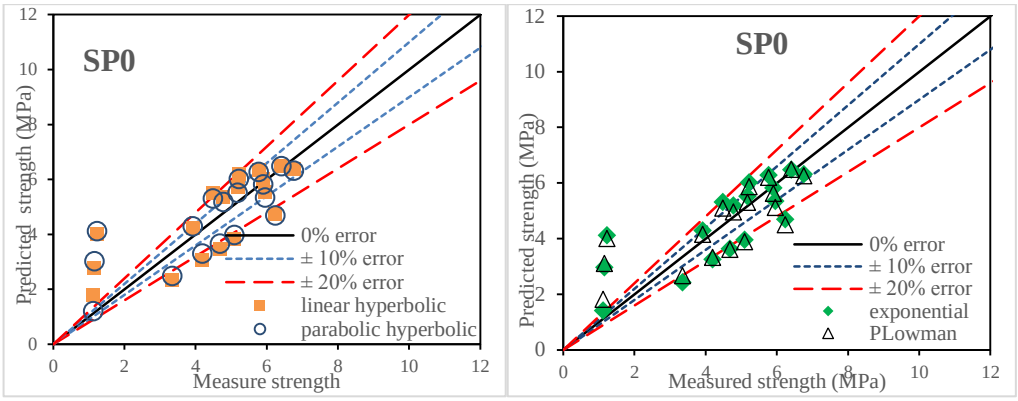

Figure 49: Measured versus predicted flexural strength by EXPeq method for SP0: (a) linear and parabolic hyperbolic model and (b) exponential and Plowman model.

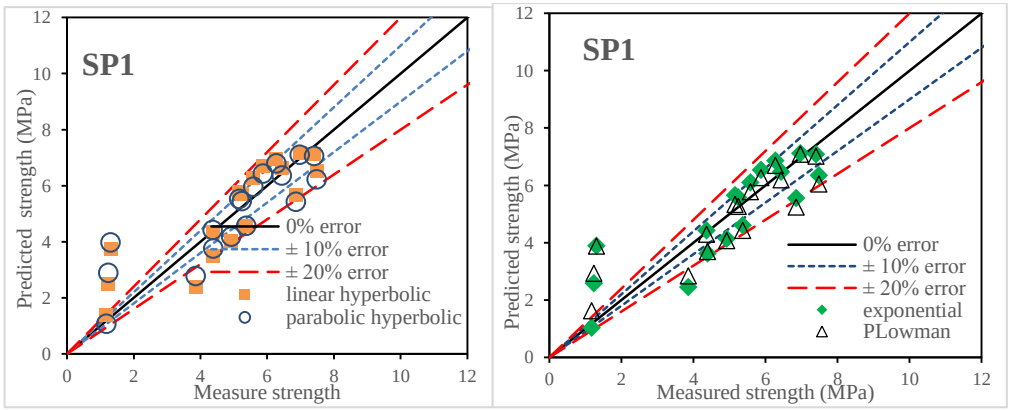

Figure 50: Measured versus predicted flexural strength by EXPeq method for SP1: (a) linear and parabolic hyperbolic model and (b) exponential and Plowman model.

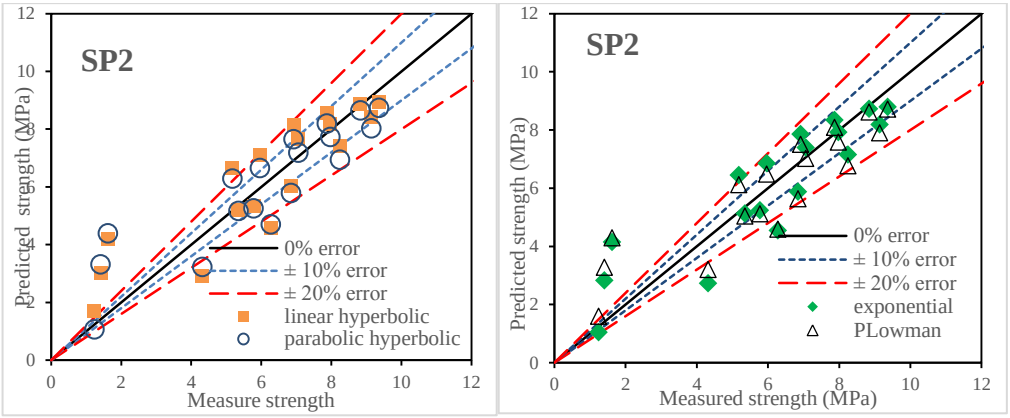

Figure 51: Measured versus predicted flexural strength by EXPeq method for SP2: (a) linear and parabolic hyperbolic model and (b) exponential and Plowman model.

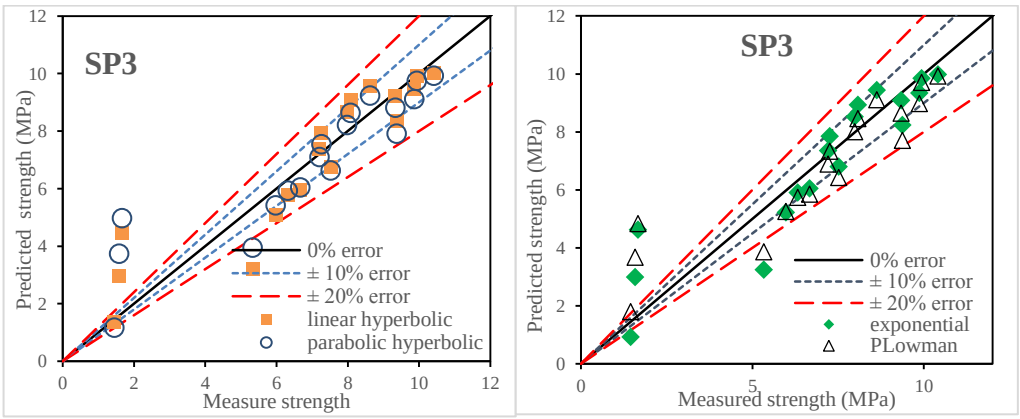

Figure 52: Measured versus predicted flexural strength by EXPeq method for SP3: (a) linear and parabolic hyperbolic model and (b) exponential and Plowman model.

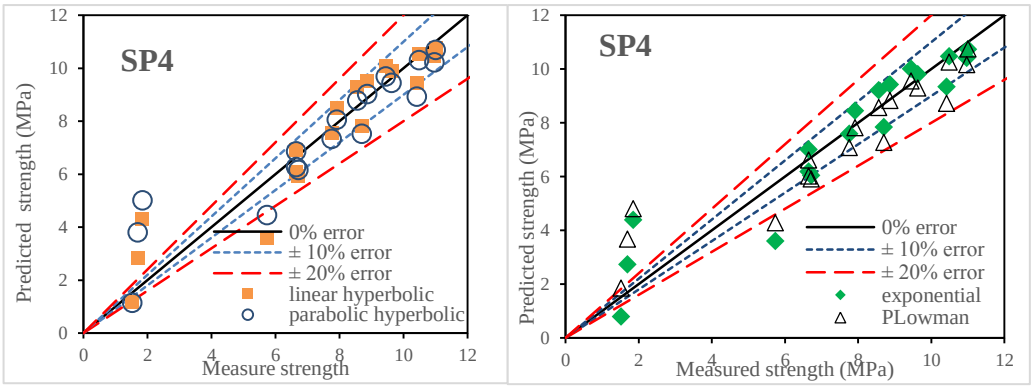

Figure 53: Measured versus predicted flexural strength by EXPeq method for SP4: (a) linear and parabolic hyperbolic model and (b) exponential and Plowman model.

5.2.6.4 Validation of Flexural Strength Models for MI

Similar to the compressive strength, the percentage of errors of flexural strength that are obtained by maturity index at 1 day is very high; however, at other ages, the range of errors is between 0 and ±20%, only one data at age of 3 days in all mixes have a percentage of error of more than ±20%, as observed in Figures 54, 55, 56, 57 and 58. At an early age of 1 day S_{PH} and S_{LOG} have a higher errors compare to S_{LH} and S_{EXP} in all mixes, however, the percentage of errors for S_{LH} and S_{EXP} at 1 day are very close to each other. At later ages (28 and 56 days) the errors of logarithmic equation (S_{LOG}) in all mixes are higher than other equations. The S_{LH} equation at later ages has the minimum error compared to other equations.

Figure 54 observes the correlation between experimental flexural strength and the predicted flexural strength of SP0 with linear hyperbolic, parabolic hyperbolic, logarithmic and exponential equations. The percentages of errors at 1 day were -60.6%, -99.5%, -92.1% and -64% for S_{LH}, S_{PH}, S_{LOG} and S_{EXP} equations respectively. However, at 56 days the percentage of errors are 0.1%, -7.2%, -13.2% and -2% for S_{LH}, S_{PH}, S_{LOG} and S_{EXP} equations respectively.

Figure 55 shows a correlation between the predicted and measured flexural strength with four equations (S_{LH}, S_{PH}, $S_{LOG,}$ and S_{EXP}) for the SP1 mixture. The percentages of errors at 1 day were -64%, -116.3%, -115% and -61% for S_{LH}, S_{PH}, S_{LOG} and S_{EXP} equations respectively. However, at 56 days the percentage of errors are 3.4%, -0.3%, -5.2% and -3.3% for S_{LH}, S_{PH}, S_{LOG} and S_{EXP} equations respectively.

Figure 56 shows the predicted and measured flexural strength of SP2. The percentages of errors at 1 day were -55.6%, -99.1%, -87.6% and -58.3% for S_{LH}, S_{PH},

S_{LOG} and S_{EXP}equations respectively. However, at 56 days the maximum percentages of errors are -1.3%, -8.8%, -14.5% and -3.2% for S_{LH}, S_{PH}, S_{LOG} and S_{EXP} equations respectively.

Figure 57 presents the estimated and measured flexural strength of SP3 mixture with four different equations. The maximum percentage of error at 1 day were -77.5%, -127.2% for S_{LH}, S_{PH} equations respectively, and on the sameday, the maximum percentage of error are -115% and -79.6% for S_{LOG} and S_{EXP} equations respectively. However, at 56 days, the percentage of errors are 0.5%, -7.2%, -13.4% and -1.1% for S_{LH}, S_{PH}, S_{LOG} and S_{EXP} equations respectively.

Figure 58 presents the estimated and measured flexural strength of SP4 mixture with four different equations. The maximum percentage of error at 1 day were -77.5%, -127.2% for S_{LH}, S_{PH} equations respectively, and on the sameday, the percentage of error are -115% and -79.6% for S_{LOG} and S_{EXP} equations respectively. However, at 56 days the maximum percentages of errors for S_{LH} and $S_{PH}$are -0.4%, -8.1%, respectively, and for S_{LOG} and S_{EXP} are -14.5% and -1.7% respectively.

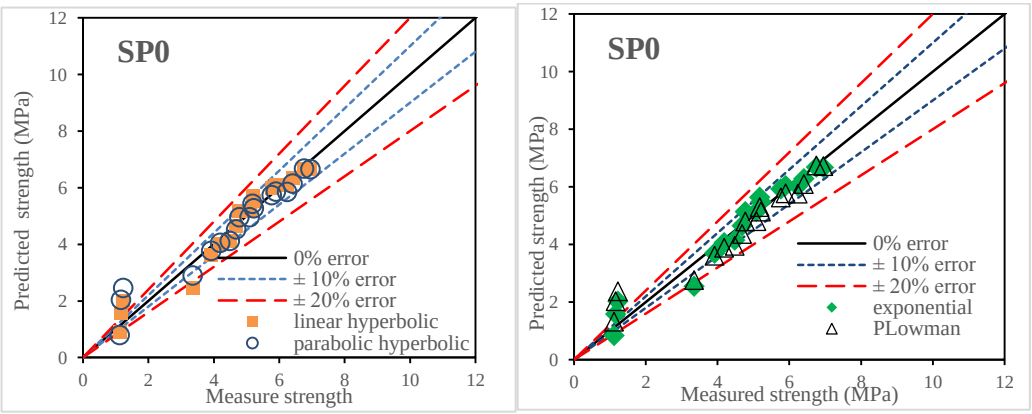

Figure 54: Measured versus predicted flexural strength by MI method for SP0: (a) linear and parabolic hyperbolic model and (b) exponential and Plowman model.

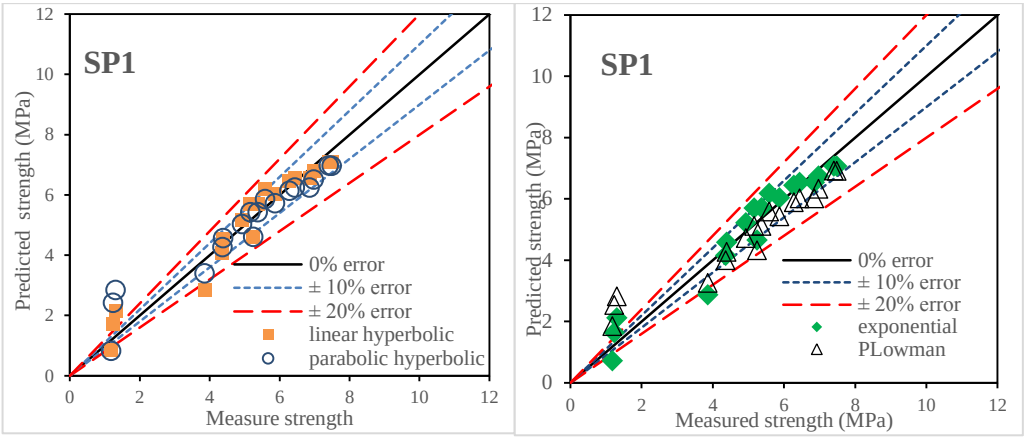

Figure 55: Measured versus predicted flexural strength by MI method for SP1: (a) linear and parabolic hyperbolic model and (b) exponential and Plowman model.

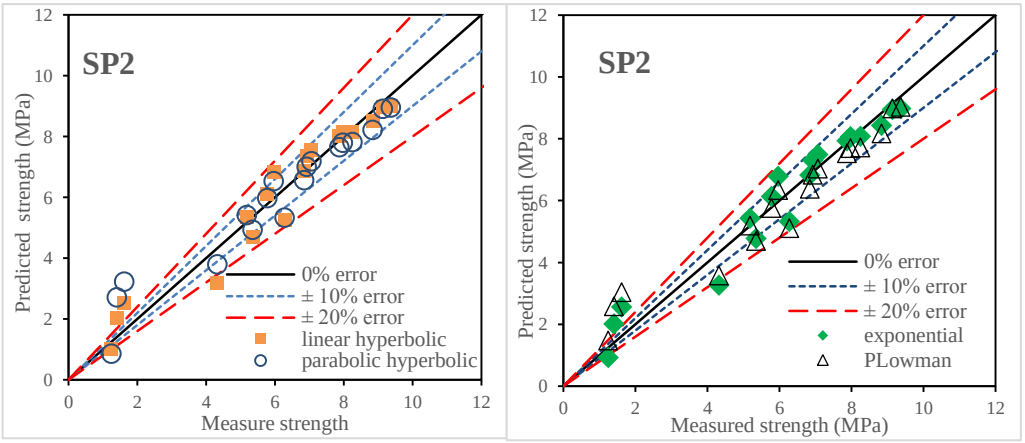

Figure 56: Measured versus predicted flexural strength by MI method for SP2: (a) linear and parabolic hyperbolic model and (b) exponential and Plowman model.

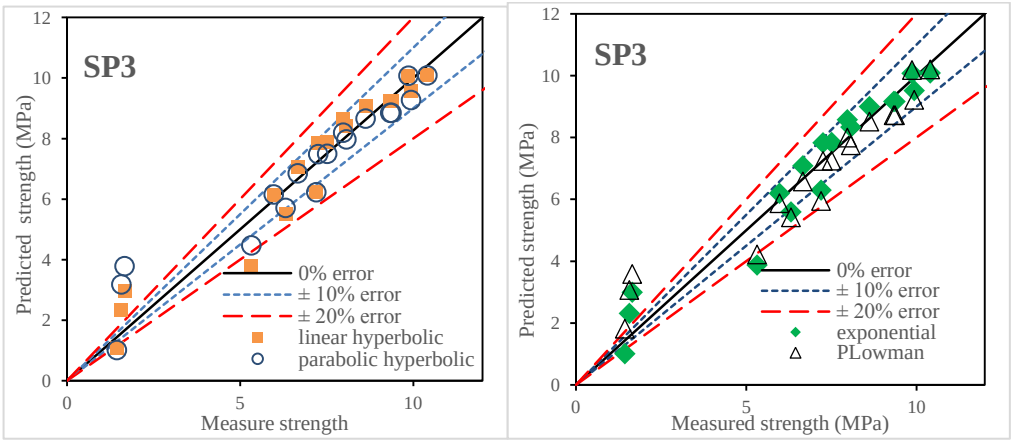

Figure 57: Measured versus predicted flexural strength by MI method for SP3: (a) linear and parabolic hyperbolic model and (b) exponential and Plowman model.

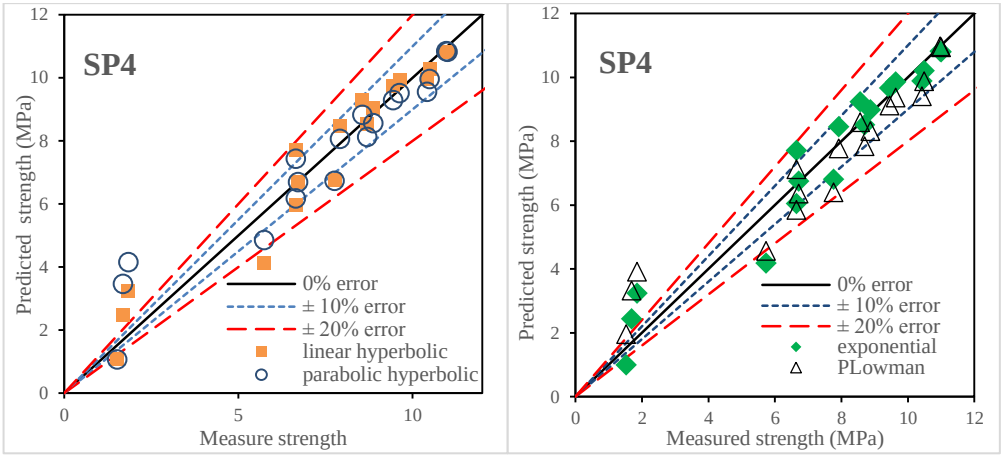

Figure 58: Measured versus predicted flexural strength by MI method for SP4: (a) linear and parabolic hyperbolic model and (b) exponential and Plowman model.

5.3 Models for Flexural Toughness

In order to predict the flexural toughness, three equivalent ages (LH_{eq}, PH_{eq} and EXP_{eq}) and maturity index were obtained for all the volume fractions of fibers at three different curing temperatures. After calculating the equivalent ages and maturity index, the flexural toughness was predicted by four models (S_{LH}, S_{PH},$S_{LOG,}$ and S_{EXP}). The results show that all four equations have a high approximation with experimental results, the range of correlation coefficient (R2) of all mixtures of all of the models are between 0.677-0.987.

5.3.1 Flexural Toughness Development for Linear Hyperbolic Equivalent Age (LH_{eq})

Figure 59 presents the experimental and predicted flexural toughness of SP0, SP1, SP2, SP3, and SP4 that were obtained by linear hyperbolic equivalent age (LH_{eq}) with four modes (S_{LH}, S_{PH}, $S_{LOG,}$ and S_{EXP}). The regressions, which are parameters of all these four models, were shown in Table 16. The ranges of correlation coefficient (R^2) are between 0.906 and 0.987. All the models have a very good correlation with experimental results. The values of R^2 for all the mixes and with all

models are higher than 0.9. However, in this method, the ranges of R^2 of all four models are very close to each other.

For SP0 mixes the rates of correlation coefficient are 0.958, 0.947, 0.957 and 0.925 for linear hyperbolic, parabolic hyperbolic, logarithmic and exponential equations respectively. For SP1, the rates of correlation coefficient are 0.931, 0.938, 0.937 and 0.939 for linear hyperbolic, parabolic hyperbolic, logarithmic and exponential equations respectively. For SP2 mixes the rates of R^2 are 0.906, 0.914, 0.914 and 0.915 for S_{LH}, S_{PH}, S_{LOG} and S_{EXP} equations respectively. The values of R^2 for SP3 for S_{LH}, S_{PH}, S_{LOG} and S_{EXP} equations are 0.951, 0.963, 0.987 and 0.963 respectively. For SP4 mix the values of the correlation coefficient for S_{LH}, S_{PH} are 0.942 and 0.939 respectively, however, this value for S_{LOG} and S_{EXP} are 0.935 and 0.938 respectively.

Table 16: Regression parameters of flexural toughness for LHeq.

V_f	equation	Regression parameters							
		S_u	**k_T**	**T_0**	**τ**	**α**	**a**	**b**	**R^2**
SP0	Linear hyperbolic	6.506	0.185	-					0.896
	Parabolic hyperbolic	8.252	0.119	1.054					0.947
	Plowman						1.491	1.115	0.893
	exponential	7.076			3.261	0.608			0.9
SP1	Linear hyperbolic	99.285	0.078	-					0.929
	Parabolic hyperbolic	139.873	0.034	0.303					0.924
	Plowman						13.8	13.87	0.923
	exponential	194.676			33.14	0.244			0.926
SP2	Linear hyperbolic	152.134	0.065	-					0.897
	Parabolic hyperbolic	219.816	0.025	0.156					0.901
	Plowman						17.69	25.03	0.896
	exponential	365.808			96.74	0.208			0.902
SP3	Linear hyperbolic	180.465	0.205	-					0.891
	Parabolic hyperbolic	209.165	0.272	0.702					0.996
	Plowman						68.69	24.58	0.888
	exponential	207.791			1.91	0.444			0.896
SP4	Linear hyperbolic	222.841	0.122	-					0.923
	Parabolic hyperbolic	269.892	0.121	-					0.921
	Plowman						71.55	30.64	0.918
	exponential	324.352			4.844	0.275			0.919

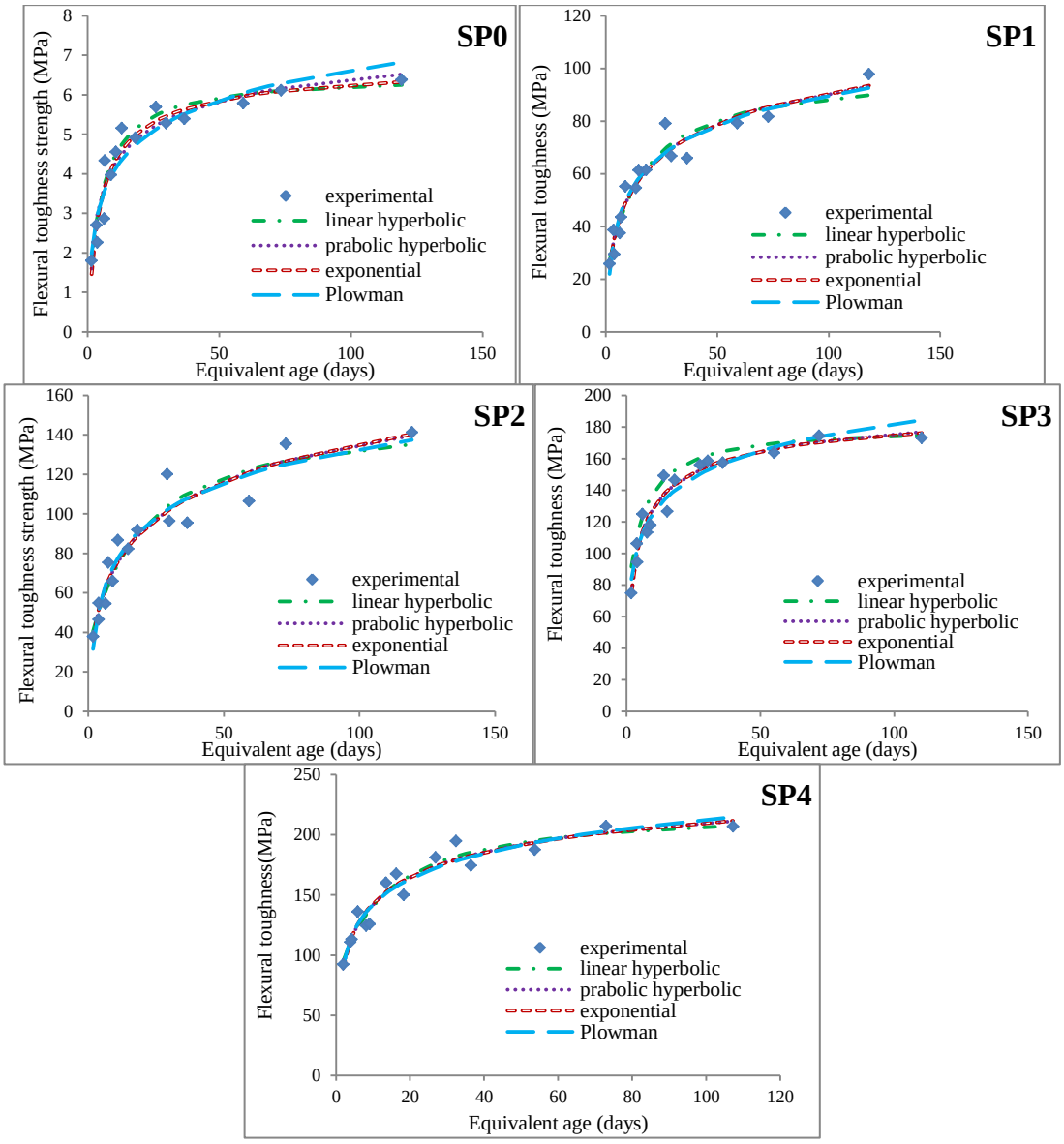

Figure 59: Predicted Flexural toughness by LHeq method.

5.3.2 Flexural Toughness Development for Parabolic Hyperbolic Equivalent Age (PH_{eq})

Figure 60 presents the experimental and predicted flexural toughness of SP0, SP1, SP2, SP3, and SP4 that were obtained by parabolic hyperbolic equivalent age (PH_{eq}) with four modes (S_{LH}, S_{PH}, S_{LOG} ,and S_{EXP}). The regressions, which are parameters of all these four models, were shown in Table 17. The ranges of correlation coefficient (R^2) were between 0.698 and 0.981. All the models have good correlation with experimental results. However, the R^2 that obtains for SP0 and SP2 are slightly

lower than other mixes, but SP3 and SP4 have a very good correlation with experimental results. For all mixes (except SP1) the logarithmic equation has the lowest value of R^2. For SP1 the lowest value of R^2 is a linear hyperbolic equation. The highest value of R^2 is for the exponential equation for all mixes (except SP0). For SP0 the highest value is in the parabolic hyperbolic equation.

For SP0 mixes the rates of correlation coefficient are 0.699, 0.72, 0.717 and 0.698 for linear hyperbolic, parabolic hyperbolic, logarithmic and exponential equations respectively. For SP1 the rates of correlation coefficient are 0.835, 0.857, 0.861 and 0.862 for linear hyperbolic, parabolic hyperbolic, logarithmic and exponential equations respectively. For SP2 mixes the rates of R^2 are 0.744, 0.759, 0.76 and 0.764 for S_{LH}, S_{PH}, S_{LOG} and S_{EXP} equations respectively. The values of R^2 of SP3 for S_{LH}, S_{PH}, S_{LOG} and S_{EXP} equations are 0.966, 0.963, 0.936 and 0.963 respectively. For SP4 mix the values of the correlation coefficient for S_{LH}, S_{PH} are 0.981 and 0.979.

Table 17: Regression parameters of flexural toughness for PHeq.

V_f	equation	Regression parameters							
		S_u	k_T	T_0	τ	α	a	b	R^2
SP0	Linear hyperbolic	6.121	0.177	-					0.955
	Parabolic hyperbolic	7.035	0.234	0.37					0.947
	Plowman						2.27	0.791	0.945
	exponential	7.925			2.468	0.322			0.959
SP1	Linear hyperbolic	91.475	0.121	-					0.94
	Parabolic hyperbolic	119.6	0.072	-					0.937
	Plowman						23.56	13.83	0.936
	exponential	185.97			25.77	0.211			0.944
SP2	Linear hyperbolic	139.78	0.062	-					0.95
	Parabolic hyperbolic	176.83	0.046	-					0.946
	Plowman						33.46	18.55	0.949
	exponential	11.503			3.077	0.593			0.954
SP3	Linear hyperbolic	176.95	0.208	-					0.94
	Parabolic hyperbolic	200.6	0.317	0.264					0.939
	Plowman						76.08	21.17	0.937
	exponential	205			1.477	0.397			0.945
SP4	Linear hyperbolic	212.97	0.137	-					0.946
	Parabolic hyperbolic	249.04	0.168	-					0.944
	Plowman						81.78	26.06	0.935
	exponential	12.100			2.350	0.783			0.947

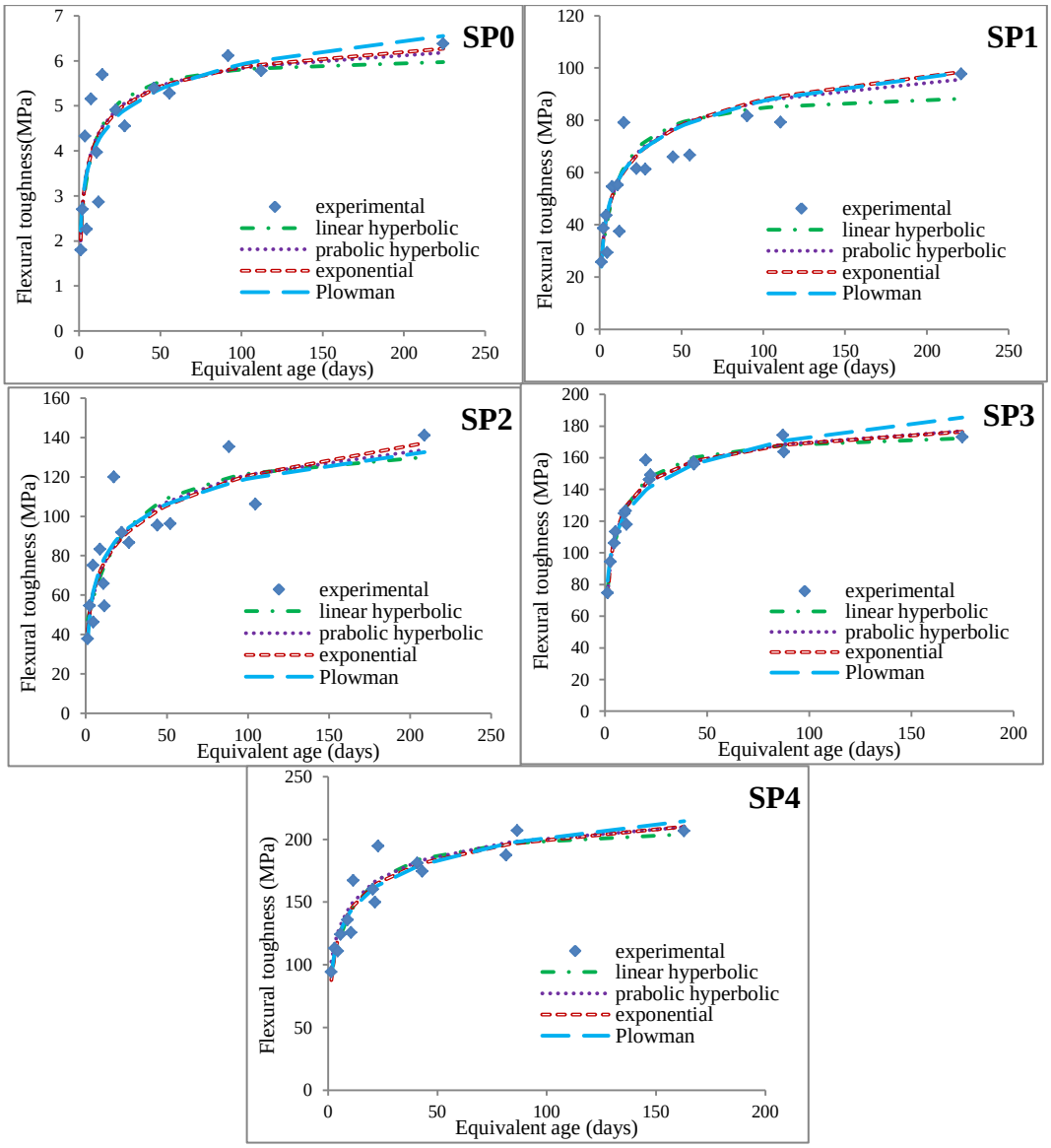

Figure 60: Predicted Flexural toughness by PHeq method.

5.3.3 Flexural Toughness Development for Exponential Equivalent Age (EXP_{eq})

Figure 61 presents the experimental and predicted flexural toughness of SP0, SP1, SP2, SP3 and SP4 that were obtained by exponential equivalent age with four models (S_{LH}, S_{PH}, S_{LOG} and S_{EXP}). The regressions, which are parameters of all these four models were shown in Table 18. The ranges of correlation coefficient (R^2) were between 0.667 and 0.985. Similar to other equivalent ages (LH_{eq} and PH_{eq}), all the models have a good correlation with experimental results. However, the R^2 that obtains for SP0 is lower than other mixes. However, SP3 and SP4 have a very good

correlation with predicted models and experimental results. In this method, the range of the R^2 for all strength development equations in this method is very similar to each other.

For SP0 mixes the rates of correlation coefficient are 0.667, 0.695, 0.694 and 0.697 for linear hyperbolic, parabolic hyperbolic, logarithmic and exponential equations respectively. For SP1, the rates of correlation coefficient are 0.849, 0.862, 0.863 and 0.865 for linear hyperbolic, parabolic hyperbolic, logarithmic and exponential equations respectively. For SP2 mixes the rates of R^2 are 0.861, 0.867, 0.862 and 0.867 for S_{LH}, S_{PH} S_{LOG} and S_{EXP} equations respectively. The values of R^2 for SP3 for S_{LH}, S_{PH}, S_{LOG} and S_{EXP} equations are 0.963, 0.962, 0.985 and 0.956 respectively. For SP4 mix the values of the correlation coefficient for S_{LH}, S_{PH} are 0.936 and 0.933 respectively, however, this value for S_{LOG} and S_{EXP} are 0.926 and 0.93 respectively.

Table 18: Regression parameters of flexural toughness for EXPeq.

V_f	equation	Regression parameters							
		S_u	**k_T**	**T_0**	**τ**	**α**	**a**	**b**	**R^2**
SP0	Linear hyperbolic	6.078	0.176	-					0.955
	Parabolic hyperbolic	6.895	0.264	0.329					0.947
	Plowman						2.354	0.759	0.945
	exponential	8.069			2.419	0.298			0.959
SP1	Linear hyperbolic	94.306	0.079	-					0.94
	Parabolic hyperbolic	123.69	0.047	-					0.937
	Plowman						20.5	13.75	0.936
	exponential	259.32			198.2	0.162			0.944
SP2	Linear hyperbolic	146.23	0.066	-					0.95
	Parabolic hyperbolic	201.04	0.032	-					0.946
	Plowman						24.52	22.23	0.949
	exponential	411.22			235.1	0.171			0.954
SP3	Linear hyperbolic	178.93	0.204	-					0.94
	Parabolic hyperbolic	205.48	0.282	0.421					0.939
	Plowman						72.3	22.81	0.937
	exponential	206.2			1.707	0.422			0.945
SP4	Linear hyperbolic	219.55	0.128	-					0.946
	Parabolic hyperbolic	263.42	0.134	-					0.944
	Plowman						74.18	29.38	0.935
	exponential	310.13			4.037	0.281			0.947

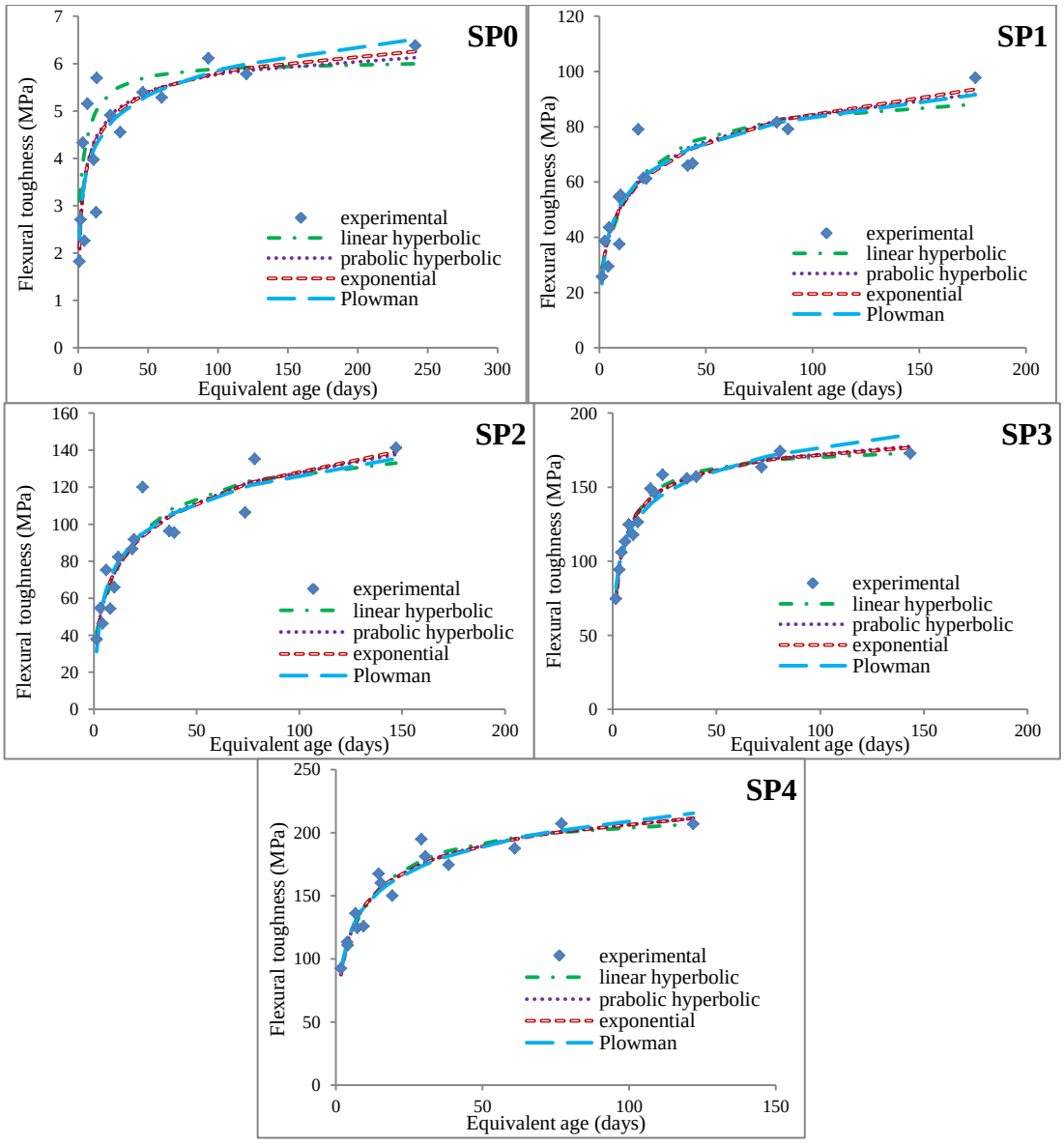

Figure 61: Predicted Flexural toughness by EXPeq method.

5.3.4 Comparison of Flexural Toughness Prediction between LH_{eq}, PH_{eq} and EXP_{eq}

As comparing the predicted flexural toughness models between different equivalent ages (LH_{eq}, PH_{eq} and EXP_{eq}), the LH_{eq} has a higher R^2 values in all mixes compared to other equivalent ages with values of approximately 0.9. The R^2 values of exponential equivalent age are lower than LH_{eq}, but it is higher than PH_{eq}, with values of approximately 0.8 and the lowest value of R^2 is for a parabolic hyperbolic equation with an approximate value of 0.7.

4.3.5 Flexural Toughness Prediction by MI

Flexural toughness was predicted for five different mixes (SP0, SP1, SP2, SP3, and SP4). Four equations (S_{LH}, S_{PH}, $S_{LOG,}$ and S_{EXP}) were used to predict the flexural strength by maturity index. Figure 62 presents the experimental and predicted flexural strength of SP0, SP1, SP2, SP3, and SP4 with four models. The regression parameters of all of these four models were shown in Table 19. The ranges of correlation coefficient (R^2) were between 0.851 and 0.984. All the models (except SP1 and SP3) have a good correlation with experimental results, the R^2 values for SP1 and SP3 are slightly lower than other mixes. In this method, the values of R^2 of all four models are very similar to each other. However, the accuracy of S_{LH} and S_{EXP} are slightly higher than S_{PH} and S_{LOG}.

For SP0 mixes the rates of correlation coefficient are 0.984, 0.969, 0.95 and 0.983 for linear hyperbolic, parabolic hyperbolic, logarithmic and exponential equations respectively. For SP1 the rates of correlation coefficient are 0.863, 0.873, 0.907 and 0.851 for linear hyperbolic, parabolic hyperbolic, logarithmic and exponential equations respectively. For SP2 mixes the rates of R^2 are 0.941, 0.951, 0.948 and 0.952 for S_{LH}, S_{PH}, S_{LOG} and S_{EXP} equations respectively. The values of R^2 of SP3 for S_{LH}, S_{PH}, S_{LOG} and S_{EXP} equations are 0.883, 0.892, 0.879 and 0.891 respectively. For SP4 mix the values of the correlation coefficient for S_{LH}, S_{PH} are 0.941 and 0.925 respectively, however, this value for S_{LOG} and S_{EXP} are 0.923 and 0.941 respectively.

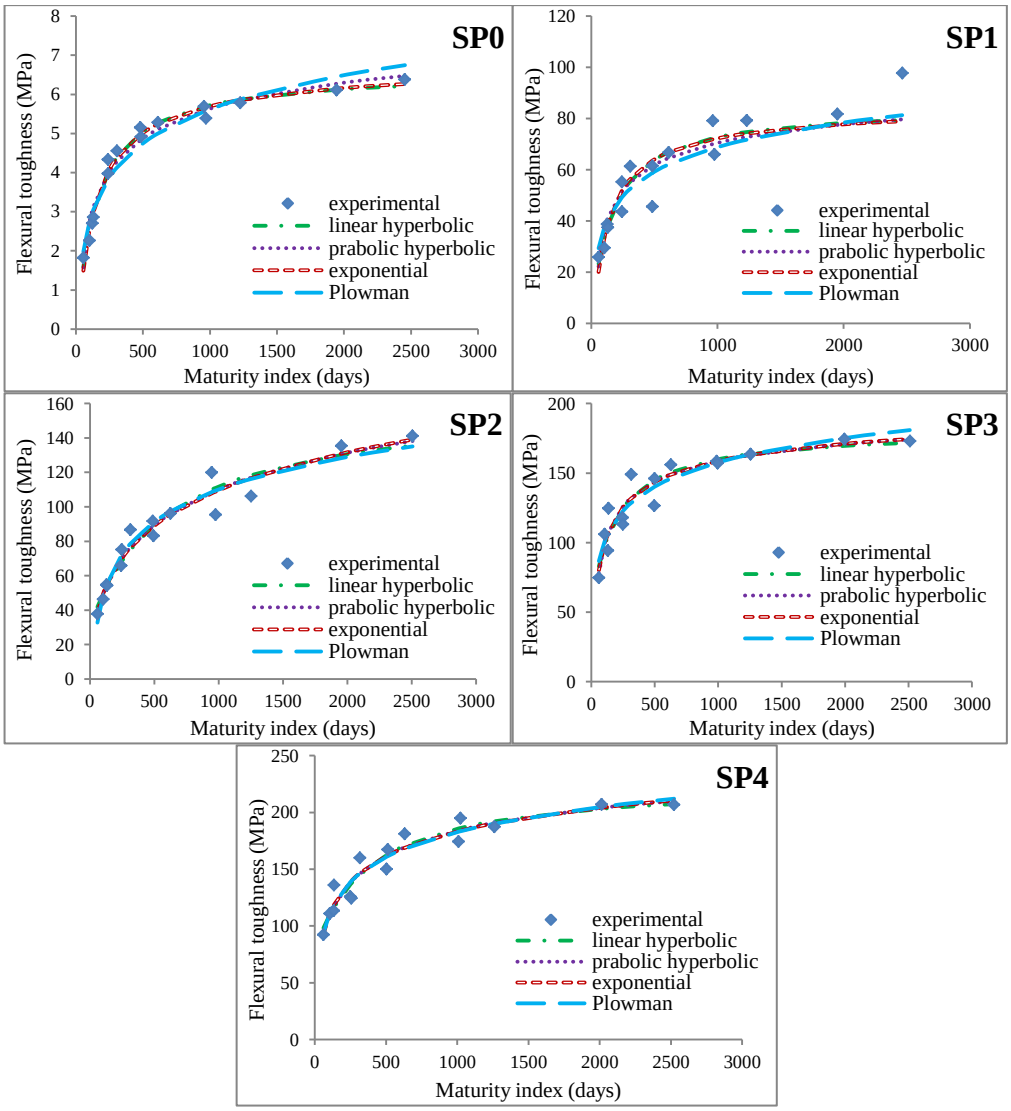

Figure 62: Predicted Flexural toughness by MI method.

Table 19: Regression parameters of flexural toughness for MI.

V_f	equation	Regression parameters							
		S_u	k_T	T_0	τ	α	a	b	R^2
SP0	Linear hyperbolic	6.597	0.006	6.88					0.955
	Parabolic hyperbolic	8.673	0.003	41.59					0.947
	Plowman						-3.06	1.257	0.945
	exponential	6.989			102.9	0.698			0.959
SP1	Linear hyperbolic	84.75	0.006	-					0.94
	Parabolic hyperbolic	102.27	0.005	42.76					0.937
	Plowman						-26.8	13.84	0.936
	exponential	86.839			97.54	0.727			0.944
SP2	Linear hyperbolic	160.85	0.002	-					0.95
	Parabolic hyperbolic	245.24	0.006	8.81					0.946
	Plowman						-78	27.22	0.949
	exponential	520.79			116.4	0.18			0.954
SP3	Linear hyperbolic	181.03	0.007	-					0.94
	Parabolic hyperbolic	208.48	0.01	25.94					0.939
	Plowman						-16.4	25.2	0.937
	exponential	211.84			55.96	0.431			0.945
SP4	Linear hyperbolic	227.18	0.004	-					0.946
	Parabolic hyperbolic	277.85	0.004	-					0.944
	Plowman						-36.4	31.73	0.935
	exponential	366.6			221.1	0.242			0.947

5.3.6 Validation of Flexural Toughness Models

Similar to compressive and flexural strength, in order to assess the accuracy of the predicted flexural strengths of each model, the additional lines are provided with ranges of ±10 and ±20% errors for the different volume fractions of the fibers.

5.3.6.1 Validation of Flexural Toughness Models for LH_{eq}

In this method, the ranges of errors for all data is between 0 and ±20%, as observed in Figures 63, 64, 65, 66 and 67. However, in SP0 mixture only two data (at 3 and 7days) have errors higher than ±20%. The maximum error occurs at 3 days for all mixes. For SP0, SP1, and SP2 at 3 days the logarithmic equation has the highest error, however, for SP3 and SP4 the highest error is for the linear hyperbolic equation. At later ages in all mixes (except SP1 and SP2) the logarithmic equation has the highest error, for SP1 and SP2 mixes at later ages the linear hyperbolic equation has the highest error.

Figure 63 observes the correlation between experimental flexural toughness and predicted flexural toughness of SP0 with linear hyperbolic, parabolic hyperbolic, logarithmic and exponential equations. The maximum percentage of error which occurs at 3 days were -28.4%, -31.7%, -30.9% and -24.6% for S_{LH}, S_{PH}, S_{LOG} and S_{EXP} equations respectively. However, at 56 days, the percentage of error values are 2.1%, -2.1%, -7% and 0.8% for S_{LH}, S_{PH}, S_{LOG} and S_{EXP} equations respectively.

Figure 64 shows a correlation between the predicted and measured flexural toughness with four equations (S_{LH}, S_{PH}, $S_{LOG,}$ and S_{EXP}) for the SP1 mixture. The maximum percentages of errors at 3 days were -17.2%, -20.5%, -20.6% and-20.4% for S_{LH}, S_{PH}, S_{LOG} and S_{EXP} equations respectively. However, at 56 days the percentages of errors are -8%, 4.7%, 5.2% and 4.3% for S_{LH}, S_{PH}, S_{LOG} and S_{EXP} equations respectively.

Figure 65 shows the predicted and measured flexural toughness of SP2. The maximum percentages of errors at 3 days were -11.2%, -14.7%, -17.4% and -15.2% for S_{LH}, S_{PH}, S_{LOG} and S_{EXP} equations respectively. However, at 56 days the percentage of errors is 4.3%, 1.1%, 2.7% and 0.6% for S_{LH}, S_{PH}, S_{LOG} and S_{EXP} equations respectively.

Figure 66 presents the estimated and measured flexural toughness of SP3 mixture with four different equations. The maximum percentage of error at 3 days were -18.2%, -7.9% for S_{LH}, S_{PH} equations respectively, and on the sameday, the maximum percentage of error are -8.9% and -7.2% for S_{LOG} and S_{EXP} equations respectively. However, at 56 days the percentages of errors are -1%, -2.2%, -6.6% and -1.9% for S_{LH}, S_{PH}, S_{LOG} and S_{EXP} equations respectively.

Figure 67 presents the estimated and measured flexural toughness of SP4 mixture with four different equations. The maximum percentages of errors at 3 days were 10%, 8.3% for S_{LH}, S_{PH} equations respectively, and on the sameday, the percentage of errors were 7.7% and 7.8% for S_{LOG} and S_{EXP} equations respectively. However, at 56 days the maximum percentage of errors for S_{LH} and S_{PH} are -0.3%, -2.2%, respectively, and for S_{LOG} and S_{EXP} are -3.8% and -2.3% respectively.

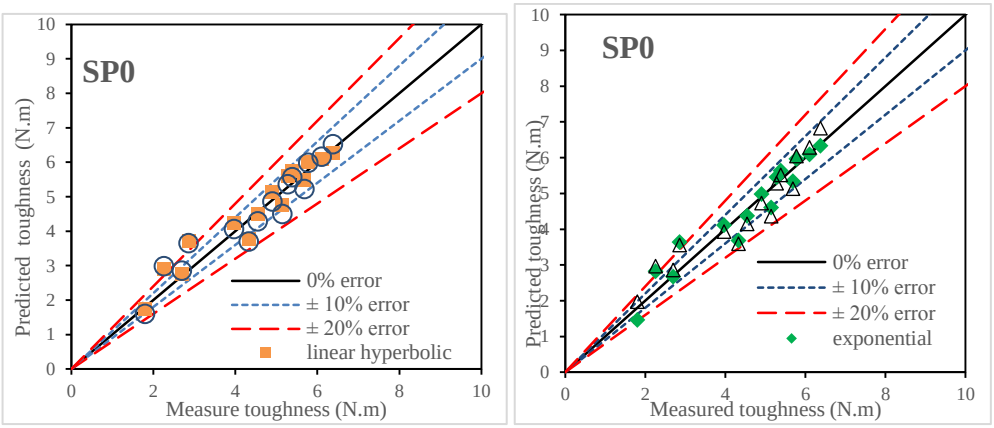

Figure 63: Measured versus predicted flexural toughness by LHeq method for SP0: (a) linear and parabolic hyperbolic model and (b) exponential and Plowman model.

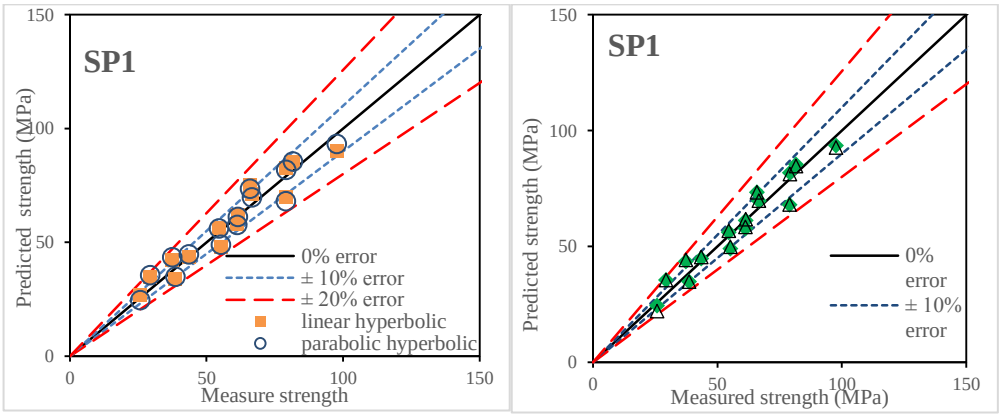

Figure 64: Measured versus predicted flexural toughness LHeq method for SP1: (a) linear and parabolic hyperbolic model and (b) exponential and Plowman model.

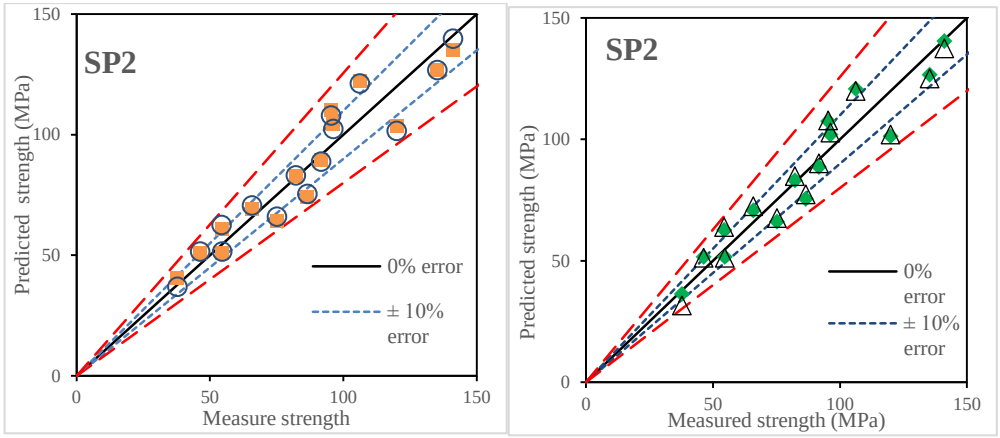

Figure 65: Measured versus predicted flexural toughness LHeq method for SP2: (a) linear and parabolic hyperbolic model and (b) exponential and Plowman model.

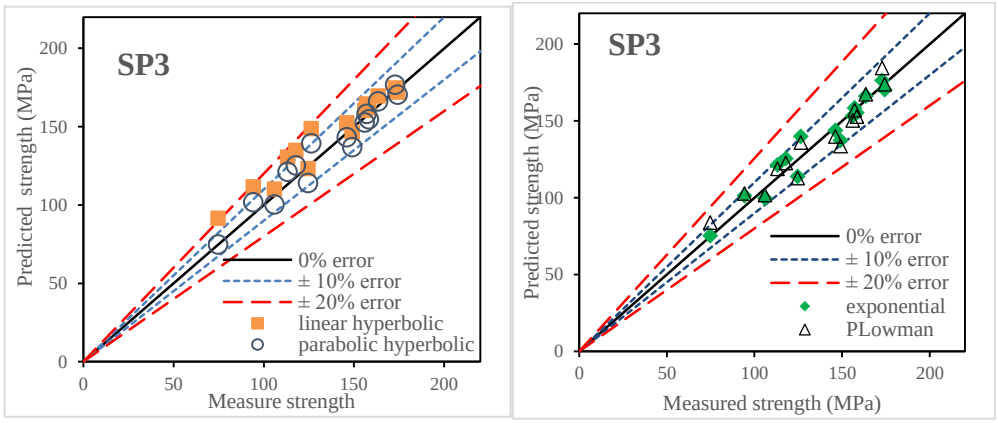

Figure 66: Measured versus predicted flexural toughness LHeq method for SP3: (a) linear and parabolic hyperbolic model and (b) exponential and Plowman model.

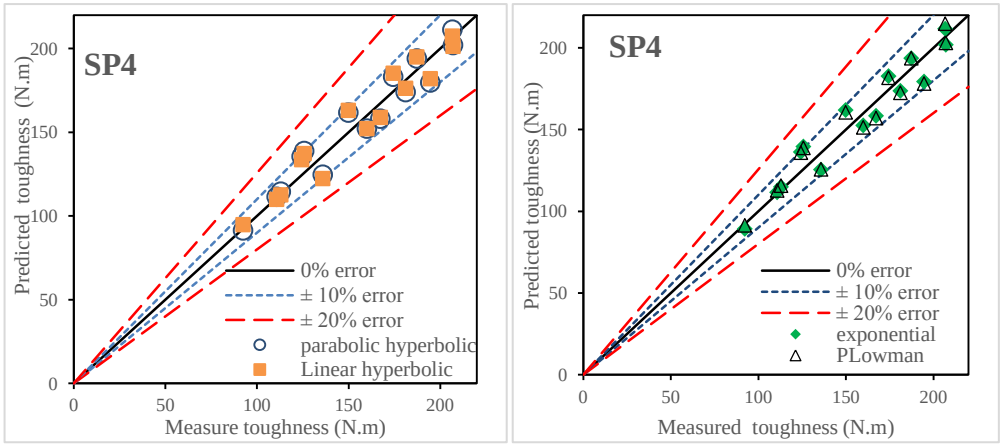

Figure 67: Measured versus predicted flexural toughness LHeq method for SP4: (a) linear and parabolic hyperbolic model and (b) exponential and Plowman model.

5.3.6.2 Validation of Flexural Toughness Models for PH_{eq}

In this method, most of the data have the ranges of errors between 0 and ±20%, as observed in Figures 68, 69, 70, 71 and 72. However, in SP0 mixture some data have errors higher ±20%, but for other mixes only one or two data in each mixture have error higher than ±20%. The maximum error occurs at 3 days for SP0, SP1 and SP2 mixes. However, for SP3 and SP4 the maximum error occurs at 7 days. At early ages for SP1, SP2 and SP4 the logarithmic equation has a higher error compared to other equations, but for SP0 and SP3 the parabolic hyperbolic and exponential equations respectively, have the highest error. At later ages, for SP0 and SP1 the exponential equation has the highest error. However, for SP2, SP3, and SP4 the logarithmic equation has a higher error compared to other equations.

Figure 68 observes the correlation between experimental flexural toughness and predicted flexural toughness of SP0 with linear hyperbolic, parabolic hyperbolic, logarithmic and exponential equations. The maximum percentage of error which occurs at 3 days were -47.5%, -55%, -52.9% and -34.5% for S_{LH}, S_{PH}, S_{LOG} and S_{EXP} equations respectively. However, at 56 days, the percentage of error values are 6.4%, 3.1%, -2.7% and 7.9% for S_{LH}, S_{PH}, S_{LOG} and S_{EXP} equations respectively.

Figure 69 shows a correlation between predicted and measured flexural toughness with four equations (S_{LH}, S_{PH}, $S_{LOG,}$ and S_{EXP}) for the SP1 mixture. The maximum percentages of errors at 3 days were -54.5%, -53.9%, -54.4% and -53% for S_{LH}, S_{PH}, S_{LOG} and S_{EXP} equations respectively. However, at 56 days the percentage of errors are 7.7%, -11.5%, -11.9% and -12.9% for S_{LH}, S_{PH}, S_{LOG} and S_{EXP} equations respectively.

Figure 70 shows the predicted and measured flexural toughness of SP2. The maximum percentages of errors at 3 days were -37.3%, -40.2%, -44.7% and -40.8% for S_{LH}, S_{PH}, S_{LOG} and S_{EXP} equations respectively. However, at 56 days the percentage of errors is 11.7%, 12.5%, 13.9% and 13.1% for S_{LH}, S_{PH}, S_{LOG} and S_{EXP} equations respectively.

Figure 71 presents the estimated and measured flexural toughness of SP3 mixture with four different equations. The maximum percentage of errors at 7 days were -9.7%, -9.7% for S_{LH}, S_{PH} equations respectively, and on the sameday, the maximum percentage of error are -7% and -10.2% for S_{LOG} and S_{EXP} equations respectively. However, at 56 days the percentage of errors are 0.4%, -2.3%, -7.2% and -2% for S_{LH}, S_{PH}, S_{LOG} and S_{EXP} equations respectively.

Figure 72 presents an estimated and measured flexural toughness of SP4 mixture with four different equations. The maximum percentage of errors at 7 days were -13.7%, -17.5% for S_{LH}, S_{PH} equations respectively, and on the sameday, the percentage of error are -13.9% and -14.9% for S_{LOG} and S_{EXP} equations respectively. However, at 56 days the maximum percentage of errors for S_{LH} and $S_{PH}$are 1.4%, -1.4%, respectively, and for S_{LOG} and S_{EXP} are -3.7% and -1.6% respectively.

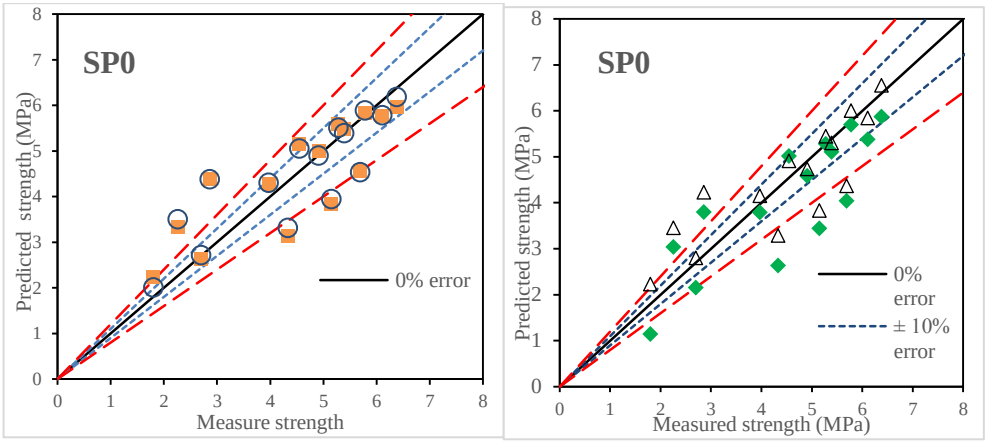

Figure 68: Measured versus predicted flexural toughness by PHeq method for SP0: (a) linear and parabolic hyperbolic model and (b) exponential and Plowman model.

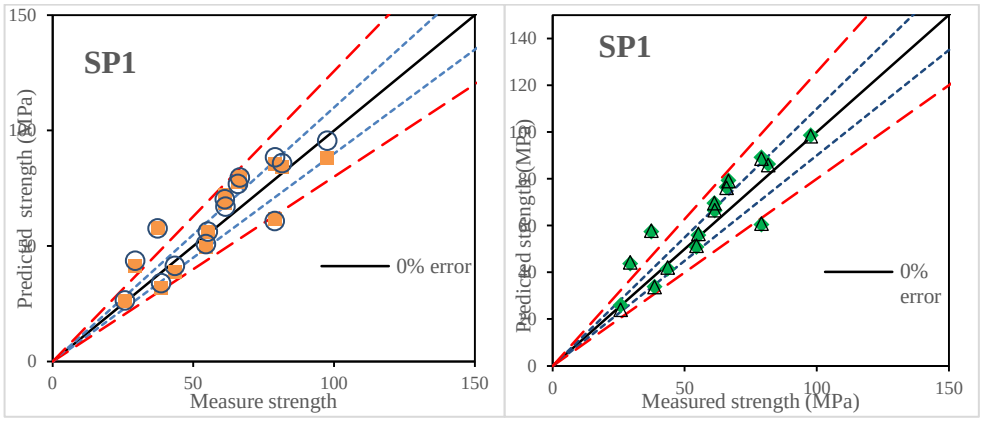

Figure 69: Measured versus predicted flexural toughness by PHeq method for SP1: (a) linear and parabolic hyperbolic model and (b) exponential and Plowman model.

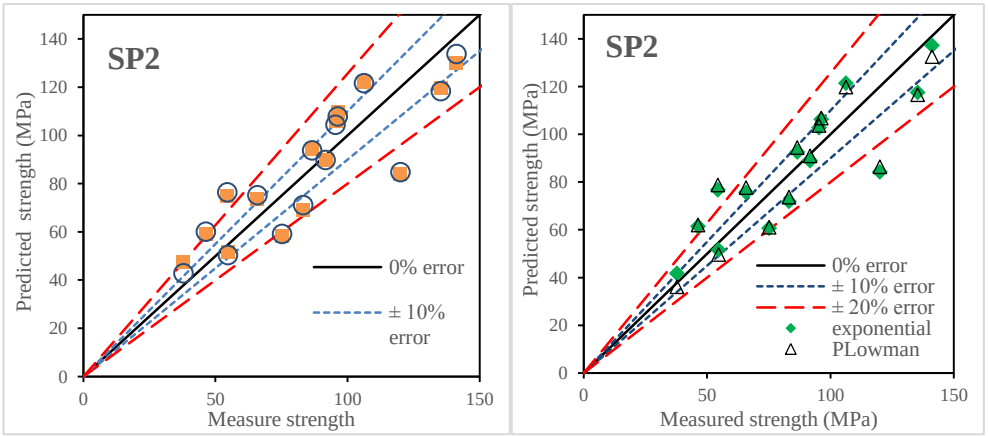

Figure 70: Measured versus predicted flexural toughness by PHeq method for SP4: (a) linear and parabolic hyperbolic model and (b) exponential and Plowman model.

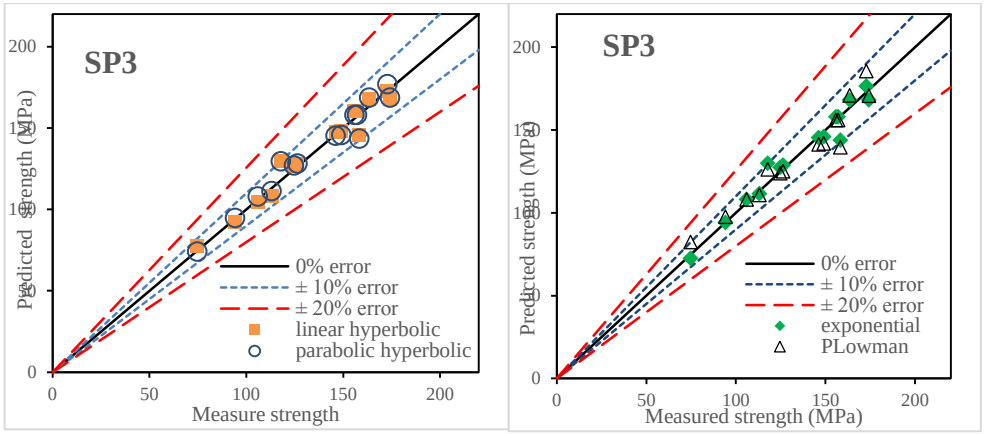

Figure 71: Measured versus predicted flexural toughness by PHeq method for SP4: (a) linear and parabolic hyperbolic model and (b) exponential and Plowman model.

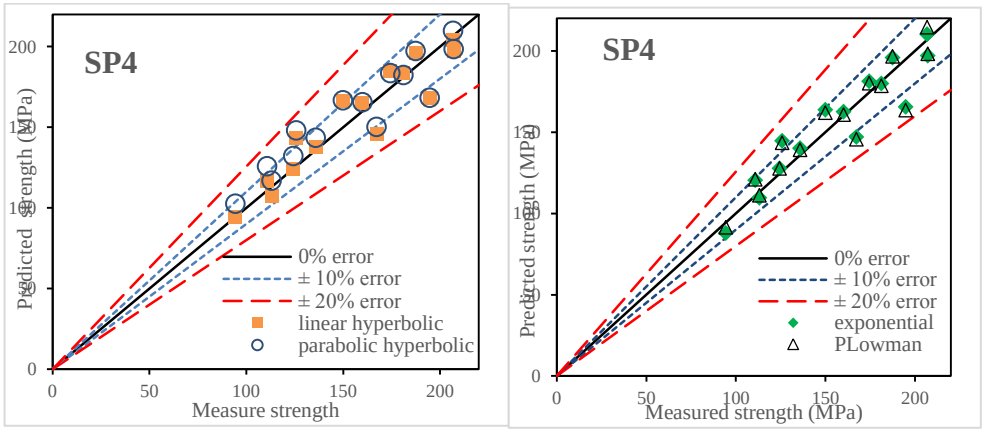

Figure 72: Measured versus predicted flexural toughness by PHeq method for SP4: (a) linear and parabolic hyperbolic model and (b) exponential and Plowman model.

5.3.6.3 Validation Flexural Toughness Models for EXP_{eq}

In this method, most of the data have the range of errors between 0 and ±20%, as observed in Figures 73, 74, 75, 76 and 77. However, in SP0 mixture some data have error higher ±20%, but for other mixes only one or two data in each mixture have error higher than ±20%. The maximum error occurs at 3 days for SP0, SP1 and SP2 mixes. However, for SP3 and SP4 the maximum error occurs at 7 days. At early ages for SP0, SP3 and SP4 the linear hyperbolic equation has a higher error compared to other equations and for SP1 and SP2 the logarithmic equation has a higher error.

However, at later ages, the linear hyperbolic equation has the highest error in all mixes.

Figure 73 observes the correlation between experimental flexural toughness and predicted flexural toughness of SP0 with linear hyperbolic, parabolic hyperbolic, logarithmic and exponential equations. The maximum percentages of errors which occur at 3 days were -83.3%, -56.8%, -55.1% and -56.1% for S_{LH}, S_{PH}, S_{LOG} and S_{EXP} equations respectively. However, at 56 days, the percentage of error values are 6%, 4%, -2.1% and 1.9% for S_{LH}, S_{PH}, S_{LOG} and S_{EXP} equations respectively.

Figure 74 shows a correlation between predicted and measured flexural toughness with four equations (S_{LH}, S_{PH}, $S_{LOG,}$ and S_{EXP}) for the SP1 mixture. The maximum percentages of errors at 3 days were -31.5%, -33.6%, -37.1% and -34.2% for S_{LH}, S_{PH}, S_{LOG} and S_{EXP} equations respectively. However, at 56 days the percentages of errors are 9.8%, 6%, 6.3% and 4.3% for S_{LH}, S_{PH}, S_{LOG} and S_{EXP} equations respectively.

Figure 75 shows the predicted and measured flexural toughness of SP2. The maximum percentages of errors at 3 days were -22.4%, -25.7%, -29.9% and -26.8% for S_{LH}, S_{PH}, S_{LOG} and S_{EXP} equations respectively. However, at 56 days the percentages of errors are 5.8%, 2.5%, 4.1% and 1.5% for S_{LH}, S_{PH}, S_{LOG} and S_{EXP} equations respectively.

Figure 76 presents an estimated and measured flexural toughness of SP3 mixture with four different equations. The maximum percentages of errors at 7 days were -8%, -8.2% for S_{LH}, S_{PH} equations respectively, and on the sameday, the maximum

percentage of error are -5.7% and -8.6% for S_{LOG} and S_{EXP} equations respectively. However, at 56 days the percentages of errors are 3.1%, 2.6%, 1.1% and 2.8% for S_{LH}, S_{PH}, S_{LOG} and S_{EXP} equations respectively.

Figure 77 presents an estimated and measured flexural toughness of SP4 mixture with four different equations. The maximum percentage of errors at 7 days were -10.6%, -11.6% for S_{LH}, S_{PH} equations respectively, and on the sameday, the percentage of error are -11.5% and -12.2% for S_{LOG} and S_{EXP} equations respectively. However, at 56 days the maximum percentage of errors for S_{LH} and $S_{PH}$are 3.3%, 3%, respectively, and for S_{LOG} and S_{EXP} are 2.6% and 3.2% respectively.

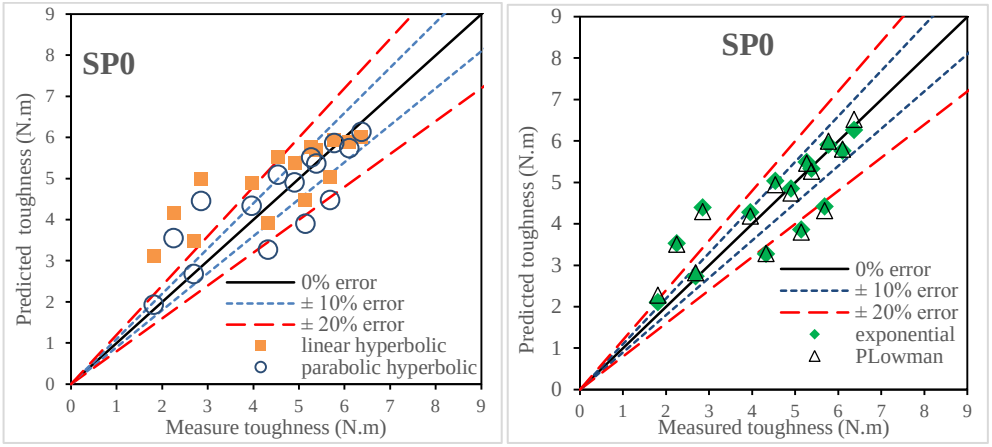

Figure 73: Measured versus predicted flexural toughness by EXPeq method for SP0: (a) linear and parabolic hyperbolic model and (b) exponential and Plowman model.

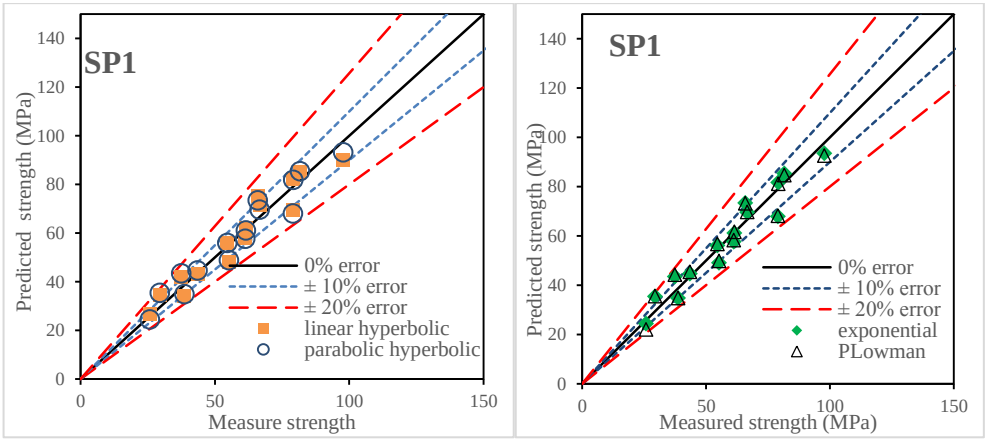

Figure 74: Measured versus predicted flexural toughness by EXPeq method for SP1: (a) linear and parabolic hyperbolic model and (b) exponential and Plowman model.

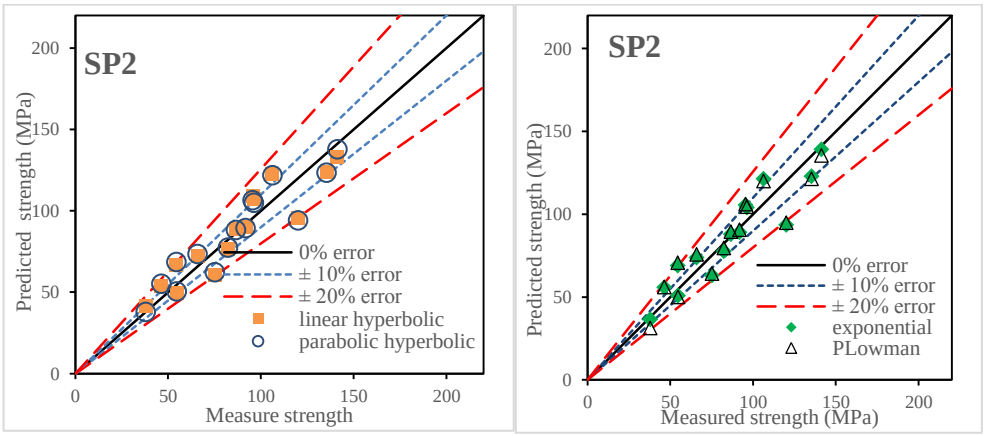

Figure 75: Measured versus predicted flexural toughness by EXPeq method for SP2: (a) linear and parabolic hyperbolic model and (b) exponential and Plowman model.

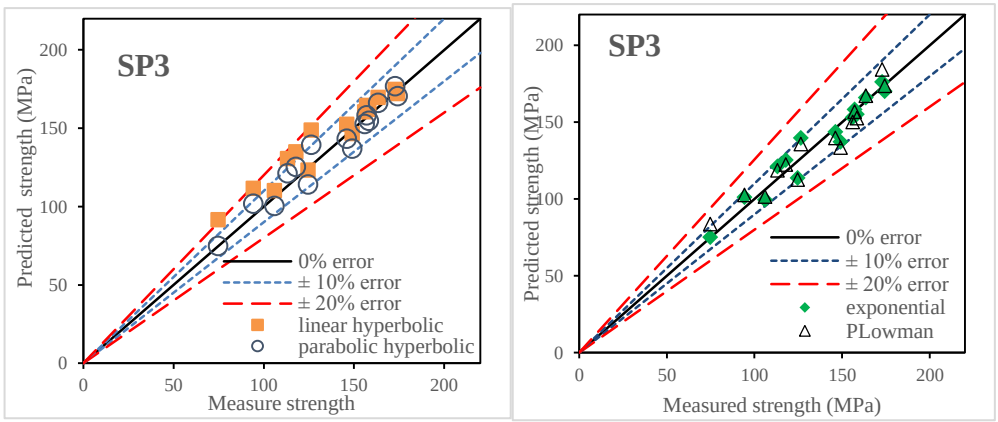

Figure 76: Measured versus predicted flexural toughness by EXPeq method for SP3: (a) linear and parabolic hyperbolic model and (b) exponential and Plowman model.

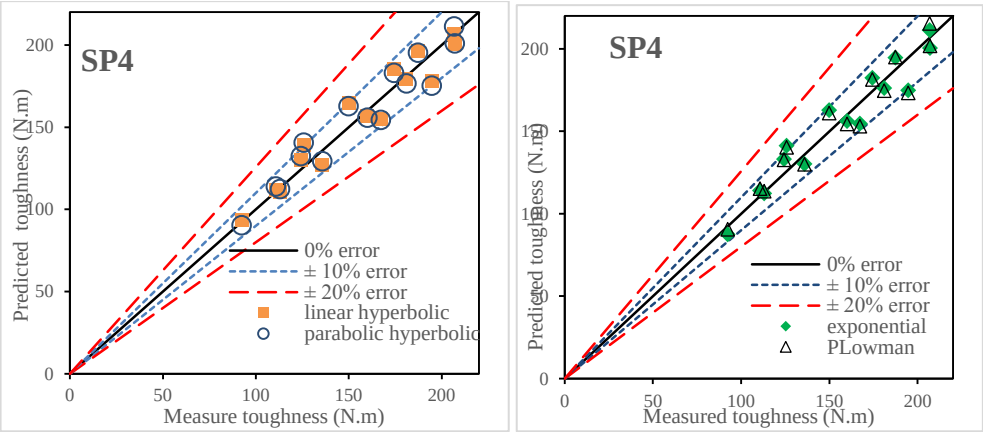

Figure 77: Measured versus predicted flexural toughness by EXPeq method for SP4: (a) linear and parabolic hyperbolic model and (b) exponential and Plowman model.

5.3.6.4 Validation of Flexural Toughness Models for MI

The range of errors of most data in this method are between 0 and ±20%, only some data at 3 and 28 days in all mixes have errors of more than ±20%, as observed in Figures 78, 79, 80, 81 and 82. The maximum errors for SP0, SP3, and SP4 occur at 3 days, however, for SP1 and SP2 maximum errors occur in 28 days. At early ages (3 and 7 days) S_{PH} and S_{LOG} have higher error compare to S_{LH} and S_{EXP} in all mixes. However, at later ages (28 and 56 days) the percentage of error forS_{LOG} equation is higher than other equations.

Figure 78 observe the correlation between experimental flexural strength and predicted flexural strength of SP0 with linear hyperbolic, parabolic hyperbolic, logarithmic and exponential equations. The maximum percentages of errors were -11.9%, -21.4%, -21.3% and -12.6% for S_{LH}, S_{PH}, S_{LOG} and S_{EXP} equations respectively. However, at 56 days the percentage of errors are 2.6%, -1.4%, -5.7% and 1.8% for S_{LH}, S_{PH}, S_{LOG} and S_{EXP} equations respectively.

Figure 79 shows a correlation between predicted and measured flexural strength with four equations (S_{LH}, S_{PH}, $S_{LOG,}$ and S_{EXP}) for the SP1 mixture. The percentages of

errors at 1 day were -38.7%, -34.8%, -29% and -39.5% for S_{LH}, S_{PH}, S_{LOG} and S_{EXP} equations respectively. However, at 56 days the percentages of errors are 8.5%, 11.4%, 13.6% and 9.1% for S_{LH}, S_{PH}, S_{LOG} and S_{EXP} equations respectively.

Figure 80 shows the predicted and measured flexural strength of SP2. The percentages of errors at 1 day were -11.4%, -10%, -9.3% and -9.7% for S_{LH}, S_{PH}, S_{LOG} and S_{EXP} equations respectively. However, at 56 days the maximum percentages of errors are -4.1%, 2.1%, 4.3% and 1.5% for S_{LH}, S_{PH}, S_{LOG} and S_{EXP} equations respectively.

Figure 81 presents an estimated and measured flexural strength of SP3 mixture with four different equations. The maximum percentages of errors at 1 day were 15.7%, 13.8% for S_{LH}, S_{PH} equations respectively, and at the sameday, the maximum percentage of error is -14.1% and -14.3% for S_{LOG} and S_{EXP} equations respectively. However, at 56 days the percentage of errors are 0.7%, -0.7%, -4.6% and -0.9% for S_{LH}, S_{PH}, S_{LOG} and S_{EXP} equations respectively.

Figure 82 presents an estimated and measured flexural strength of SP4 mixture with four different equations. The maximum percentages of errors were 14%, 12.9% for S_{LH}, S_{PH} equations respectively, and on the sameday, the percentage of error is 12.2% and 12.5% for S_{LOG} and S_{EXP} equations respectively. However, at 56 days the maximum percentages of errors for S_{LH} and $S_{PH}$is -0.2%, -1.5%, respectively, and for S_{LOG} and S_{EXP} are -2.5% and -1.8% respectively.

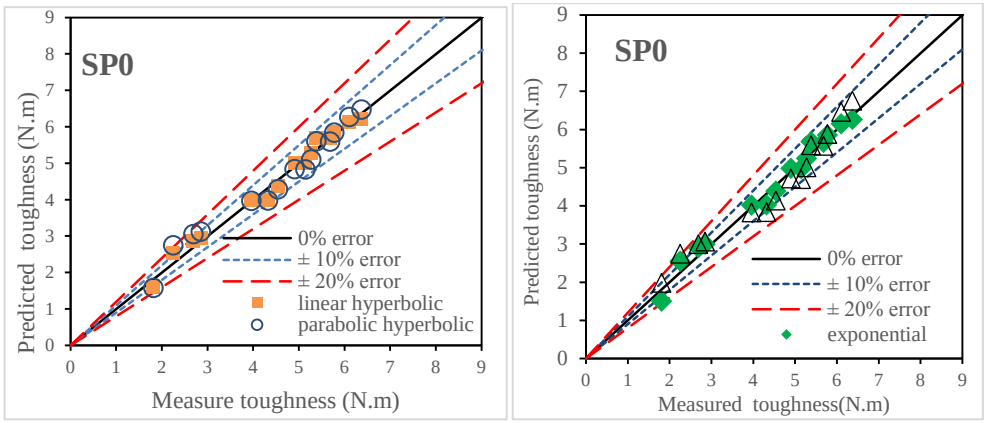

Figure 78: Measured versus predicted flexural toughness by MI method for SP0: (a) linear and parabolic hyperbolic model and (b) exponential and Plowman model.

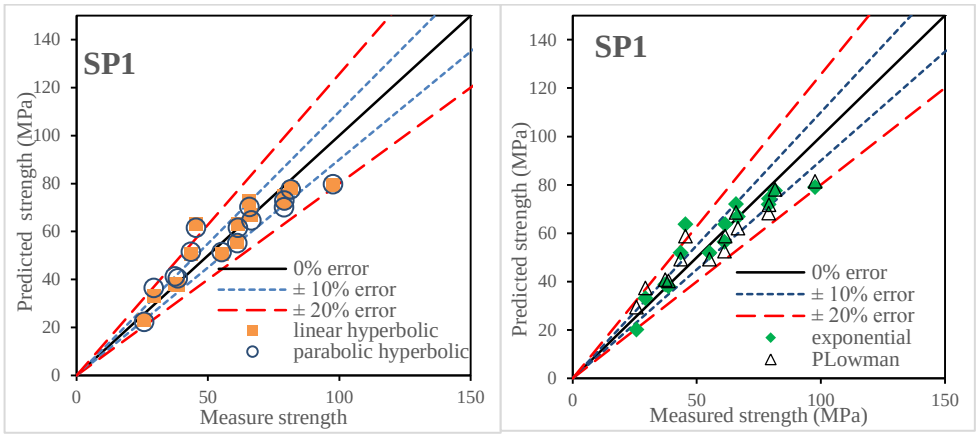

Figure 79: Measured versus predicted flexural toughness by MI method for SP1: (a) linear and parabolic hyperbolic model and (b) exponential and Plowman model.

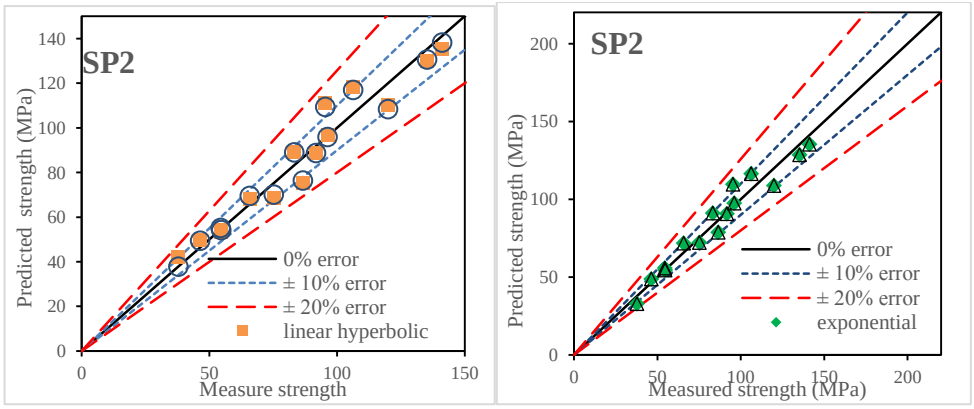

Figure 80: Measured versus predicted flexural toughness by MI method for SP2: (a) linear and parabolic hyperbolic model and (b) exponential and Plowman model.

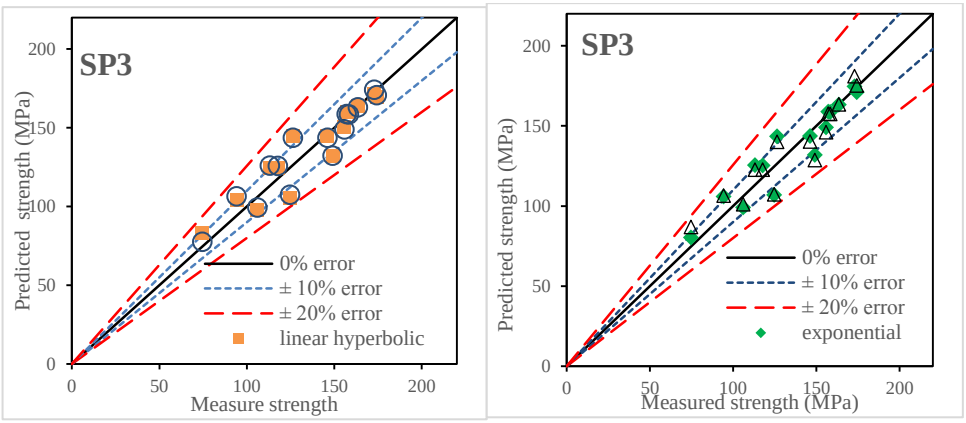

Figure 81: Measured versus predicted flexural toughness by MI method forSP3: (a)linear and parabolic hyperbolic model and (b) exponential and Plowman.

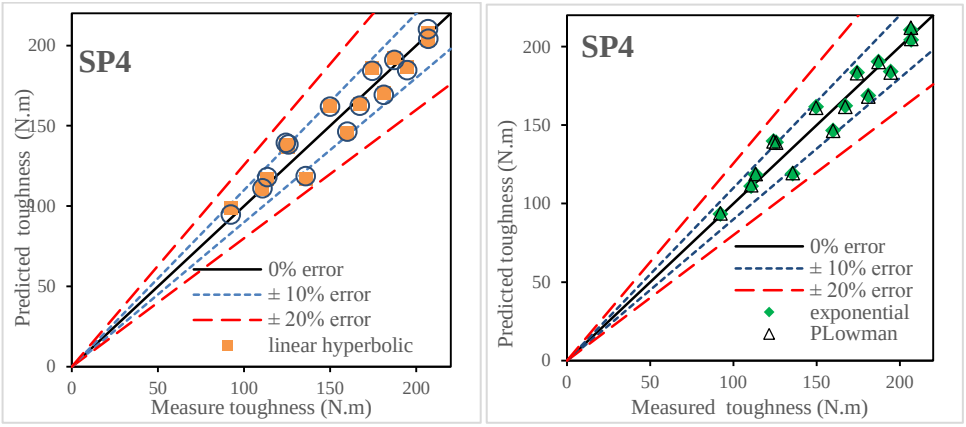

Figure 82: Measured versus predicted flexural toughness by MI method for SP4: (a) linear and parabolic hyperbolic model and (b) exponential and Plowman model.

5.4 Splitting Tensile Strength Models

Similar to other mechanical properties of concrete, the splitting tensile strength were predicted for five different mixes (SP0, SP1, SP2, SP3 and SP4) at ages of 1, 3, 7, 10, 14, 28 and 56 days and curing temperatures of 8 °C, 22 °C and 32 °C.

A similar study was performed to predict the splitting tensile strength. Splitting tensile strength was predicted for five different mixes (SP0, SP1, SP2, SP3 and SP4). Four equations were used to predict flexural strength (S_{LH}, S_{PH}, S_{LOG} and S_{EXP}). Equivalent age were calculated by three methods (LH_{eq}, PH_{eq}, EXP_{eq}).The all

estimated splitting tensile strength had a good correlation with the experimental results. The R^2 values were between 0.814 and 0.991.

5.4.1 Splitting Tensile Strength Development for Linear Hyperbolic Equivalent Age (LH_{eq})

Figure 83 presents the experimental and predicted splitting tensile strength of SP0, SP1, SP2, SP3 and SP4 that obtained by linear hyperbolic equivalent age (LH_{eq}) with four modes (S_{LH}, S_{PH}, S_{LOG} and S_{EXP}). The regressions, which are parameters of all these four models, were shown in Table 20. The range of correlation coefficient (R^2) was between 0.821 and 0.991. All the models have a very good correlation with experimental results. However, the values of the SP2 mixture are lower than other mixes. For SP0, SP1 and SP2 mix the S_{LH} equation has the highest value compared to other equations, but for SP3 and SP4 mixes, the highest value of $R^2$is for S_{PH} equation. S_{LOG} has the same as other properties have the lowest (R^2) are all mixes.

For SP0 mixes the rates of correlation coefficient are 0.956, 0.949, 0.837 and 0.946 for linear hyperbolic, parabolic hyperbolic, logarithmic and exponential equations respectively. For SP1 the rates of correlation coefficient are 0.97, 0.965, 0.948 and 0.964 for linear hyperbolic, parabolic hyperbolic, logarithmic and exponential equations respectively. For SP2 mixes the rates of R^2 are 0.847, 0.834, 0.821 and 0.828 for S_{LH}, S_{PH}, S_{OG} and S_{EXP} equations respectively. The values of R^2 for SP3 for S_{LH}, S_{PH}, S_{LOG} and S_{EXP} equations are 0.967, 0.991, 0.927 and 0.983 respectively. For SP4 mix the values of the correlation coefficient for S_{LH}, S_{PH} are 0.931 and 0.951 respectively, however, this value for S_{LOG} and S_{EXP} are 0.94 and 0.95 respectively.

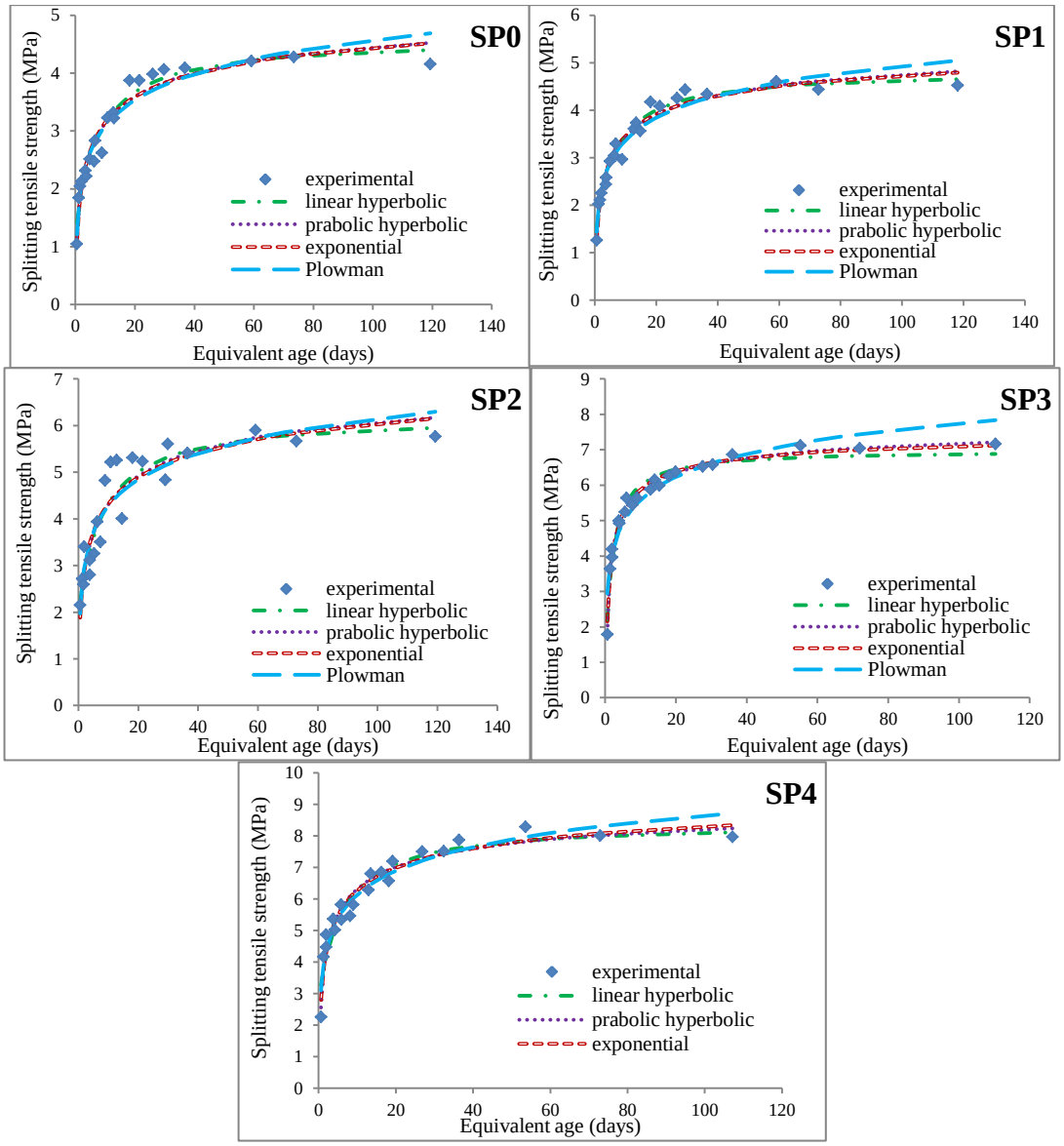

Figure 83: Predicted Splitting tensile strength by LHeq method.

Table 20: Regression parameters of splitting tensile strength for LHeq.

V_f	equation	Regression parameters							
		S_u	k_T	T_0	τ	α	a	b	R^2
SP0	Linear hyperbolic	4.602	0.18	-					0.955
	Parabolic hyperbolic	5.512	0.176	0.151					0.947
	Plowman						1.596	0.647	0.945
	exponential	6.016			2.69	0.33			0.959
SP1	Linear hyperbolic	4.826	0.255	-					0.94
	Parabolic hyperbolic	5.748	0.228	0.214					0.937
	Plowman						1.806	0.679	0.936
	exponential	5.93			1.905	0.375			0.944
SP2	Linear hyperbolic	6.22	0.183	-					0.95
	Parabolic hyperbolic	7.5	0.175	-					0.946
	Plowman						2.4	1.815	0.949
	exponential	8.942			3.059	0.269			0.954
SP3	Linear hyperbolic	6.988	0.592	-					0.94
	Parabolic hyperbolic	7.998	0.769	0.489					0.939
	Plowman						3.423	0.939	0.937
	exponential	7.607			0.904	0.566			0.945
SP4	Linear hyperbolic	8.41	0.25	-					0.946
	Parabolic hyperbolic	9.484	0.411	0.279					0.944
	Plowman						3.635	1.088	0.935
	exponential	10.516			1.4	0.337			0.947

5.4.2 Splitting Tensile Strength Development for Parabolic Hyperbolic Equivalent Age (PH_{eq})

Figure 84 presents the experimental and predicted splitting tensile strength of SP0, SP1, SP2, SP3, and SP4 that are obtained by parabolic hyperbolic equivalent age (PH_{eq}) with four modes (S_{LH}, S_{PH}, S_{LOG} and S_{EXP}). The regression parameters of all these four models were shown in Table 21. The ranges of correlation coefficient (R^2) were between 0.852 and 0.957. The R^2 values that were obtained for SP0, SP1, and SP2 is slightly lower than SP3 and SP4. In this method, values of R^2thatobtained by S_{PH} and S_{EXP} are very similar to each other in all mixes. However, all the R^2 values obtained by this method in all mixes (except SP3) have little difference with each other.

For SP0 mixes the rates of correlation coefficient are 0.852, 0.864, 0.855 and 0.863 for linear hyperbolic, parabolic hyperbolic, logarithmic and exponential equations respectively. For SP1 the rates of correlation coefficient are 0.871, 0.884, 0.867 and

0.883 for linear hyperbolic, parabolic hyperbolic, logarithmic and exponential equations respectively. For SP2 mixes the rates of R^2 are 0.847, 0.835, 0.821 and 0.828 for S_{LH}, S_{PH}, S_{LOG} and S_{EXP} equations respectively. The values of R^2 of SP3 for S_{LH}, S_{PH} S_{LOG} and S_{EXP} equations are 0.927, 0.957, 0.881 and 0.918 respectively. For SP4 mix the values of the correlation coefficient for S_{LH}, S_{PH} are 0.923 and 0.946 respectively, however, this value for S_{LOG} and S_{EXP} are 0.932 and 0.946 respectively.

Table 21: Regression parameters of splitting tensile strength for PHeq.

V_f	equation	Regression parameters							
		S_u	k_T	T_0	τ	α	a	b	R^2
SP0	Linear hyperbolic	4.331	0.201	-					0.955
	Parabolic hyperbolic	4.904	0.299	0.017					0.947
	Plowman						1.829	0.519	0.945
	exponential	5.678			1.767	0.288			0.959
SP1	Linear hyperbolic	4.55	0.284	-					0.94
	Parabolic hyperbolic	5.192	0.382	0.09					0.937
	Plowman						2.054	0.548	0.936
	exponential	5.615			1.223	0.336			0.944
SP2	Linear hyperbolic	6.102	0.185	-					0.95
	Parabolic hyperbolic	7.156	0.203	-					0.946
	Plowman						2.507	0.734	0.949
	exponential	8.374			2.335	0.27			0.954
SP3	Linear hyperbolic	6.887	0.634	-					0.94
	Parabolic hyperbolic	7.723	0.949	0.448					0.939
	Plowman						3.594	0.828	0.937
	exponential	7.459			0.785	0.552			0.945
SP4	Linear hyperbolic	8.188	0.276	-					0.946
	Parabolic hyperbolic	9.207	0.452	0.155					0.944
	Plowman						3.791	0.983	0.935
	exponential	10.187			1.156	0.326			0.947

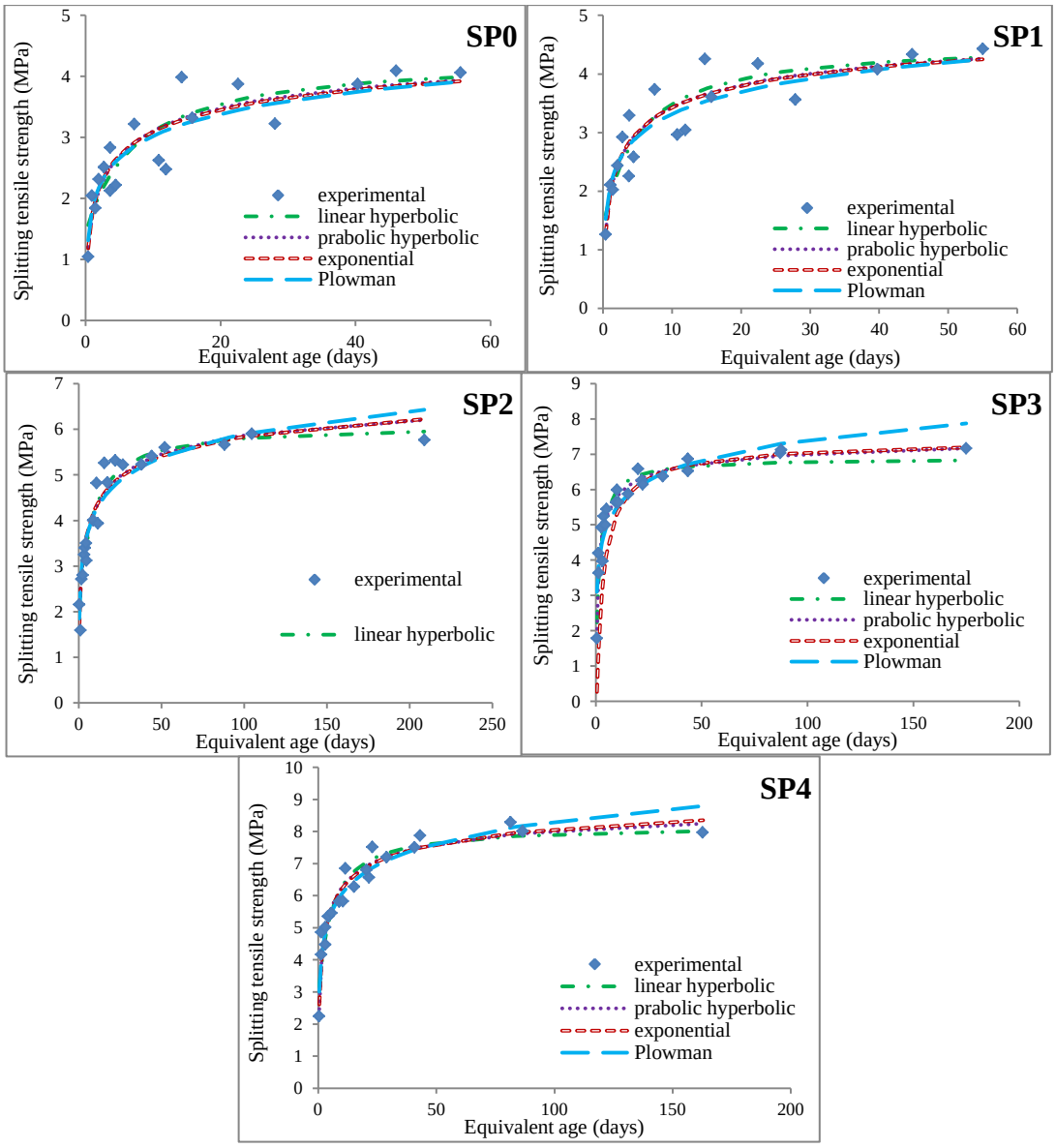

Figure 84: Predicted Splitting tensile strength by PHeq method.

5.4.3 Splitting Tensile Strength Development for Exponential Equivalent Age (EXP_{eq})

Figure 85 presents the experimental and predicted compressive strength of SP0, SP1, SP2, SP3 and SP4 that were obtained by exponential equivalent age (EXP_{eq}) with four modes (S_{LH}, S_{PH}, S_{LOG} and S_{EXP}). The regression parameters of all these four models were shown in Table 22. The range of correlation coefficient (R^2) was between 0.832 and 0.982. Similar to other equivalent ages (eq_{LH} and eq_{PH}), all the models had a very good correlation with experimental results. However, the value of R^2 that was obtained for SP0 was lower than other mixes. For the other mechanical properties the ranges of the R^2 values having all the strength development equations with this method is very similar to each other. In this method, the values of R^2 obtained by S_{PH} and S_{EXP} are approximately the same.

For SP0 mixes the rates of correlation coefficient are 0.832, 0.847, 0.838 and 0.847 for linear hyperbolic, parabolic hyperbolic, logarithmic and exponential equations respectively. For SP1 the rates of correlation coefficient are 0.924, 0.928, 0.908 and 0.927 for linear hyperbolic, parabolic hyperbolic, logarithmic and exponential equations respectively. For SP2 mixes the rates of R^2 are 0.918, 0.901, 0.882 and 0.891 for S_{LH}, S_{PH}, S_{LOG} and S_{EXP} equations respectively. The values of R^2 for SP3 for S_{LH}, S_{PH}, S_{LOG} and S_{EXP} equations are 0.950, 0.982, 0.918 and 0.977 respectively. For SP4 mix the values of the correlation coefficient for S_{LH}, S_{PH} are 0.938 and 0.958 respectively, however, this value for S_{LOG} and S_{EXP} are 0.946 and 0.957 respectively.

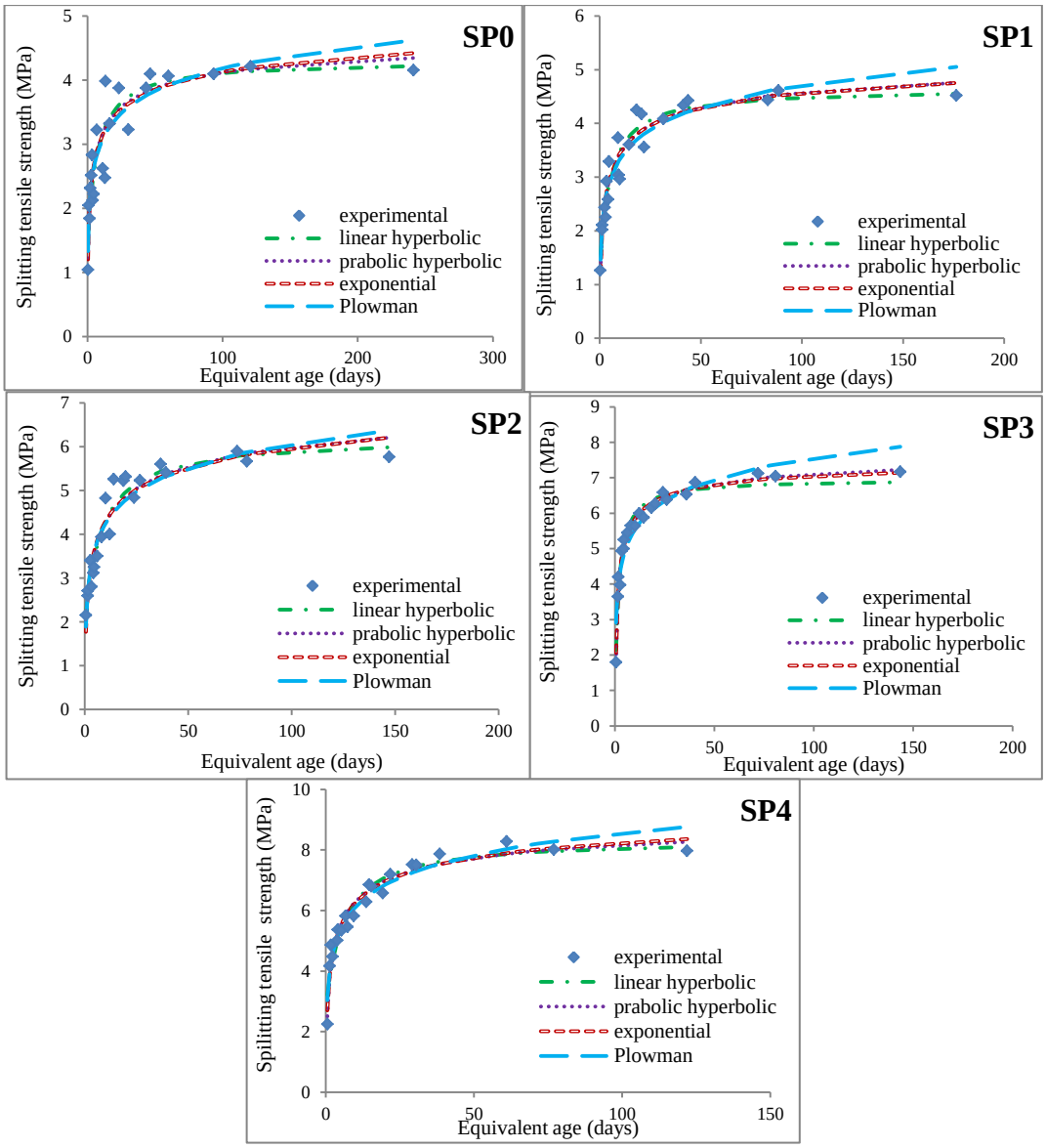

Figure 85: Predicted Splitting tensile strength by EXPeq method.

Table 22: Regression parameters of splitting tensile strength for EXPeq.

V_f	equation	Regression parameters							
		S_u	k_T	T_0	τ	α	a	b	R^2
SP0	Linear hyperbolic	4.303	0.202	-					0.955
	Parabolic hyperbolic	4.837	0.322	-					0.947
	Plowman						1.86	0.503	0.945
	exponential	5.676			1.684	0.279			0.959
SP1	Linear hyperbolic	4.65	0.262	-					0.94
	Parabolic hyperbolic	5.406	0.306	0.134					0.937
	Plowman						1.954	0.599	0.936
	exponential	5.677			1.46	0.361			0.944
SP2	Linear hyperbolic	6.209	0.179	-					0.95
	Parabolic hyperbolic	7.42	0.178	-					0.946
	Plowman						2.421	0.792	0.949
	exponential	8.734			2.829	0.273			0.954
SP3	Linear hyperbolic	6.955	0.589	-					0.94
	Parabolic hyperbolic	7.907	0.786	0.388					0.939
	Plowman						3.52	0.877	0.937
	exponential	7.616			0.824	0.532			0.945
SP4	Linear hyperbolic	8.352	0.256	-					0.946
	Parabolic hyperbolic	9.439	0.41	0.944					0.944
	Plowman						3.669	1.061	0.935
	exponential	10.416			1.341	0.336			0.947

5.4.4 Comparison of Strength Development between LH_{eq}, PH_{eq} and EXP_{eq}

As comparing the predicted splitting tensile strength models between different equivalent ages ($LH_{eq,}$ PH_{eq} and EXP_{eq}), the LH_{eq} and EXP_{eq} have higher R^2 values compare to PH_{eq} with values of approximately 0.9 in all mixes. The R^2 value of PH_{eq} is lower than other equivalent, with values of approximately 0.7.

5.4.5 Splitting Tensile Strength Development for Maturity Index

In this study, the splitting tensile strength was also predicted by maturity index for five different mixes (SP0, SP1, SP2, SP3, and SP4). Furthermore, four equations (S_{LH}, S_{PH}, $S_{LOG,}$ and S_{EXP}) were used to predict the flexural strength by maturity index. Figure 86 presents the experimental and predicted splitting tensile strength of SP0, SP1, SP2, SP3, and SP4 that were obtained from maturity index with four modes (S_{LH}, S_{PH}, $S_{LOG,}$ and S_{EXP}). The regression parameters of all of these four models were shown in Table 23. The range of correlation coefficient (R^2) was

between 0.814 and 0.977. All the models have a very good correlation with experimental results in all mixes. However, the R^2 values for SP2 are slightly lower than other mixes. In this method, the values of R^2 of all four models in all mixes are slightly closer to each other. For SP0, SP1 and SP2 mix the linear hyperbolic equation has the highest value of R^2, but for SP3 and SP4 mixes, the parabolic hyperbolic equation has the highest value.

For SP0 mixes the rates of correlation coefficient are 0.923, 0.92, 0.912 and 0.918 for linear hyperbolic, parabolic hyperbolic, logarithmic and exponential equations respectively. For SP1 the rates of correlation coefficient are 0.948, 0.939, 0.931 and 0.936 for linear hyperbolic, parabolic hyperbolic, logarithmic and exponential equations respectively. For SP2 mixes the rates of R^2 are 0.849, 0.829, 0.814 and 0.823for S_{LH}, S_{PH}, S_{LOG} and S_{EXP} equations respectively. The values of R^2 of SP3 for S_{LH}, S_{PH}, S_{LOG} and S_{EXP} equations are 0.946, 0.977, 0.911 and 0.962 respectively. For SP4 mix the values of the correlation coefficient for S_{LH}, S_{PH} are 0.909 and 0.93 respectively, however, this value for S_{LOG} and S_{EXP} are 0.918 and 0.925 respectively.

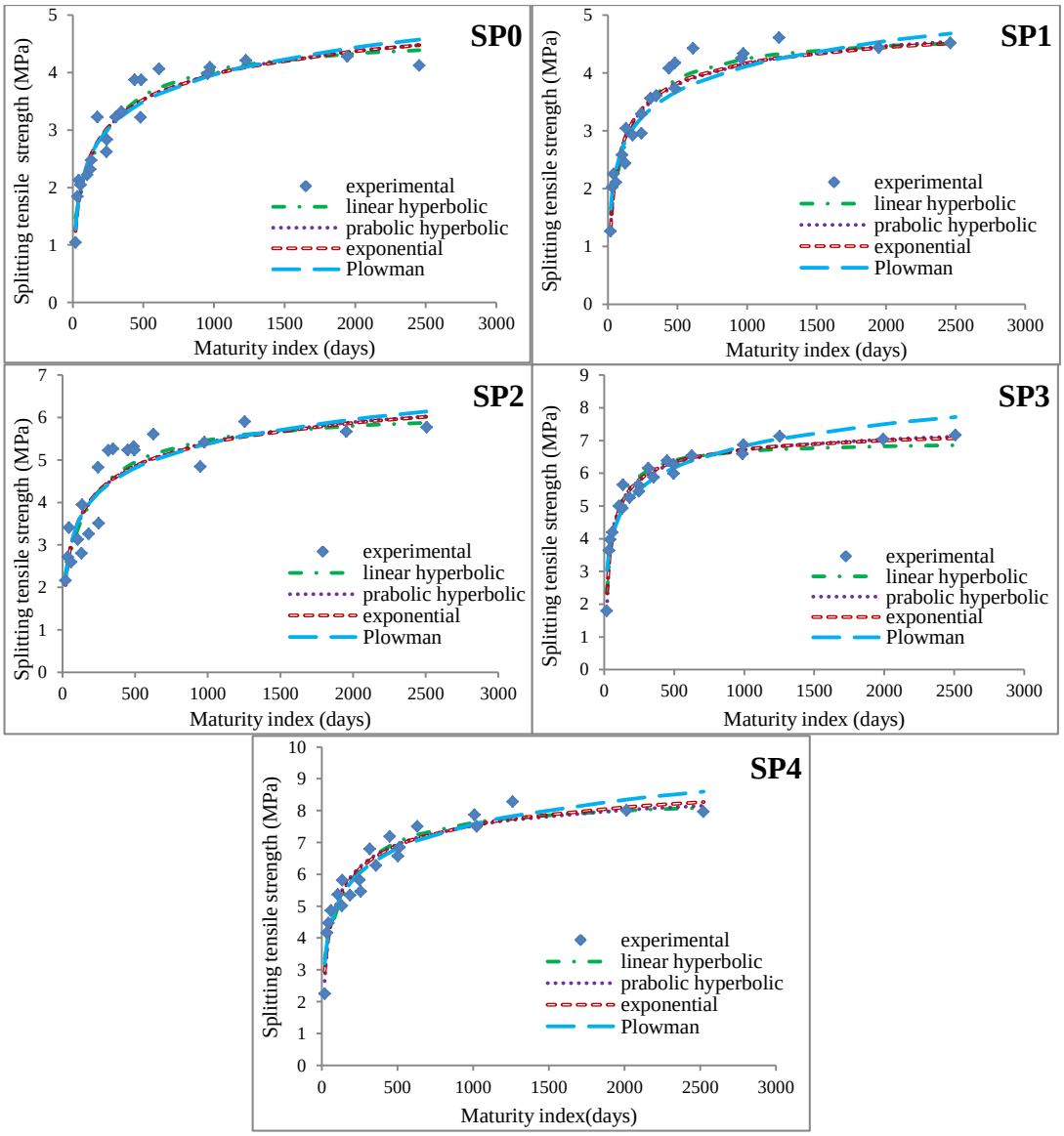

Figure 86: Predicted Splitting tensile strength by MI method.

Table 23: Regression parameters of splitting tensile strength for MI.

V_f	equation	Regression parameters							
		S_u	k_T	T_0	τ	α	a	b	R^2
SP0	Linear hyperbolic	4.686	0.006	-					0.955
	Parabolic hyperbolic	5.742	0.005	3.45					0.947
	Plowman						-0.74	0.681	0.945
	exponential	6.575			104.5	0.303			0.959
SP1	Linear hyperbolic	4.719	0.009	-					0.94
	Parabolic hyperbolic	5.407	0.011	10.22					0.937
	Plowman						-0.21	0.627	0.936
	exponential	5.266			40.8	0.456			0.944
SP2	Linear hyperbolic	6.204	0.007	-					0.95
	Parabolic hyperbolic	7.492	0.007	-					0.946
	Plowman						2.136	1.838	0.949
	exponential	8.8104			76.88	0.277			0.954
SP3	Linear hyperbolic	7.932	0.03	16.38					0.94
	Parabolic hyperbolic	6.981	0.021	-					0.939
	Plowman						0.187	0.962	0.937
	exponential	7.587			25.72	0.579			0.945
SP4	Linear hyperbolic	8.442	0.009	-					0.946
	Parabolic hyperbolic	9.465	0.015	9.394					0.944
	Plowman						-0.07	1.106	0.935
	exponential	10.63			40.53	0.335			0.947

5.4.6 Validation of Splitting Tensile Strength Models

Same procedure was done for all mixes to assess the accuracy of the splitting tensile strength.

5.4.6.1 Validation of Splitting Tensile Strength Models for LH_{eq}

In this method the ranges of errors for all data are between 0 and ±20%, only one data at age of 1 day has error higher than ±20%. Figures 87, 88, 89, 90 and 91 observe measured splitting tensile strength versus estimated splitting tensile strength for SP0, SP1, SP2, SP3 and SP4 respectively. The maximum error occur at age of 1 day for all mixes (except SP2), however, for SP2 mixture the maximum error occur at age of 7 days. At 1 day for SP0, SP1 and SP4 mixes, the S_{LH} has highest error and for SP2 and SP3 mixes the S_{LOG} has highest error. At later ages (28 and 56 days) the errors of logarithmic equation (S_{LOG}) in all mixes are higher than other equations. The S_{LH} at later ages has the minimum error compare to other equations.

Figure 87 observe the correlation between experimental splitting tensile strength and predicted flexural strength of SP0 with linear hyperbolic, parabolic hyperbolic, logarithmic and exponential equations. The maximum percentage of errors were -36%, -10.7%, -15.9% and -6.7 % for S_{LH}, S_{PH}, S_{LOG} and S_{EXP} equations respectively. However, at 56 days the percentage of errors are -1.8%, -3.4%, -9.4% and -4.7% for S_{LH},S_{PH}, S_{LOG} and S_{EXP} equations respectively.

Figure 88 shows correlation between predicted and measured splitting tensile strength with four equations (S_{LH}, S_{PH}, S_{LOG} and S_{EXP}) for SP1 mixture. The maximum percentage of errors day were 21%, 2.3%, -14% and 1.2% for S_{LH},S_{PH}, S_{LOG} and S_{EXP} equations respectively. However, at 56 days the percentage of errors are -3%, -6.6%, -11.7% and -6% for S_{LH},S_{PH}, S_{LOG} and S_{EXP} equations respectively.

Figure 89 shows the predicted and measured splitting tensile strength of SP2. The maximum percentage of error is -14.6%, -18.7%, -20.3% and -20.1% for S_{LH}, S_{PH}, S_{LOG} and S_{EXP} equations respectively. However, at 56 days the maximum percentages of errors are –3.2%, -7%, -9.2% and -6.7% for S_{LH}, S_{PH}, S_{LOG} and S_{EXP} equations respectively.

Figure 90 presents estimated and measured splitting tensile strength of SP3 mixture with four different equations. The maximum percentages of errors were -22.11%, -1.3% for S_{LH},S_{PH} equations respectively and at same day the maximum percentage of error are -66.44% and -20.38% for S_{LOG} and S_{EXP} equations respectively. However, at 56 days the percentage of errors are 4%, -0.6%, -9.4% and 0.6% for S_{LH}, S_{PH}, S_{LOG} and S_{EXP} equations, respectively.

Figure 91 presents estimated and measured splitting tensile strength of SP4 mixture with four different equations. The maximum percentage of errors at 1 day were -45.4%, -13.7% for S_{LH},S_{PH} equations respectively and at same day the percentage of error are -37.8% and -24.6% for S_{LOG} and S_{EXP} equations respectively. However, at 56 days the maximum percentage of errors for S_{LH} andS_{PH} are -1.8%, -3.4% respectively, and for S_{LOG} and S_{EXP} are -9.4% and -4.7% respectively.

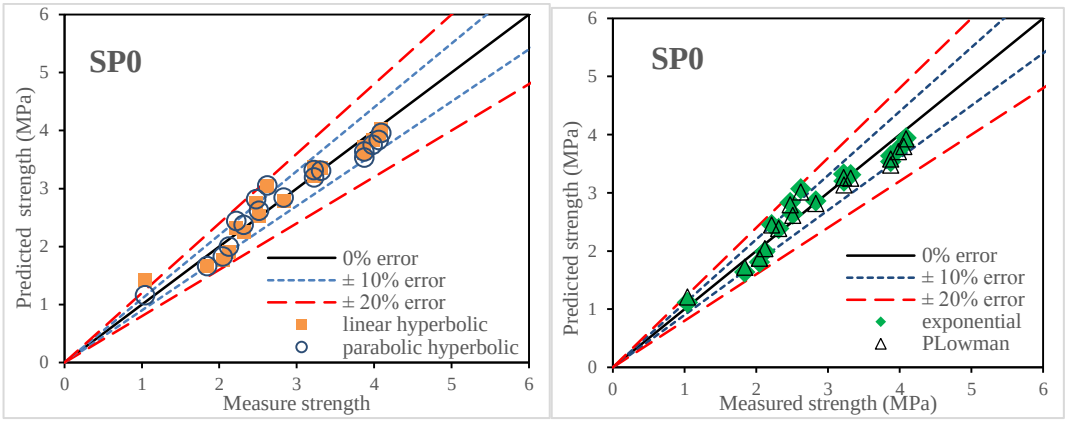

Figure 87: Measured versus predicted splitting tensile strength by LHeq method for SP0: (a) linear and parabolic hyperbolic model and (b) exponential and Plowman model.

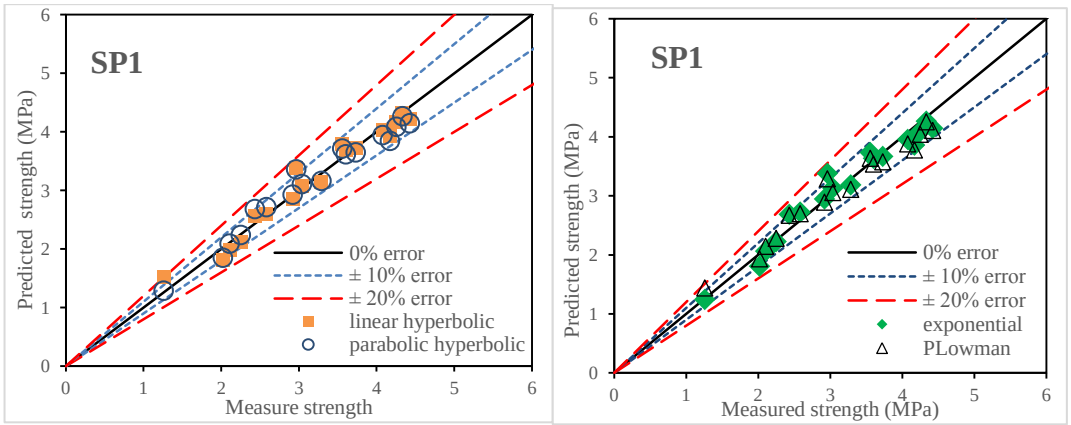

Figure 88: Measured versus predicted splitting tensile strength by LHeq method for SP1: (a) linear and parabolic hyperbolic model and (b) exponential and Plowman model.

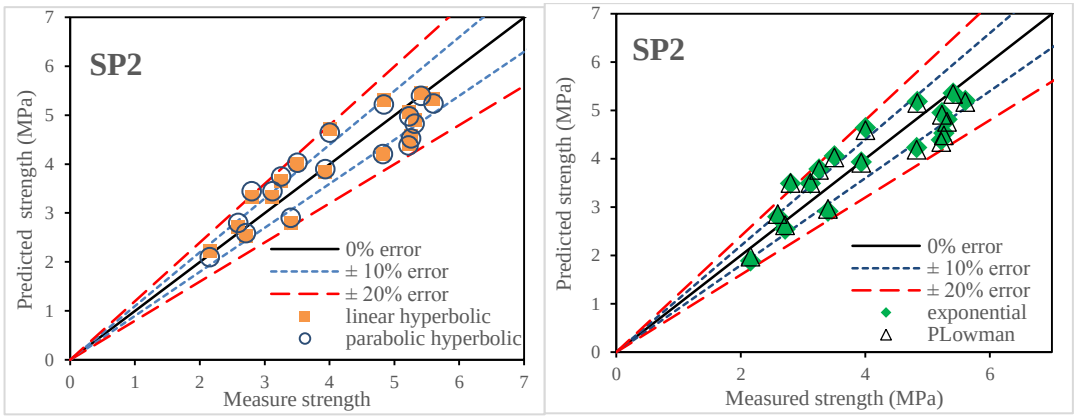

Figure 89: Measured versus predicted splitting tensile strength by LH_{eq} method for SP2: (a) linear and parabolic hyperbolic model and (b) exponential and Plowman model.

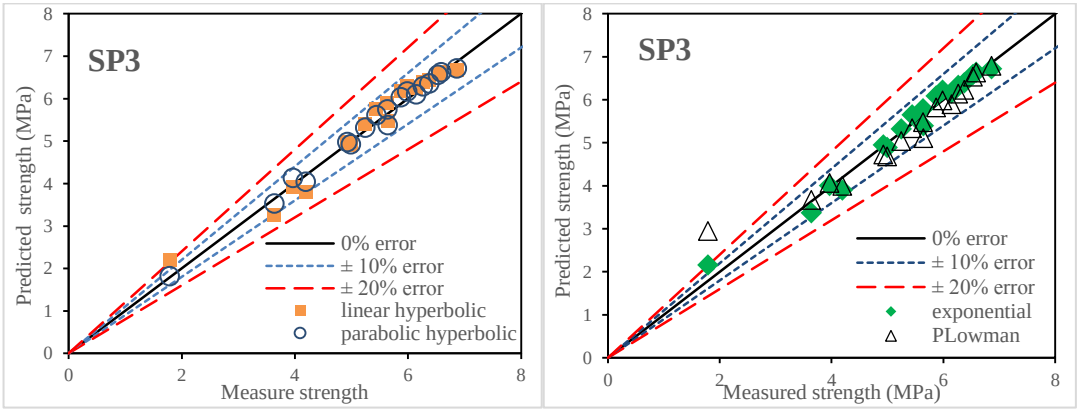

Figure 90: Measured versus predicted splitting tensile strength by LH_{eq} method for SP3: (a) linear and parabolic hyperbolic model and (b) exponential and Plowman model.

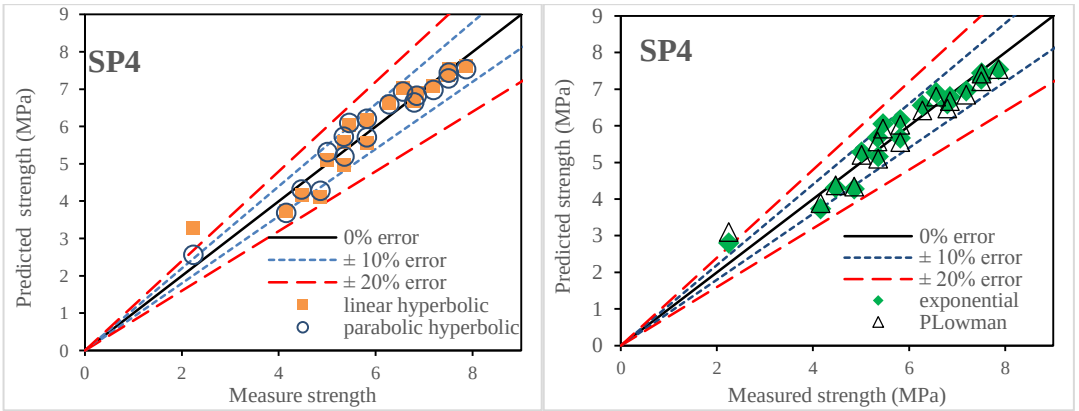

Figure 91: Measured versus predicted splitting tensile strength by LHeq method for SP4: (a) linear and parabolic hyperbolic model and (b) exponential and Plowman model.

5.4.6.2 Validation of Splitting Tensile Strength Models for PH_{eq}

Like LH_{eq}, the ranges of errors of all data in this method are also between 0 and ±20%. However, only one data at age of 1 day has error higher than ±20%. Figures 92, 93, 94, 95 and 96 show the validation of SP0, SP1, SP2, SP3 and SP4 respectively. At age of 1 day in all mixes, the percentage of errors for S_{LH} and S_{LOG} equations, are higher than S_{PH} and S_{EXP} equations. At later ages (28 and 56 days) the errors of logarithmic equation (S_{LOG}) in all mixes are higher than other equations. The percentage error of linear hyperbolic equation at later ages is lower than other equation.

Figure 92 observe the correlation between experimental splitting tensile strength and predicted splitting tensile strength of SP0 with linear hyperbolic, parabolic hyperbolic, logarithmic and exponential equations. The maximum percentage of error is -49.9%, -15.4%, -25.9% and -13.4% for S_{LH},S_{PH}, S_{LOG} and S_{EXP} equations respectively. However, at 56 days the percentage of errors are -2.1%, -5.3%, -11.7% and -6.8% for S_{LH},S_{PH}, S_{LOG} and S_{EXP} equations respectively.

Figure 93 shows correlation between predicted and measured splitting tensile strength with four equations (S_{LH}, S_{PH}, S_{LOG} and S_{EXP}) for SP1 mixture. The maximum percentage of errors were -26.4%,-2.9%, -21% and -1.4% for S_{LH},S_{PH}, S_{LOG} and S_{EXP} equations respectively. However, at 56 days the percentage of errors are 0.9%, -3.6%, -10.9% and -4.3% for S_{LH}, S_{PH}, S_{LOG} and S_{EXP} equations, respectively.

Figure 94 shows the predicted and measured splitting tensile strength of SP2. The maximum percentages of errors were -55.2%, -58.6%, -63.4% and -56.2% for S_{LH},

S_{PH}, S_{LOG} and S_{EXP} equations respectively. However, at 56 days the maximum percentage of errors are 3.2%, -7.6%, -11.4% and -7.9% for S_{LH},S_{PH}, S_{LOG} and S_{EXP} equations, respectively.

Figure 95 presents estimated and measured splitting tensile strength of SP3 mixture with four different equations. The maximum percentages of errors at 1 day were -24.7%, -2.3% for S_{LH}, S_{PH} equations respectively and at same day the maximum percentage of errors are -73.1% and -85.2% for S_{LOG} and S_{EXP} equations respectively. However, at 56 days the percentages of errors are 4.8%, 0%, -9.8% and -0.4% for S_{LH}, S_{PH}, S_{LOG} and S_{EXP} equations, respectively.

Figure 96 presents estimated and measured splitting tensile strength of SP4 mixture with four different equations. The maximum percentages of errors were -140.6%, -9.6% for S_{LH},S_{PH} equations respectively and at same day the percentage of error are -33.8% and -16.3% for S_{LOG} and S_{EXP} equations, respectively. However, at 56 days the maximum percentage of errors for S_{LH} andS_{PH} are 0.6%, -3.5%, respectively, and for S_{LOG} and S_{EXP} are -10.4% and -4.8%, respectively.

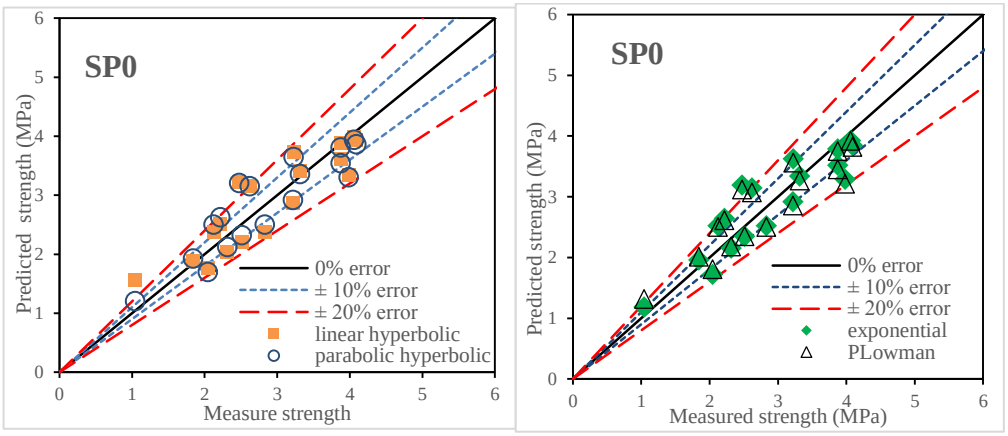

Figure 92: Measured versus predicted splitting tensile strength by PHeq method for SP0: (a) linear and parabolic hyperbolic model and (b) exponential and Plowman model.

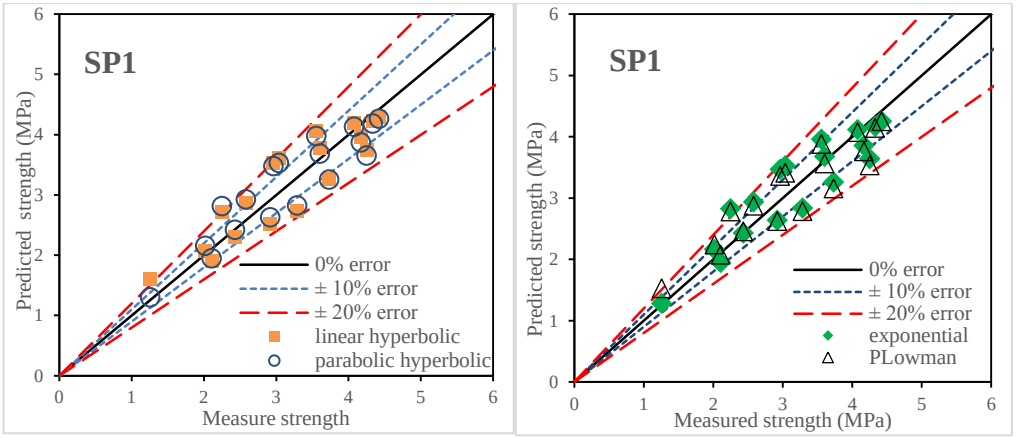

Figure 93: Measured versus predicted splitting tensile strength by PHeq method for SP1: (a) linear and parabolic hyperbolic model and (b) exponential and Plowman model.

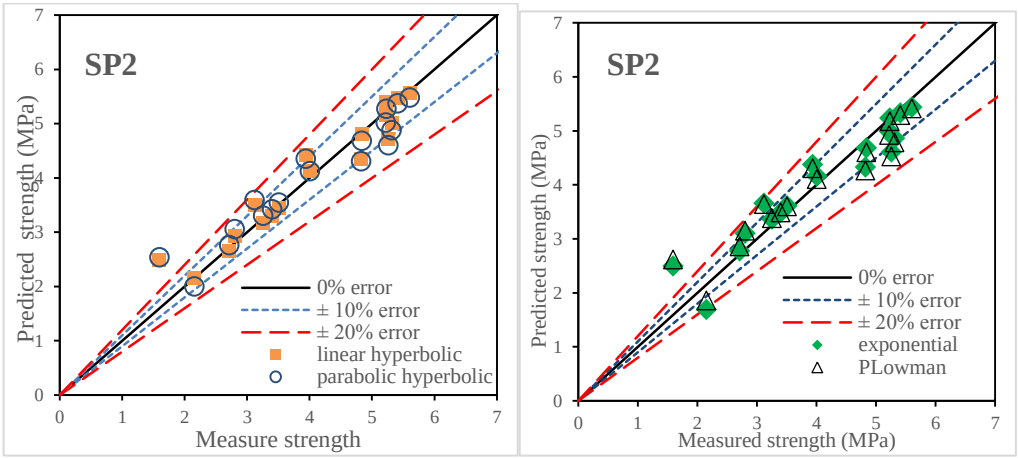

Figure 94: Measured versus predicted splitting tensile strength by PH_{eq} method for SP2: (a) linear and parabolic hyperbolic model and (b) exponential and Plowman model.

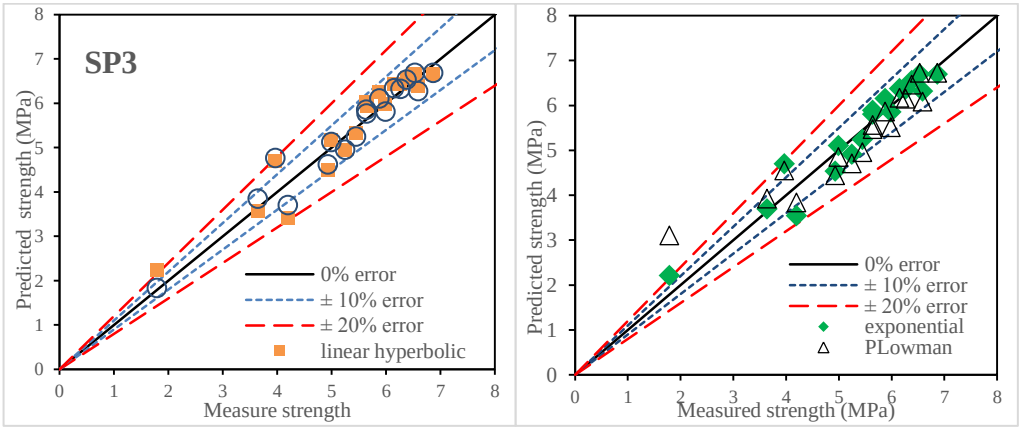

Figure 95: Measured versus predicted splitting tensile strength by PHeq method for SP3: (a) linear and parabolic hyperbolic model and (b) exponential and Plowman model.

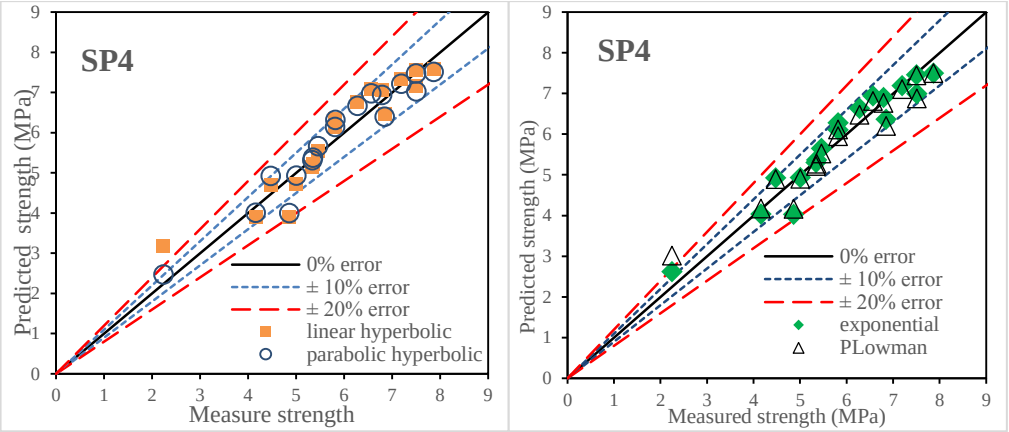

Figure 96: Measured versus predicted splitting tensile strength by PHeq method for SP4: (a) linear and parabolic hyperbolic model and (b) exponential and Plowman model.

5.4.6.3 Validation of Splitting Tensile Strength Models for EXP_{eq}

Figures 97, 98, 99, 100 and 101 exhibits the measured splitting tensile strength versus estimated flexural strength for SP0, SP1, SP2, SP3 and SP4 mixes respectively. As shown in these figures the ranges of errors of all data in this method are also between 0 and ±20%. However, only one data at age of 1 day has error higher than ±20%. The maximum errors occur in all mixes (except SP2) at age of 1 day, however, for SP2 the maximum error occur at 7 days. At age of 1 day the S_{LH} and S_{LOG} equations have higher error compare to other equations in all mixes. The highest error at later ages is for S_{LOG}. However, at later ages linear hyperbolic equation has minimum error compare to other equations. The percentage of errors at 56 day for S_{PH} and S_{EXP} seems to be similar.

Figure 97 observes the correlation between experimental splitting tensile strength and predicted splitting tensile strength of SP0 with linear hyperbolic, parabolic hyperbolic, logarithmic and exponential equations. The maximum errors at 1 day were -52.7%,-16.8%, -27.7% and -15.4% for S_{LH},S_{PH}, S_{LOG} and S_{EXP} equations

respectively. However, at 56 days the percentages of errors are -1.6%, -4.6%, -11.3% and -6.5% for S_{LH}, S_{PH}, S_{LOG} and S_{EXP} equations respectively.

Figure 98 shows correlation between predicted and measured splitting tensile strength with four equations (S_{LH}, S_{PH}, S_{LOG} and S_{EXP}) for SP1 mixture. The maximum percentage of errors at 1 day were -21.2%,-0.5%, -16.1% and 3.5% for S_{LH}, S_{PH}, S_{LOG} and S_{EXP} equations respectively. However, at 56 days the percentage of errors are 0.7%, -5.3%, -11.8% and -5.2% for S_{LH}, S_{PH}, S_{LOG} and S_{EXP} equations respectively.

Figure 99 shows the predicted and measured splitting tensile strength of SP2. The maximum percentages of errors at 1 day were -11.5%, -16.2%, -18.8% and -1.8% for S_{LH}, S_{PH}, S_{LOG} and S_{EXP} equations respectively. However, at 56 days the maximum percentages of errors are -3.8%, -7.6%, -10.5% and -7.6% for S_{LH}, S_{PH}, S_{LOG} and S_{EXP} equations respectively.

Figure 100 presents estimated and measured compressive strength of SP3 mixture with four different equations. The maximum percentages of errors at 1 day were -19.6%, -0.9% for S_{LH},S_{PH} equations respectively and at same day the maximum percentage of error are -62.7% and -15.4% for S_{LOG} and S_{EXP} equations respectively. However, at 56 days the percentage of errors are 4.1%, -0.8%, -9.9% and -0.3% for S_{LH}, S_{PH}, S_{LOG} and S_{EXP} equations respectively.

Figure 101 presents estimated and measured compressive strength of SP4 mixture with four different equations. The maximum percentages of errors at 1 day were -42.8%, -11.5% for S_{LH},S_{PH} equations respectively and at same day the percentage of

error are -35% and -20.3% for S_{LOG} and S_{EXP} equations respectively. However, at 56 days the maximum percentage of errors for S_{LH} andS_{PH} are -1.6%, -3.8% respectively, and for S_{LOG} and S_{EXP} are -10% and -4.9% respectively.

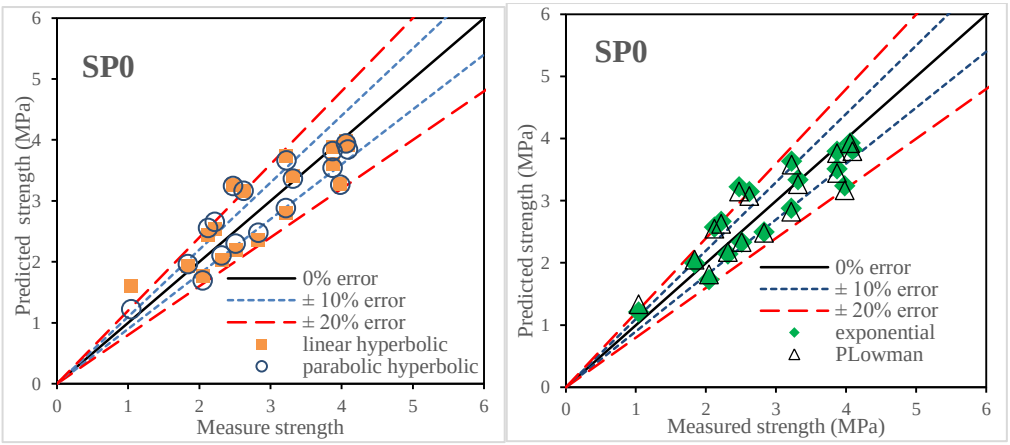

Figure 97: Measured versus predicted splitting tensile strength by EXPeq method for SP0: (a) linear and parabolic hyperbolic model and (b) exponential and Plowman model.

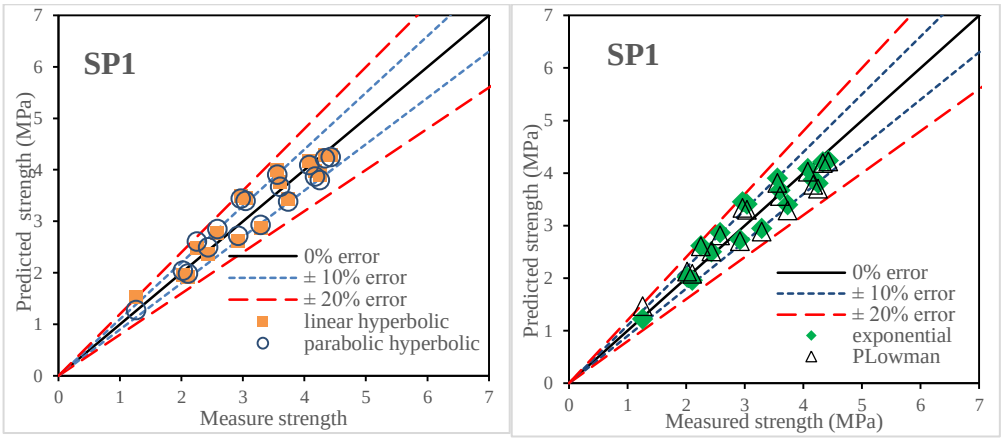

Figure 98: Measured versus predicted splitting tensile strength by EXPeq method for SP4: (a) linear and parabolic hyperbolic model and (b) exponential and Plowman model.

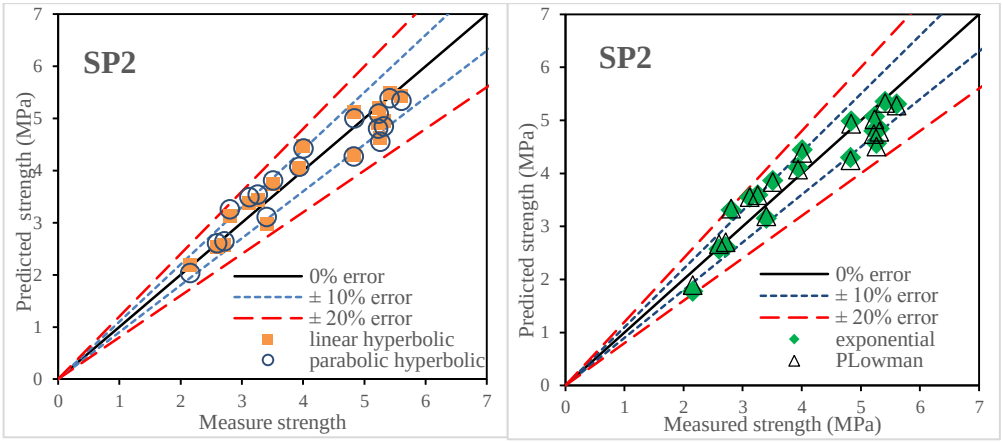

Figure 99: Measured versus predicted splitting tensile strength by EXPeq method for SP2: (a) linear and parabolic hyperbolic model and (b) exponential and Plowman model.

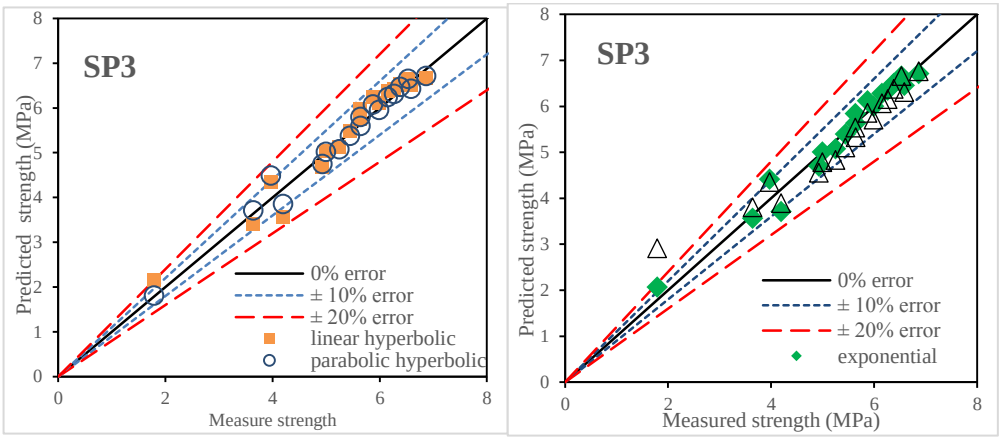

Figure 100: Measured versus predicted splitting tensile strength by EXPeq method for SP3: (a) linear and parabolic hyperbolic model and (b) exponential and Plowman model.

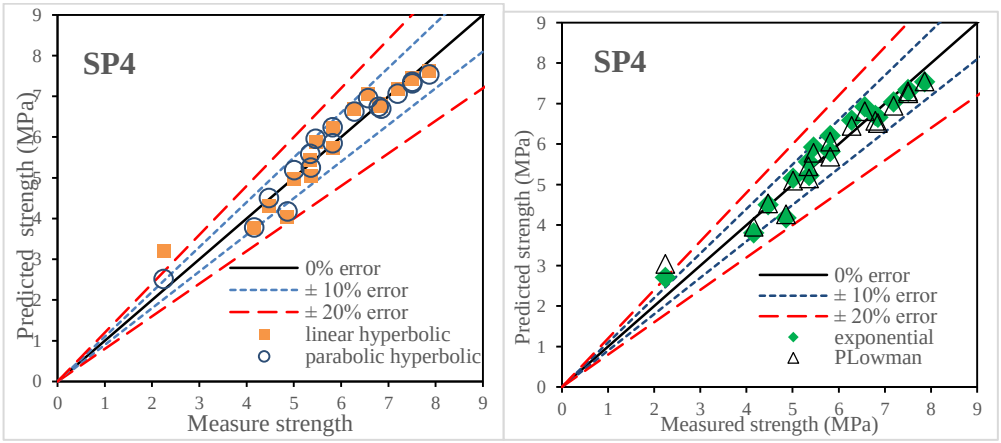

Figure 101: Measured versus predicted splitting tensile strength by EXPeq method for SP4: (a) linear and parabolic hyperbolic model and (b) exponential and Plowman model.

5.4.6.4 Validation of Splitting Tensile Strength Models for MI

In this method, the ranges of errors for most of the data are between 0 and ±20%, however, some of the data at the ages of 1, 3, 7 and 10 days have an error higher than ±20%. Figures 102, 103, 104, 105 and 106 observe the measured splitting tensile strength versus estimated splitting tensile strength for SP0, SP1, SP2, SP3 and SP4 respectively. The maximum error occurs at an age of 1 day for all mixes (except SP2), however, for SP2 mixture the maximum error occurs at an age of 7 days. In both 1 and 56 days of logarithmic equation (S_{LOG}) in all mixes are higher than other equations in all mixes.

Figure 102 observes the correlation between experimental splitting tensile strength and the predicted flexural strength of SP0 with linear hyperbolic, parabolic hyperbolic, logarithmic and exponential equations. The maximum percentages of errors were -4.1%, -22.8%, -22.9% and -19.4% for S_{LH}, S_{PH}, S_{LOG} and S_{EXP} equations respectively. However, at 56 days the percentages of errors are -6.4%, -8.6%, -10.9% and -8.6% for S_{LH}, S_{PH}, S_{LOG} and S_{EXP} equations, respectively.

Figure 103 shows a correlation between the predicted and measured splitting tensile strength with four equations (S_{LH}, S_{PH}, $S_{LOG,}$ and S_{EXP}) for the SP1 mixture. The maximum percentage of errors day were 24%, -5.3%, -31% and -3.2% for S_{LH}, S_{PH}, S_{LOG} and S_{EXP} equations respectively. However, at 56 days the percentage of errors are 0.2%, -0.6%, -3.6% and 0.2% for S_{LH}, S_{PH}, S_{LOG} and S_{EXP} equations respectively.

Figure 104 shows the predicted and measured splitting tensile strength of SP2. The maximum percentages of errors were -27.5%, -30.6%, -31.7% and -32.2% for S_{LH}, S_{PH}, S_{LOG} and S_{EXP} equations respectively. However, at 56 days the maximum

percentages of errors are -1.9%, -4.5%, -6.5% and -4.3% for S_{LH}, S_{PH}, S_{LOG} and S_{EXP} equations respectively.

Figure 105 presents an estimate and measured the compressive strength of SP3 mixture with four different equations. The maximum percentages of errors were -30.5%, -3.5% for S_{LH}, S_{PH} equations respectively, and on the sameday, the maximum percentages of errors are -69.8% and -30.5% for S_{LOG} and S_{EXP} equations respectively. However, at 56 days the percentages of errors are 4.4%, 0.6%, -7.7% and 1.3% for S_{LH}, S_{PH}, S_{LOG} and S_{EXP} equations respectively.

Figure 106 presents an estimate and measured the splitting tensile strength of SP4 mixture with four different equations. The maximum percentages of errors at 1 day were -49.1%, -17.7% for S_{LH}, S_{PH} equations respectively, and on the sameday, the percentage of error are -42.3% and -30.9% for S_{LOG} and S_{EXP} equations respectively. However, at 56 days the maximum percentages of errors for S_{LH} and S_{PH} are -1.5%, -2.3%, respectively, and for S_{LOG} and S_{EXP} are -7.9% and -3.8% respectively.

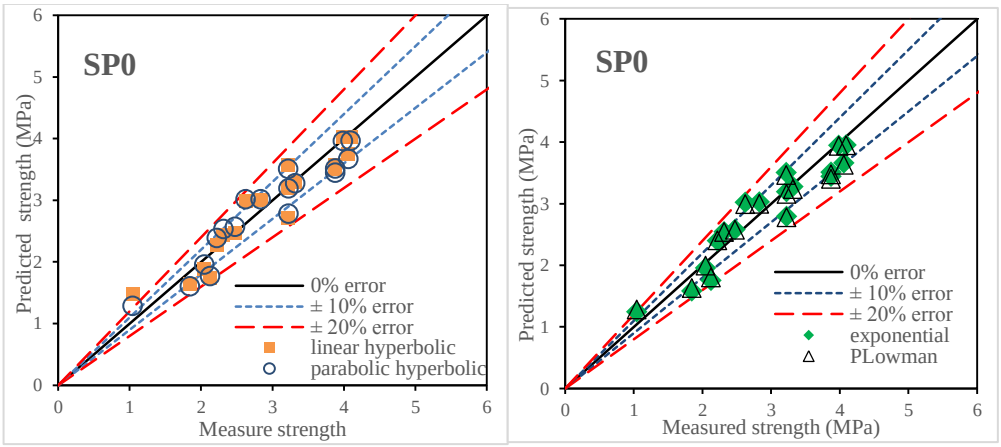

Figure 102: Measured versus predicted splitting tensile strength by MI method for SP0: (a) linear and parabolic hyperbolic model and (b) exponential and Plowman model.

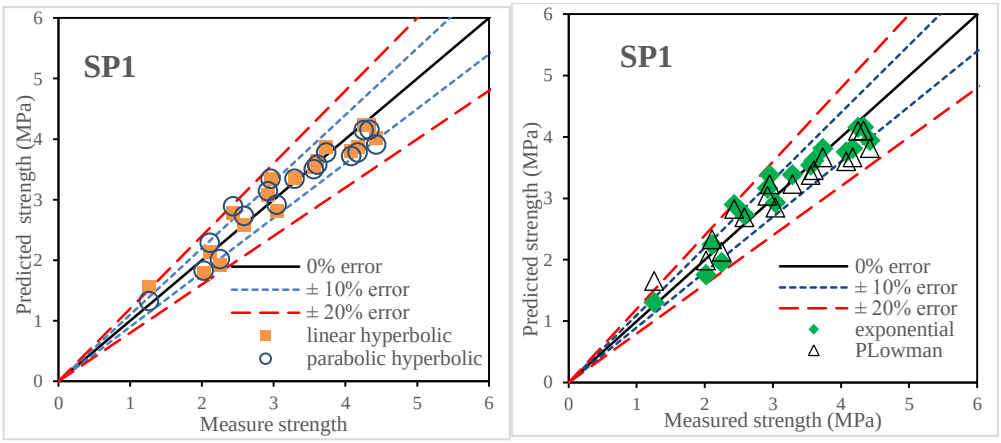

Figure 103: Measured versus predicted splitting tensile strength by MI method for SP1: (a) linear and parabolic hyperbolic model and (b) exponential and Plowman model.

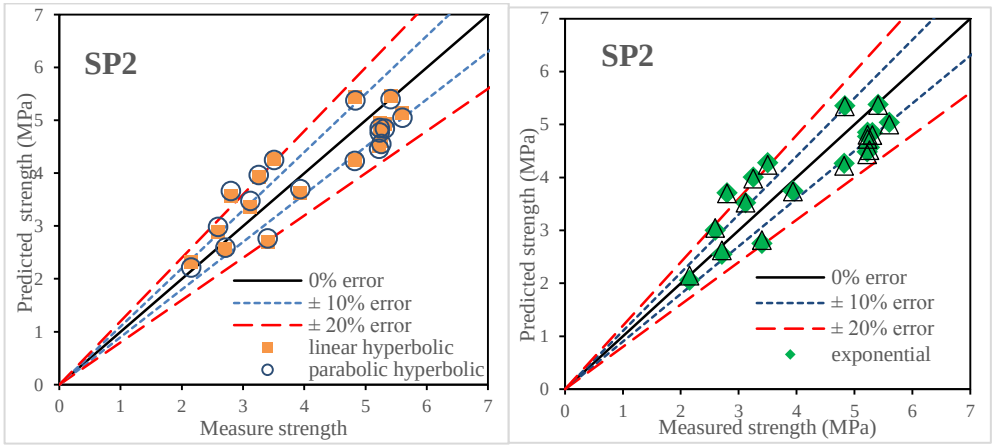

Figure 104: Measured versus predicted splitting tensile strength by MI method for SP4: (a) linear and parabolic hyperbolic model and (b) exponential and Plowman model.

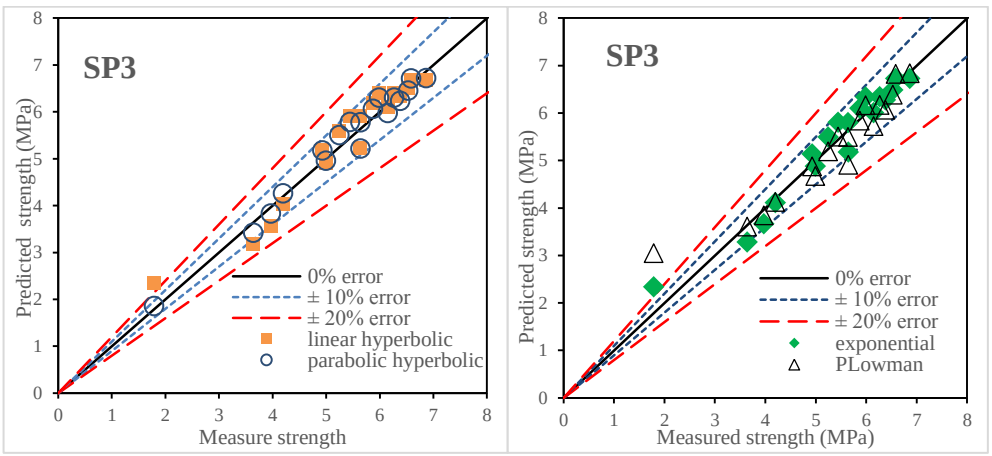

Figure 105: Measured s versus predicted splitting tensile strength by MI method for SP3: (a) linear and parabolic hyperbolic model and (b) exponential and Plowman model.

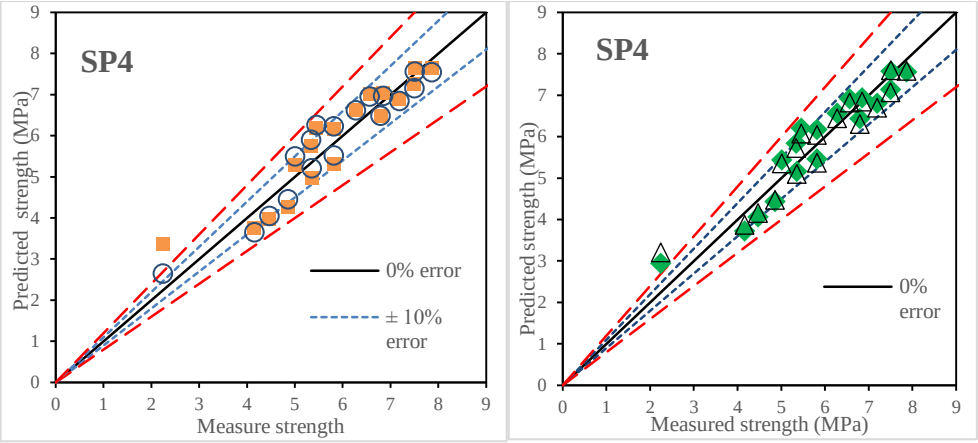

Figure 106: Measured versus predicted splitting tensile strength by MI method for SP4: (a) linear and parabolic hyperbolic model and (b) exponential and Plowman model.

Chapter 6

CONCLUSION

In this study, four mechanical properties of steel fiber reinforced concrete (compressive strength, flexural strength, flexural toughness and splitting tensile strength) were evaluated with two maturity method (Nurse-Saul and Arrhenius). The results show that both maturity methods can be acceptable for predicting all of these four properties. However, the Nurse-Saul method had a better result in all concrete properties when compared to Arrhenius method.

The apparent activation energy was determined by three alternative methods (linear hyperbolic, parabolic hyperbolic and exponential). At 2% volume fractions of fibers, the PH method was 39% higher than LH method, however, EXP method was 16% higher than LH method. The models obtained by linear hyperbolic had a very good correlation with experimental results.

The activation energy of steel-fiber reinforced concrete decreased by increasing the volume fraction of the fibers and at a 2% volume fraction, the activation energy decreased 24% compared to plain concrete.

The equivalent age and maturity index were calculated for five different mixes. The equivalent age was determined by three methods (eq_{LH}, eq_{PH}, and eq_{EXP}). The results show that the models obtained by eq_{LH} had a very good correlation with experimental results.

Maturity relation for four concrete properties of all mixes was obtained by four equations (S_{LH}, S_{PH}, S_{LOG}, and S_{EXP}). The models predicted by all the equations have a good correlation with experimental results. However, the accuracy of S_{LH} and S_{EXP} are slightly higher than S_{PH} and S_{LOG}. The accuracy of S_{LOG} is slightly lower than the other equations.

The range of R^2 for compressive strength for all models is between 0.671-0.97. However, the models obtained by the eq_{LH} method and its range of R^2 are between 0.881-0.946, for the eq_{PH} method the range of R^2 is between 0.702-0.857, for the eq_{EXP} method, the range of R^2 is between 0.671-0.895 and for the maturity index method, the range of R2 is between 0.906-0.97.

The range of R^2 for flexural strength for all models is between 0.684-0.968. However, the models obtained by the eq_{LH} method, the range of R^2 are between 0.883-0.937, for the eq_{PH} method the range of R^2 is between 0.711-0.840, the strength value of the eq_{EXP} method, the range of R^2 are between 0.684-0.915 and for the maturity index, the range of R^2 is between 0.91-0.968.

The range of R^2 for flexural toughness for all models is between 0.677-0.987. However, the models obtained by eq_{LH} method, the range of R^2 is between 0.906-0.987, for eq method the range of R2 is between 0.698-0.981, for the strength value of eq_{EXP} method, the range of R^2 is between 0.677-0.895 and for the maturity index, the range of R^2 is between 0.851-0.984.

The range of R^2 for splitting tensile strength for all models is between 0.814-0.991. However, the models obtained by eq_{LH} method, the range of R^2 are between 0.821-

0.991, for eq_{PH} method the range of R^2 is between 0.852-0.957, for the strength value of eq_{EXP} method, the range of R^2 is between 0.832-0.972 and for the maturity index, the range of R^2 is between 0.814-0.977.

The percentage of errors for all models for compressive and flexural strength at 1 day is very high, due to lower curing period. At later ages (3, 7, 10, 14, 28 and 56 days) the range of errors is approximately lower than ±20%. However, for flexural strength at an age of 3 days, some data have error higher than ±20%. At 1 day for all methods, the parabolic hyperbolic and Plowman equations have higher error compared to linear hyperbolic and exponential equations. However, at 56 days the Plowman equation has the highest error in all models.

For splitting tensile strength the percentage of error for most of the data is very low. Only one data at age of 1 day has an error higher than ±20%. However, for MI method some data at 1, 3, 7 and 10 days have an error higher than ±20%. At 1 day the linear hyperbolic and Plowman equations have a higher error compared to other equations in all mixes. However, at 56 days the Plowman equation has the highest error in all mixes.

For the flexural toughness, most of the data have error lower than ±20%. However, some data at ages of 3 and 7 days have an error higher than ±20%. At ages of 1 and 56 days, S_{LH} and S_{LOG} equations have a higher error compared to S_{PH} and S_{EXP} equations.

The temperature histories at early ages (first 24 hours) slightly increased by increasing the volume fraction of fibers, due to the transfer of heat via hydration by

steel fibers. However, after 24 hours temperature histories of all volume fractions of fibers at all curing temperatures are approximately same as plain concrete.

The compressive strength slightly increased at all curing temperatures, by increasing the volume fraction of fibers. The concretes cured at 32°C has a higher compressive strength at early ages (up to 10 days) but at later ages (14, 28 and 56 days) the cross-over effects occur and the compressive strength at 32°C curing temperatures decreased compared to 22 °C with the same volume fraction of fibers. However, at 56 days the compressive strength of concrete that cured at 32 °C has the same value with concrete which cured at 8 °C.

By increasing the volume fraction of fibers, the flexural strength increased at all curing temperatures. At 32°C curing temperature, the flexural strength of the samples has higher values, when compared to those at 8°C and 22°C curing temperatures; however, at 28 and 56 days, the values obtained from samples of 22°C and 32°C curing temperatures were approximately the same.

Flexural toughness significantly increased by increasing volume fractions of fiber. In all mixes at ages of 3, 7, 14 and 28 days the flexural toughness that cured at 32 °C has higher values, when compared to 8 °C and 22 °C curing temperatures but at 56 days due to the completion of hydration process, the values obtained from 22 °C and 32 °C were approximately the same.

The same was observed for other properties of concrete in this study. Increasing the curing temperature leads to an increase in the splitting tensile strength at early ages. Splitting tensile strength for concrete that cured at 32°C has higher tension values at

early ages compared to other curing temperatures (8°C and 22°C); At 56 days, approximately the same tension value was obtained for all volume fractions of fibers as concrete cured at 22 °C and 32°C.

6.1 Recommendations of future studies

1. The maturity relationship of steel fiber reinforced concrete should be evaluated for ultra-high performance concrete.
2. The maturity relationship of steel fiber reinforced concrete should be evaluated at high temperature (more than 30 °C).
3. There should be an evaluationof the maturity relationship of SFRC for other properties of concrete such as modulus of elasticity, impact resistance and compressions toughness.
4. There should be an evaluationof the effects of aspect ratio of steel fibers on the maturity relationship of steel fiber reinforced concrete.
5. The maturity relationship can be evaluated for some other types of fiber such as polypropylene and carbon fibers.
6. Maturity method can be evaluated by different curing methods such as autoclave and steam curing.

REFERENCES

Ahmad, I., Ali H., Azhar, S., Markert, L., Vanwhervin, D., & Escobar, L. (2006). Utilization of maturity method for concrete quality assurance in bridge substructure in Florida, in: *Proceedings of the 85th Annual Meeting of the Transportation Research Board (on CD Rom),* Washington DC.

Alexander, K. M., & Taplin, J. H. (1962). Concrete Strength, Cement Hydration and the Maturity Rule, *Australian Journal of Applied Science,* V.13, pp. 277- 284.

American Concrete Institute-ACI. (1997). State of art report on fiber reinforced concrete. ACI544.1R_96, *American Concrete Institute,* Farmington Hills, MI, US:

American Concrete Institute-ACI. (1988). Design consideration for fiber reinforced concrete. ACI544.4R_88, *American Concrete Institute,* Farmington Hills, MI, US:

ASTM C78. (2015). Standard test method for flexural strength of concrete (using simple beam with third-point loading). C 78/C78M, *ASTM International,* West Conshohocken, US, DOI: 10.1520/C0078_C0078M_15B.

ASTM C403. (2008). Standard Test Method for Time of Setting of Concrete Mixtures by Penetration Resistance. C403/C403M-08, *Annual Book of ASTM Standards,* V.04.02, ASTM, Philadelphia, doi: 10.520/C403_C403M-08.

ASTM C496. (2006). Standard Test Method for Splitting Tensile Strength of Cylindrical Concrete Specimens. *Annual Book of ASTM Standards,* Philadelphia,

ASTM C1074. (2011). Standard Practice for Estimating Concrete Strength by Maturity Method. C 1074, *Annual Book of ASTM Standards,* V.04.02, ASTM, Philadelphia, pp.689-696, doi: 10.1520/C1074_11.

Barnett, S.J., Soutsos, M.N., Millard, S.G., & Bungey J. H. (2006). Strength development of mortars containing ground granulated blast-furnace slag: Effect of curing temperature and determination of apparent activation energies. *Cement and Concrete Research,* V36, pp. 434-440, doi: 10.1016/j.cemconres.2005.001

Bentur, A., and Mendess, S. (2007). Fiber Reinforced Cementitious Composites. *Taylor & Francis,* London and New York.

Bergstrom, S. G. (1953). Curing Temperature, Age and Strength of Concrete, Magazine *of Concrete Research,* V.5, No.14, pp.61-66.

Bernhardt, C. J. (1956). Hardening of the Concrete at Different Temperatures, RILEM Symposium on Winter Concreting, *Danish Institute for Building Research,* Session B-II, Copenhagen,

Bickley, J. A. (1993). Field manual for maturity and pullout testing on highway structures, Strategic Highway Research Program Report (SHRPC-376*), National Research Council*, Washington, D.C.

Boubekeur, T., Ezziane, K., & Kadri E. H. (2014). Estimation of mortars compressive strength at different curing temperature by maturity method. *Construction and Building Materials,* V. 71, pp.299-307, DOI: 10.1016/j.conbuildmat.2014.08.084.

British Standards Institution - BSI. BS 1881-104. (1983). *Testing Concrete Part 104: Method for Determination of Vebe Time.* London: BSI.

Brooks, A.G., Schindier, A. K. & Robert, W. (2007). Maturity method evaluated for various cementitious materials. *Journal of Materials in Civil Engineering,* V.19, No.12.

Carino, N. J. (2004). The maturity method". In: Malhotra VM, Carino NJ, editors, *Handbook on Nondestructive Testing of Concrete*, 2nd edition, CRC Press.

Carino, N. J. (1984). The Maturity Method: Theory and Application. *Cement, Concrete, and Aggregates,* CCAGDP, V.6, No.2, winter pp.61-73, 1984.

Carino, N. J., & Tank, R. C. (1992). Maturity Functions for Concretes Made with Various Cements and Admixtures. *ACI Materials Journal,* V.89, No.2, pp.188-196.

Carino, N. J., Lew, H. S., & Volz, C. K. (1983). Early Age Temperature Effects on Concrete Strength Prediction by the Maturity Method. *ACI Journal,* V.80, No.2, pp.93-101.

Carino, N. J., & Lew, H. S. (1983). Temperature Effects on Strength-Maturity Relations of Mortar, *ACI Journal,* V.80, No.3, pp.177-182.

Clarke, C. (2009). Concrete shrinkage prediction using maturity and activation energy. Master of Science, *University of Maryland*.

Eren, Ö., Marar, K., & Çelik, T. (1999). Effects of silica fume and steel fibers on some mechanical properties of high-strength fiber-reinforced concrete. *Journal of Testing and Evaluation,* V .27,No.6,pp.380-387.

Eren, Ö. (2009). Strength prediction of concrete by non-destructive methods. *Eastern Mediterranean University*. MEKB-07-12,

Ferreira, L., Branco, F.G., Costa, H.S.S., Julio, E., & Maranha, P. (2015). Characterization of alkali-activated binders using maturity method. *Construction and Building Materials,* V.95, pp.377-344.

Freisleben Hansen, P., & Pedersen, E. J. (1977). Maturity Computer for Controlled Curing and Hardening of Concrete. *Nordisk Betong,* V.1, pp.19-34, DOI: 10.1016/j.conbuildmat.2015.07.068.

Freiesleben, H. P, & Pedersen, E. J. (1985). Curing of concrete structures. *CEB Information,* Bulletin 166.

Chengju, G. (1989). Maturity of Concrete: Method for Predicting Early-Stage Strength. ACI Materials Journal, V.86, No.4, pp.341-353, 1989.

Galobardes, I., Cavalaro, S. H,Goodier, C. I., Austin, S., & Rueda, A. (2015). Maturity method to predict the evaluation of the properties of spray concrete. *Construction and Building Materials,* V.79, pp.357-369, Doi: 10.1016/j.conbuildmat.2014.12.038.

Gauthier, E., & Regourd, M. (1982). The Hardening of Cement in Function of Temperature. *Proceedings of the RILEM International Conference on Concrete at Early Ages*, V.1, Ecole Nationale des Pones et Chausses, Paris, pp.145-150, 1982.

Concrete Solution. (2008). Glacier North West, Po Box 1730 Seattle WA 98111, Retrieved from www.glaciernw.com.

Han, M. C., & Han, C. G. (2010). Use maturity method to estimate the setting time of concrete containing super retarding agents, *Cement and Concrete Composites*, V.32, pp. 164-172, DOI: 1016/j.conbuildmat.2009.11.008.

Henault, J.W. (2012) Assessing CONDOT's Portland cement concrete testing methods phase II – Final report, *Connecticut Department of Transportation Bureau of Engineering and Construction*, Newington, CT.

Hosten, M. A., & Johnson, R. I. (2011). Implementation of the concrete maturity meter forMaryland, State Highway Administration Research Report, Report no. MD-11-SP708B4, *Office of Policy and Research Maryland State Highway Administration*, Baltimore, MD.

Jonasson, J. E. (1985). Early Strength Growth in Concrete-Preliminary Test Results Concerting Hardening at Elevated Temperatures, *The 3th RILEM Symposium on Winter Concreting*, Espoo, Finland, RILEM, pp.249-254.

Kada-Benameur, H., Wirquin, E., & Duthoit, B. (2000). Determination of Apparent Activation Energy of Concrete by Isothermal Calorimetry, *Cement and Concrete Research,* V.30, pp.301-305.

Kamkar, S. & Eren, Ö. (2017). Evaluation of maturity method for steel fiber reinforced concrete, *KSCE Journal of Civil Engineering,* doi: 10.1007/s12205-017-1761-9.

Kee, C. F. (1971). Relation Between Strength and Maturity of Concrete, *ACI Journal, Proceedings,* V.68, No.3, pp.196-203.

Kjellsen, K. O., & Detwiller, R. J. (1993). Later-Age Strength Prediction by a Modified Maturity Model, *ACI Materials Journal,* V.90, No.3, pp.220-227.

Knudsen, T. (1982). Modelling hydration of Portland cement: effect of particle size distribution. *Engineering foundation conference on characterization and performance prediction of cement and concrete.*

Lachemi, A., Hossain, K. M. A., Anagnostpoulos, C., & Sabouni, A. R. (2007). Application of maturity method to slip forming operations: Performance validation. *Cement and Concrete Composites,* V.29, pp. 290-299.

Lacome, M. L., Blankespoor, A. & Rens, K. M. (2000). A valid non-destructive evaluation and forensic tool. *ASCE,* Forensic Engineering.

Lamond, J. F. & James, H. (2006). Significance of tests and properties of concrete and concrete making materials. *ASTM international,* STP 169D.

Maage, M., & Helland, S. (1988). Cold Weather Concrete Curing Planned and Controlled by Microcomputer. *Concrete International: Design and Construction,* V.10, No.10, pp.34-39, 1988.

Malhotra, V. M., & Carino, N. J. (1991*). Handbook on Non-destructive Testing of Concrete,* CRC Press, pp. 3-5, 1991.

Marar, K., Eren, Ö., & Yitmen, I. (2011). Compression specific toughness of normal strength steel fiber reinforced concrete (NSSFRC) and high strength steel fiber reinforced concrete (HSSFRC). *Materials Research,* V.14, No. 2, pp.239-247, DOI: 101590/s1516-1439201 1005000042.

McIntosh, J D. (1956). The Effects of Low-Temperature Curing on the Compressive Strength of Concrete. RILEM Symposium on Winter Concreting. *Danish Institute for Building Research,* Session B-II, Copenhagen.

McIntosh, J. D. (1949). Electrical Curing of Concrete. *Magazine of Concrete Research,* V.1, No.1, pp.21-28.

Mindess, S., & Young, J. F. (1981). *Concrete,* Prentice-Hall Inc., Eaglewood Cliffs, New Jersey, USA.

Myers, J. J. (2000). The use of the maturity method as a quality control tool for high-performance concrete bridge decks. In Proc. PCI/FHWA/FIB Int. Symp. on High Performance Concrete, L.S. Johal, Ed., *Precast/Prestressed Institute,* Chicago, 316.

Nixon, J. M, Schindler A. K, Barnes, R. W, & Wade, S. A. (2008). Evaluation maturity method to estimate concrete strength in field applications. *Highway Research Center and Department of Civil Engineering at Auburn University*, ALDOT Research Project 930-590.

Nokken, M. R. (2015). Electrical conductivity to determine maturity and activation energy in concretes. *Materials and Structures,* doi: 10.1617/s11527-015-0644-0

Neville, A. M., & Brooks, J. J. (2005). *Concrete Technology,* Revised edition-2001 standards update. pp. 78-93.

Nurse, R. W. (1949). Steam Curing of Concrete. *Magazine of Concrete Research*, V.1, No.2, pp.79-88.

Pinto, R.C.A., & Hover, K. (1996). Application of maturity functions to high-strength concretes, in *High-Strength Concrete:* An International Perspective, ACI SP 167, J.A. Bickley, Ed., *American Concrete Institute,* Farmington Hills, MI, 229.

Plowman, J. M. (1956). Maturity and the Strength of Concrete. *Magazine of Concrete Research,* V.8, No.22, pp.13-22.

Rastrup, E. (1954). Heat of Hydration. *Magazine of Concrete Research*, V.6, No. 17, pp.127-140.

Roy, D. M. & Idorn, G.M. (1982). Hydration, structure, and properties of blast furnace slag cements, mortars and concrete. *J. Am. Conc. Inst.*,79(6), 444.

Saul, A. G. A. (1951). Principles underlying the steam curing of concrete at Atmospheric pressure. *Magazine of Concrete Research,* V.2, No.6, pp.127-140.

Sofi, M., Mendis, P. A., & Baweja, D. (2012). Estimating early-age in situ strength development of concrete slabs. *Construction and Building Materials,* V.29, pp.659-666, DOI: 10.1016/j.conbuildmat.2011.10.019.

Soutsos, M. N., Turu'allo, G., Owens, K., Kwasny, J., Barnett, S. J., & Basheer, P. A. M. (2013). Maturity testing of lightweight self-compacting and vibrated concretes. *Construction and Building Materials,* V.47, pp.118-125, DOI: 10.1016/j.conbuildmat.2013.04.045.

Tank, R. C., & Carino, N. J. (1991). Rate Constant Functions for Strength Development of Concrete. *ACI Materials Journal,* V.88, No.1, pp.74-83.

Turcry, P., Loukili, A., Barcelo, L., & Casabonne, J. M. (2002). Can the maturity concept be used to separate the autogenous shrinkage and thermal deformation of cement paste at early age?. *Cement and Concrete Research,* V.32, pp.1443-1450.

Verbeck, G.J., & Helmuth, R. H. (1968). Structure and physical properties of cement paste, in *Proc. Fifth Int. Symp. on the Chemistry of Cement,* Part III, Tokyo, 1−32.

Wade, S. A., Barnes, R. W., Schindler, A. K., & Nixon, J. M. (2008). Evaluation of the maturitymethod to estimate concrete strength in field applications. *Highway Research Center and Department of Civil Engineering at Auburn University,* Report no. 2 ALDOT Research Project 930–590,

Waller, V., d'Aloïa, L., Caussingh, F., & Lecrux, S. (2004). Using the maturity method in concrete cracking control at early ages. *Cement and Concrete Composites*, V24, pp 589-599, 2004, doi: 10.1016/S0958-9465(03)00080-5.

Ykici, T.A., & Chen, H.L, (2015). Use of maturity method to estimate compressive strength of mass concrete, *Constructions and Building Materials*, V.95, pp.802-812, doi: /dx.doi.org/10.1016/j.conbuildmat.2015.07.026.

Zhanng, J., Cusson, D., Monteiro, P., & Harvey, J. (2008). New perspectives on maturity method and approach for high performance concrete applications. *Cement and Concrete Research*, Doi: 10.116/j.ceconres.2008.08.001.

APPENDICES

Table A1: Results of Compressive strength

Age		Compressive strength results					
(Days)	**1**	**3**	**7**	**10**	**14**	**28**	**56**
				8 °C			
SP0	7.63	21	29.3	32.35	37.1	44	47.7
SP1	7.8	21.25	31.1	34.76	38.55	45.2	48.5
SP2	8.06	22.4	32.85	35.3	39.1	46.8	51.55
SP3	8.41	22.6	34.1	36.45	41.1	49	52.6
SP4	8.57	22.7	37.8	36.95	44.3	51.56	54.7
				22 °C			
SP0	8.05	23.05	32.5	37.4	48.3	51.7	52.23
SP1	8.32	23.35	34.25	43.25	51.2	53.4	53.9
SP2	8.94	23.7	35.4	45.45	53.55	55.7	56.3
SP3	9.07	24.41	36.2	46.6	55.2	57	58.4
SP4	9.09	25.65	40.45	48.7	56.75	60.1	60.88
				32 °C			
SP0	8.53	28.5	36.05	41.15	46.3	49.85	48.6
SP1	9.46	32.1	41.45	45.35	47.2	52.45	51.75
SP2	9.51	35.35	43.5	46.4	49.06	52.95	53.5
SP3	9.73	38	44	47.7	50.3	53.85	53.9
SP4	10.25	39.6	46.1	49.05	52.05	55.46	54.65

Table A2: Results of Flexural Strength

Age		Flexural strength results					
(Days)	**1**	**3**	**7**	**10**	**14**	**28**	**56**
				8 °C			
SP0	1.12	3.35	4.191	4.685	5.091	6.241	6.959
SP1	1.180	3.860	4.391	4.930	5.376	6.860	7.489
SP2	1.245	4.324	6.281	5.779	6.85	8.253	9.144
SP3	1.450	5.330	5.981	6.670	7.520	9.376	9.872
SP4	1.521	5.736	6.713	6.65	8.7	10.418	10.972
				22 °C			
SP0	1.16	3.92	4.782	5.18	5.9	6.76	7.124
SP1	1.240	4.370	5.163	5.590	6.440	7.406	7.759
SP2	1.41	5.354	5.97	7.067	7.98	9.369	9.567
SP3	1.580	6.320	7.260	7.980	9.340	10.414	10.665
SP4	1.69	6.65	7.915	8.56	9.63	11.004	11.445
				32 °C			
SP0	1.16	3.92	4.782	5.18	5.9	6.76	7.124
SP1	1.240	4.370	5.163	5.590	6.440	7.406	7.759
SP2	1.41	5.354	5.97	7.067	7.98	9.369	9.567
SP3	1.580	6.320	7.260	7.980	9.340	10.414	10.665
SP4	1.69	6.65	7.915	8.56	9.63	11.004	11.445

Table A3: Results of Flexural Toughness

Age	Flexural toughness results				
(Days)	**3**	**7**	**14**	**28**	**56**
			8 °C		
SP0	1.82	2.7	4.33	5.15	5.69
SP1	25.77	38.65	43.55	54.56	79.06
SP2	37.89	54.7	75.25	113.23	124.42
SP3	74.75	94.35	113.23	126.52	158.47
SP4	92.43	113.15	124.42	167.4	194.83
			22 °C		
SP0	2.26	3.97	4.91	5.39	6.11
SP1	29.4	55.23	61.47	65.89	81.63
SP2	46.41	65.89	91.77	95.46	135.35
SP3	106.1	117.93	146.21	157.23	174.31
SP4	110.89	125.85	150	174.48	207.16
			32 °C		
SP0	2.86	4.55	5.28	5.78	6.38
SP1	37.44	61.25	66.66	79.17	97.72
SP2	54.46	86.65	96.29	106.3	141.23
SP3	124.75	149.1	156	163.6	172.94
SP4	135.98	160.14	181.25	187.46	206.87

Table A4: Results of Splitting Tensile Strength

Age		Splitting tensile strength results					
(Days)	**1**	**3**	**7**	**10**	**14**	**28**	**56**
				8 °C			
SP0	1.043	2.046	2.315	2.513	2.831	3.219	3.983
SP1	1.260	2.108	2.435	2.922	3.290	3.734	4.254
SP2	2.156	2.597	2.803	3.256	3.507	4.006	4.839
SP3	1.790	4.197	4.930	5.249	5.446	5.990	6.587
SP4							
				22 °C			
SP0	1.842	2.219	2.623	3.317	3.875	4.092	4.279
SP1	2.022	2.584	2.965	3.606	4.172	4.335	4.436
SP2	2.715	3.121	4.825	5.262	5.315	5.412	5.665
SP3	3.642	4.995	5.639	5.876	6.266	6.866	7.04
SP4	4.162	5.36	5.822	6.282	6.569	7.868	8.011
				32 °C			
SP0	2.125	2.477	3.225	3.875	4.061	4.211	4.152
SP1	2.253	3.041	3.559	4.079	4.427	4.610	4.52
SP2	3.403	3.939	5.223	5.232	5.606	5.9	5.768
SP3	3.969	5.644	6.150	6.38	6.531	7.125	7.167
SP4	4.475	5.82	6.797	7.195	7.505	8.283	7.968

Table B1: Equivalent Age Values with LH Method.

Age		Equivalent age with LH method					
(Days)	**1**	**3**	**7**	**10**	**14**	**28**	**56**
				8 °C			
SP0	0.55	1.54	3.4	4.79	6.57	13.07	26.01
SP1	0.58	1.64	3.55	4.94	6.78	13.46	26.76
SP2	0.59	1.74	3.82	5.33	7.33	14.6	29.05
SP3	0.6	1.84	4	5.57	7.66	15.27	30.39
SP4	0.61	1.91	4.22	5.92	8.14	16.26	32.4
				22 °C			
SP0	1.21	3.73	8.9	12.86	18.22	36.82	73.45
SP1	1.2	3.71	8.84	12.76	18.07	36.51	72.85
SP2	1.3	3.82	8.91	12.77	18.07	36.51	72.85
SP3	1.3	3.82	8.91	12.77	18.02	35.96	71.95
SP4	1.26	3.83	9	12.92	18.21	36.41	72.9
				32 °C			
SP0	1.98	6.34	10.82	21.5	29.86	59.2	119.33
SP1	2	6.29	14.79	21.13	29.4	59.03	118.1
SP2	2.06	6.26	14.61	20.83	28.85	57.87	115.68
SP3	1.97	5.97	13.92	19.86	27.52	55.19	110.31
SP4	1.97	5.83	13.5	19.15	26.88	53.64	107.22

Table B2: Equivalent Age Values with PH Method.

Age		Equivalent age with PH method					
(Days)	**1**	**3**	**7**	**10**	**14**	**28**	**56**
				8 °C			
SP0	0.37	0.95	1.96	2.71	3.64	7.2	14.24
SP1	0.38	1.03	2.07	2.82	3.79	7.46	14.72
SP2	0.41	1.15	2.39	3.27	4.41	8.74	17.3
SP3	0.55	1.34	2.77	3.8	5.15	10.13	20.01
SP4	0.45	1.45	3.08	4.26	5.79	11.57	22.98
				22 °C			
SP0	1.41	4.47	10.84	15.8	22.61	46.02	91.66
SP1	1.4	4.44	10.76	15.67	22.41	44.78	90.10
SP2	1.61	4.67	10.86	15.58	22.14	44.08	88.22
SP3	1.48	4.53	10.69	15.39	21.78	43.54	87.22
SP4	1.46	4.5	10.62	15.29	21.6	43.21	86.58
				32 °C			
SP0	3.62	11.91	28.07	40.32	55.57	112.01	224.16
SP1	3.73	11.89	27.84	39.73	54.97	110.5	221
SP2	3.79	11.5	26.67	37.94	52.09	104.61	208.89
SP3	3.17	9.59	22.27	31.71	43.63	87.6	174.95
SP4	3.06	8.97	20.6	29.10	40.92	81.52	162.85

Table B3: Equivalent Age Values with EXP Method.

Age		Equivalent age with EXP method					
(Days)	**1**	**3**	**7**	**10**	**14**	**28**	**56**
				8 °C			
SP0	0.35	0.9	1.84	2.54	3.4	6.72	13.28
SP1	0.44	1.22	2.51	3.45	4.67	9.23	18.27
SP2	0.51	1.35	3.15	4.36	5.95	11.91	23.71
SP3	0.5	1.53	3.24	4.47	6.1	12.14	24.1
SP4	0.55	1.75	3.83	5.34	7.32	14.64	29.14
				22 °C			
SP0	1.44	4.57	11.1	16.19	23.19	46.43	93.26
SP1	1.32	4.16	10.01	14.54	20.71	41.46	83.22
SP2	1.42	4.14	9.99	13.84	19.59	39.11	78.21
SP3	1.38	4.22	9.93	14.28	20.17	40.32	80.75
SP4	1.31	4.03	9.48	13.63	19.21	38.42	76.95
				32 °C			
SP0	3.9	12.83	30.24	43.44	59.81	120.59	241.32
SP1	2.95	9.41	22.08	31.53	43.72	88.43	176.31
SP2	2.63	8	18.63	26.55	36.64	73.54	146.94
SP3	2.58	7.82	18.2	25.94	35.8	71.84	143.53
SP4	2.25	6.66	15.37	21.78	30.58	61	121.91

Table B4: Maturity Index Values

Age		Maturity Index					
(Days)	**1**	**3**	**7**	**10**	**14**	**28**	**56**
				8 °C			
SP0	9.5	25.29	53.75	74.92	100.79	200.18	396.65
SP1	9.75	27.71	56.51	76.38	102.79	203.31	401.65
SP2	9.75	28.46	59.13	80.42	108.13	214.74	424.85
SP3	9.38	29.79	60.04	81.21	109	216.5	428.02
SP4	9.17	30.42	63.54	86.96	116.92	233.68	463.39
				22 °C			
SP0	23.21	71.42	169.42	244.04	344.71	689.76	1382.06
SP1	22.71	71.42	169.42	244.04	345.81	690.28	1383.4
SP2	25.04	74.29	173.33	248.21	349.33	697.53	1395.55
SP3	24.83	75.46	177.25	254.25	357.96	715.8	1432.95
SP4	24.96	76.46	179.46	258	363.04	729.41	1457.3
				32 °C			
SP0	31.79	100.17	236.04	338.29	471.58	946.59	1894.63
SP1	31.63	101	237.42	339.54	473.83	950.93	1903.28
SP2	34.33	104.75	244.92	349.71	485.75	973.99	1947.76
SP3	34.46	104.83	245.04	349.88	486.5	975.11	1949.74
SP4	35/46	106.13	246.46	350.83	491.38	981.55	1962.37